POLITECNICO DI TORINO

Master of Science in Civil Engineering

Master's thesis

A new approach for the evaluation of the feasibility of cold asphalt mixtures for flexible pavement maintenance

Supervisors

prof. Ezio Santagata
prof. Davide Dalmazzo
prof. Pier Paolo Riviera
prof. Shane Underwood

Candidate

Stefano Marini

July 2018

To my family,

to my friends

ABSTRACT

This research is the result of a work conducted by both Giuseppe Pullara and Stefano Marini at the Road Materials Laboratory of Politecnico di Torino and at North Carolina State University.

Pothole patching is becoming an important issue in the maintenance activities of the administration all around the world; although the increasing road accidents and the economic loss due to potholes, no standards are present in Italy and only some recommendations can be found in other states.

To repair potholes, usually cold mix asphalts are used: they are a mixture of aggregates and bituminous binder, usually emulsion or cutback, that can be stockpiled for a long period after the production and can be used at low temperature, allowing emergency repairs under harsh water condition.

The main objective of this research is to evaluate the performances of different cold mix asphalts available in Italy, starting from the analysis of the basic properties, such as the composition and the compaction characteristics.

The performances were evaluated with reference to two different conditions:
- Low level of compaction, for which Indirect Tensile Strength (ITS) and California Bearing Ratio (CBR) were performed;
- High level of compaction, for which the resilient modulus, the quick shear resistance and the wheel tracking test were performed.

From this research it is possible to say that generally cold mix asphalts have poor properties, they are usually difficult to compact, with only two materials that have a voids content lower than 10% after 180 rounds in the Gyratory Shear Compactor.

Abstract

Regarding the performances, lots of samples collapsed during the curing period before the test. Only one out of seven materials completed all the test procedure, while for four materials it was impossible to achieve some results during the ITS test.

In addition to the performances evaluation, the compaction characteristics were deeply analyzed in the Civil, Construction and Environmental Engineering department of the North Carolina State University, where different analytical models were studied and developed.

The objective of this phase was to obtain a predictive model that can simulate the deformation of the materials using the Gyratory Shear Compactor.

SINTESI

Questa ricerca è il risultato di un lavoro condotto da Giuseppe Pullara e Stefano Marini presso il laboratorio di materiali stradali del Politecnico di Torino e presso la North Carolina State University.

La riparazione di buche stradali sta diventando un problema importante nelle attività di manutenzione tra le amministrazioni di tutto il mondo. Nonostante il problema delle buche causi un incremento di incidenti stradali e una notevole perdita dal punto di vista economico, in Italia non è presente alcuna normativa, mentre in altri Stati è possibile trovare solamente delle indicazioni a riguardo.

I conglomerati bituminosi a freddo sono i materiali più utilizzati per il riempimento di buche stradali: essi sono composti da un mix di aggregati e legante bituminoso, solitamente emulsione o bitume flussato. Queste miscele possono essere stoccate per un lungo periodo dopo la produzione e possono essere utilizzate a basse temperature, permettendo interventi di emergenza anche durante condizioni metereologiche avverse.

Il principale obiettivo di questo studio è la valutazione delle performances di differenti conglomerati a freddo disponibili in Italia, partendo dall'analisi delle proprietà base quali la composizione e le caratteristiche di compattazione.

Le performances sono state analizzate con riferimento a due diverse condizioni:
- Basso livello di compattazione, per il quale sono state effettuate le prove di resistenza a trazione indiretta (ITS) e California Bearing Ratio (CBR);
- Alto livello di compattazione, per il quale sono state effettuate le prove di modulo resiliente, quick shear e ormaiamento.

Da questo studio è possibile concludere come i conglomerati a freddo abbiano scarse proprietà e come siano solitamente difficili da compattare, con solo due materiali che raggiungono un contenuto di vuoti inferiore al 10% dopo 180 giri nella pressa a taglio giratoria.

Riguardo alle performances, molti campioni sono collassati durante il periodo di condizionamento prima dei test. Solamente uno dei sette materiali ha completato tutte le prove, mentre per quattro è stato impossibile registrare dei risultati durante la prova ITS.

In aggiunta, sono state analizzate nel dettaglio le caratteristiche di compattazione, presso il Civil, Construction and Environmental Engineering Department della North Carolina State University, dove sono stati studiati e sviluppati diversi modelli analitici.

L'obiettivo in questa fase è stato quello di ottenere un modello predittivo che potesse simulare la deformazione dei materiali durante la compattazione con la pressa a taglio giratorio.

ACKNOWLEDGMENTS

TABLE OF CONTENTS

LIST OF TABLES

LIST OF FIGURES

LIST OF GRAPHS

1. INTRODUCTION

This thesis presents the work realized both at the Road Materials Laboratory of Politecnico di Torino and at North Carolina State University.

The work started after the request from GTT (Gruppo Torinese Trasporti), the society that provides public transport in Turin, to analyses the characteristics and the behavior of two cold mix asphalts that they use for road repair, due to a lack of performances of the used mixes and the difficulties that the company has in choosing the right product.

After a literature review, to analyze the state of the art around the world, a first period of understanding was done, in which different tests were performed to find the best approach for this kind of mixtures.

Then, the research developed with the support of some cold mix asphalt producers, that provide different materials to test; at the end seven different CMA were analyzed.

A detailed analysis of the compaction performances was performed during two months in North Carolina State University, with the aim of developing an analytical model that could predict the behavior of the analyzed CMA.

1.1. BACKGROUND

1.1.1. POTHOLES

Pothole repairs is a major maintenance item in the budget of many administration, and for these, the annual appearance of potholes is a major public relations concern.

In spite of considerable progress made in pavement materials and pavement mechanics, pothole repair remains an area in which little progress has been made. Clearly, there is a need for long-lasting, cost-effective materials and construction technologies for repairing potholes (Marasteanu, 2018).

Potholes are defined as bowl-shaped holes of various sizes in the pavement surface, which minimum plan dimension is 150 mm. They can be divided into different severity levels, from low to moderate, in relation to their number and depth.(Miller & Bellinger, 2003)

Potholes occur on asphalt-surfaced pavements subjected to a broad spectrum of traffic levels, from two-lane rural routes to multi-lane interstate highways (Wilson P & Romine R, 2001).

1.1.2. PATCHING

Patching is the procedure used to fill and repair potholes; it can be described as a portion of pavement surface, greater than 0.1 m^2, that has been removed and replaced or as additional material applied to the pavement after original construction. As for potholes, patching can be divided into different severity levels (Miller & Bellinger, 2003).

Pothole patching is generally performed either as an emergency repair in the winter or during other adverse conditions to address an immediate safety, or as routine maintenance scheduled for warmer and drier periods (Wilson P & Romine R, 2001).

1.1.3. IMPACT ON SOCIETY

In 1999, it was estimated that more than $1 billion was spent annually in the United States on pothole and spall repair and costs have increased since then. With such a large expenditure of tax dollars, it is important to ensure that the funds are spent in a cost-effective manner and that the investments in patching result in improved pavement performance and longer service lives (McDaniel, Olek, Behnood, Magee, & Pollock, 2014).

Potholes are a scourge of rich and poor countries alike. The American Automobile Association calculated that 16 million drivers in the United States suffered pothole damage to their vehicles in the past five years. The bill to fix it was about $3 billion a year. In India, meanwhile, the cost of potholes is often paid in a harsher currency than dollars. There, more than 3,000 people a year are killed in accidents involving them.

Also cash-strapped governments often ignore the problem, letting roads deteriorate. In Britain, for example, some $17 billion would be needed to make all roads pothole-free (The Economist Group Limited, 2016).

A group of researchers form the American Auburn University and from the Italian Centro Nazionale di Tecnologie dell'Asfalto have analyzed and synthetized more than 20 studies related to patching problems.

They have concluded that the regularity and the degree of deterioration of the roads, due to the presence of potholes or some defects on the surface course, are the two main factors that influence the rolling motion of the tires and so the fuel consumption.

It has been calculated that a modest improvement of the road surfaces can lead to a saving of 91 billion liters of petrol and 34 billion liters of diesel; according to the oil price in 2011, this means a total saving of about 12.5 billion dollars each year (SITEB - buonasfalto.it, 2018).

1.2. PROBLEM STATEMENT

Although the increasing numbers of crashes, injuries and deaths caused by potholes, and the immense economic loss due to damages, nowadays the repair of potholes is usually performed with materials that are only good on a short–term base. For this reason, it is required an improvement in the methods and techniques and especially to give road agencies some kind of help to deal with these problems (ERA-NET ROAD, 2012).

As a consequence of all the mentioned problems, maintenance management programs are increasing in importance and complexity, but administrations must deal with rising costs, decreasing numbers of employees, and decreasing budgets.

It is increasingly important to efficiently manage an activity as pervasive and expensive as pavement patching (McDaniel et al., 2014).

1.3. OBJECTIVE OF THE STUDY

The objective of this research project is to analyze and evaluate the performances of different cold mix asphalts available in Italy, used for patching applications.

After a first literature review, presented in chapter 2: _Literature review_, the study was developed in four main parts:

- Characterization of the materials, to understand their basic properties, described in chapter 3: _Testing: basic properties, composition and compaction characteristics_;

- Testing of cold mix asphalts, trying to understand which laboratory test can be performed and which are useless. These tests can be divided into low compaction analysis (chapter 4: _Testing: low compaction strength_) and high compaction analysis (chapter 5: _Testing: high compaction strength_).

- Development of analytical models for the evaluation of compaction properties of cold bituminous mixtures, proposed in chapter 6. _Modelling_

- Development of a test protocol for cold mix asphalts analysis, in order to create a standard procedure to characterize them and to understand their field of application.

2. LITERATURE REVIEW

2.1. INTRODUCTION

Although the behavior of Hot Mix Asphalt (HMA) is somewhat well understood and there is extensive knowledge about its performance, the inability to produce and store HMA in small quantities to be used as required make them unsuitable for pothole and other localized repairs. To fill this need, Cold Mix Asphalt (CMA) is normally used, as its characteristics allow users to have immediate availability in stock, and use it when and where needed (Diaz, 2016).

While different kind of tests were developed to characterize CMA, most of them don't analyze the performance of these mixes. Often the characterization includes the workability, the particle size gradation, the binder content and other aggregates tests.

In particular, there is a need of standard procedures for cold mix asphalts both in the design and in the test phase; to make easier for the producers and administration the choice of the right mix.

In this study it was analyzed the existing literature regarding cold mix asphalts and their composition and properties. It was found that, in particular in Italy, there is not a defined procedure to characterize them; moreover, no standards are present regarding the quality and performance of patching materials.

Some regulations were found in the USA, but they are different from state to state.

2.2. CAUSES AND RELATIVE PROBLEMS

Failure in pavements can be the result of repeated loading, shearing, or deflection of materials due to the action of traffic, poor underlying support, adverse weather conditions (freeze-thaw action), or combinations of these factors. (Maher, Gucunski, Yanko, & Petsi, 2001).

The creation of a pothole usually follows a general pattern wherein water finds a way into the base of the pavement (usually through a crack); traffic loading can cause the base or subgrade to soften and finally to wash away (pumping). As the fines continue to be pumped out, the pavement surface loses support and the asphalt will begin to break up. If the pothole remains unrepaired, the distressed area can increase in size, making repairs more difficult and costly.

Although less common, potholes are also caused by fatigue and/or low-temperature cracking. As potholes usually occur on roads with high traffic volume, the need for a speedy repair is essential (Chatterjee, White, Smit, & River, 2006).

Although the presence of water is the primary cause, potholes can also result from non-structural causes such as chemical spillages; mechanical damage to surfacing from vehicle rims and/or accidents and fires; damage caused by falling rocks in cuttings; animal hooves on road surfaces in hot weather; and poor road design over certain subgrades (Paige-Green, Maharaj, & Komba, 2010).

Another reason for the growing quantity of potholes in the roads is linked to the increasing traffic, both in the number of vehicle, the load and speed. In this way the roads are subjected to higher stresses, bigger than the ones for which they were designed.

In general, potholes derive from low quality of the building material combined with a low monitoring made by the administrations. In particular, it should be necessary an adequate planning of the precautionary maintenance, to avoid that little failures became big potholes.

2. Literature review

From the administrative point of view, in Italy the public biddings are often based exclusively on the price, only sometimes they compare the quality and performances of the materials.

In this way the repairs will have a short duration, due to the low quality of the chosen cheap mixtures; this leads to a more frequent need of maintenance, with a loss of money, and to a decrease in safety of the roads (SITEB - buonasfalto.it, 2018).

2.3. MATERIALS

Usually there are three types of cold mixes available (Wilson P & Romine R, 2001).

The first of these is cold mix produced by a local asphalt plant, using the available aggregate and binder.

The second type is cold mix produced according to specifications set by the agency that will use the mix. The specifications normally include the acceptable types of aggregate and asphalt, as well as acceptance criteria for the agency to purchase the material.

The third type is proprietary cold mix, these are produced by companies that test the local aggregate, design the mixes, and monitor production to ensure the quality of the product.

AGGREGATES

Due to the lack of standards regarding cold mix asphalt and the fact that the environment in which they are used is the same of HMA, the type of aggregate should be the same for both the products.

The critical properties for the aggregates are particle size distribution, maximum size, angularity and shape, surface texture and compatibility with the binder.

Usually proprietary cold mix asphalts are sold referring to their dimensional class, expressed as the ratio between the sieve corresponding to 100% of retained and the one with 100% of passing.

The particle size distribution affects the densification level of the mix, the workability and the mechanical characteristics.

Regarding the grading, different researches were made; from a research of the NCHRP (National Cooperative Highway Research Program), they discovered that a single-size aggregate mixture has a good workability and cures fast after the compaction thanks to the great amount of voids that allows a quick escape of volatiles. In this case the resistance of the patch is obtained with the aggregate interlock (NCHRP, 1979).

2. Literature review

In 1981 it was found that an ideal bituminous patching mixture should have aggregates smaller than 9.5mm and less than 2% fines; this has the following advantages (Kandhal & Mellott, 1981):

- The mix is pliable and workable;
- Due to the increased surface area, more bituminous binder can be incorporated into the mix to improve the durability;
- The mix remains pliable for a prolonged period of time and continues to densify easily under traffic and will continue to adapt to the changing geometry of the pothole.

This lead to the following suggested particle size distribution:

Sieve [mm]	Percent passing	
	specific	preferred
9.5	100	100
4.75	40-100	85-100
2.36	15-40	10-40
1.18	-	0-10
0.075	0-2	0-2

Table 2.1: Suggested particle size distribution - Kandhal & Mellott, 1981

The maximum size of the aggregate is an important parameter, because it affects both the workability and the final stability of the patch. Large maximum size aggregates are preferred when good stability is desired.

Different size of patching mixtures should be available, a large size aggregates for lower lift of deep hole and a small size for the upper lift or small holes.

The shape of the aggregates affects the skeleton of the mixture and its properties; usually grains should have a cubical or spheroidal shape, without a predominant dimension. It should be avoided the presence of flat or elongated particles, that will reduce the mechanical resistance.

Surface texture influences bitumen and cement adhesion; it is typically classified as either rough or smooth and will influence the tenacity with which the bitumen adheres to the coarse aggregate. Aggregates with rough surface texture bond more firmly with bitumen than relatively smooth rounded material (Buertey, Atsrim, & Offei, 2016).

The *Figure 2.1* (British Standard Institute, 1995) below shows the various expected shapes of a crush rock from any quarry, these range from angular in (a), rounded in (b), flaky in (c), elongated in (d) and flaky and elongated in (e).
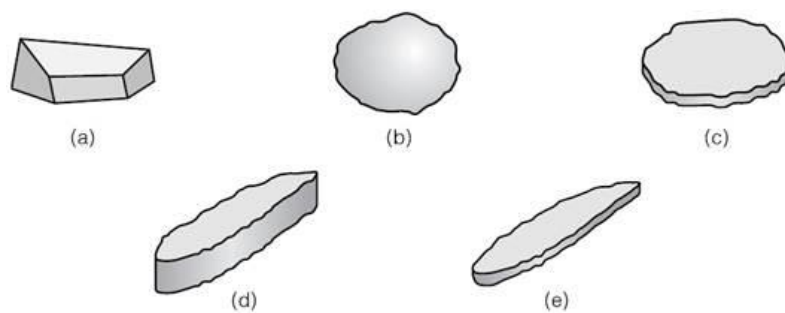
Figure 2.1: Expected shapes of a crush rock - British Standard Institute, 1995

Other required characteristics are(Santagata et al., 2016):

- Resistance to fragmentation, abrasion and impact;
- Resistance to smoothness;
- Durability;
- Resistance to wear.

Another important test should be performed to ensure compatibility of aggregate ad binder when producing a cold mix pothole patching material.

Bitumen

Available types of binder in CMA are (ERA-NET ROAD, 2012):

- cutback bitumen;
- bitumen emulsion;
- proprietary products.

A cutback asphalt is simply a combination of asphalt cement and petroleum solvent, typically kerosene. They are used because they reduce asphalt viscosity for lower temperature uses. After the application, the petroleum solvent evaporates leaving behind asphalt cement residue on the surface to which it was applied.

Cutback bitumen are divided in three categories, depending on the viscosity grade (Bahonar Brokerage (IME CO), 1999):

- Rapid-Curing (RC): the cutback bitumen is solved in gasoline; the evaporation is quick;
- Medium-Curing (MC): the cutbacks are prepared dissolving bitumen in kerosene, which evaporates slower than gasoline;
- Slow-Curing (SC): cutback may be achieved from solving bitumen in gasoil or fuel oil or directly from distillation of crude oil.

Cutback bitumens are most commonly used as the binder for cold-mix asphalt patches, they are combined with well-graded blends of aggregates to produce dense asphalt mixtures. The cutbacks used can be classified by type as either medium curing or slow curing.

Emulsion are classified by their surficial particle charge, the residual binder content, presence of fluxes and polymers and the breaking speed. These parameters are synthesized in an alphanumeric code, according to the UNI EN 13308 (Santagata et al., 2016).

Bitumen emulsions are also widely used in the repair of asphalt pavements. A limitation of emulsions is the relatively short time they take to break and cure; therefore, only slow-setting emulsions should be used for cold mixtures.

2. Literature review

Proprietary products are usually covered by patent, so their composition is unknown; often they are made with cutback bitumen or emulsion in different quantities.

From a research of the Virginia Department of Transportation (VDOT), it has been discovered that these types of mixtures usually have an excessive binder content; this can lead to early failure of the patches.

The ideal residual binder content should respect these limits in the following tests (Prowell & Franklin, 1995):

- Coating test: > 90% coated
- Stripping test: > 90% coated
- Boil test: > 85% coated
- Draindown test: < 8%
- Workability test: < 3.0 at 4°C

The coating test is required to ensure that a sufficient residual binder content is present to coat completely the aggregates; it is designated as AASHTO TP40-94.

The stripping test is designated as AASHTO TP41-94 and consist in placing a 100 grams sample in one liter of distilled water at 60°C for 16 to 18 hours.

The boil test is another type of stripping test, developed by the VDOT in 1993 and designed as VTM13; it is made by boiling in water for 10 minutes a sample of 200 grams.

The draindown is calculated as the percentage of the sample's initial binder content after 24 hours at 60°C; the standard procedure is described in the AASHTO TP42-94.

The workability is evaluated pressing a soil penetrometer against a sample in a cubical box; this test was developed by the Pennsylvania Transportation Institute and it is designed as AASHTO TP43-94.

ADDITIVES

Manufacturers of proprietary products generally use a cutback or an emulsion and then add some type of antistripping agent, polymer, or fiber. These materials are added to improve the strength, bonding, and durability of the repair material.

In most cases, anti-stripping additives are required, because, if the correct type and quality is chosen, they can reduce moisture damage. Moreover, they should retain their coating in the stockpile and during storage under adverse weather conditions, during the handling and in the pothole after placing (Kandhal & Mellott, 1981).

Other type of additives used are short fibers, that can increase the cohesion of the mixtures; the problem is that they usually decrease the workability.
Nowadays there is a trend to make products that are green and eco-sustainable, for this reason some new kind of fibers are used, that comes from part-worn tires.

MIXTURE

The bituminous mixtures are multi-phase systems composed by (Santagata et al., 2016):

- Solid phase: aggregates that are the lytic skeleton;

- Binder phase: bitumen and filler give cohesion to the system;

- Gaseous phase: the porosity contains air that allows the thermic expansion of binder.
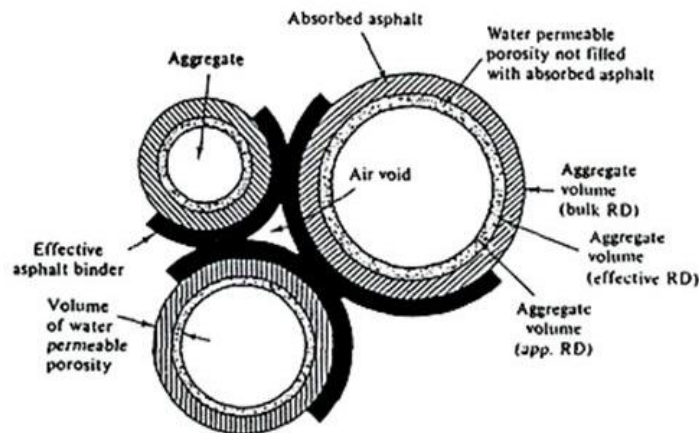
Figure 2.2: Asphalt mixture showing net or effective asphalt,

absorbed asphalt and air voids - Santagata et al., 2016

In the *Figure 2.2* the solid core is covered by two rings that describe the surface porosity of the particles, so the volume occupied by the surfaces' voids. The external ring includes the overall volume occupied by the particles and represents the part of surface's porosity filled with bitumen (absorbed asphalt).

The internal ring is the zone that is not reached by the bitumen; the black ring is the bitumen film that surrounds the particles and has a binder role (effective asphalt binder).

It is fundamental to analyze the bonding properties between aggregates and the covering binder film; the presence of water can determine a loss of adhesion between the two components, due to a chemical-mechanical action.

This phenomenon is called moisture damage and consist in the breakage and asportation of the binder film from the aggregate surface. In this way, the cohesion of the mix is compromised and the performances are reduced.

2. Literature review

It is desirable for patching materials to be both workable (ease with which mixture can be placed in field) and stable (ability to stay in place under load) in all seasons. To increase workability, an adequate amount of soft binder can be used. If the binder is too soft, however, the mixture can face instability problems in summer. Certain aggregates, such as sands and uncrushed gravels, can improve mixture workability but can also lead to pushing and shoving under traffic (Estakhri, Jimenez, & Button, 1999).

One main problem in the design phase is that, until now, there is not a strict correlation between laboratory parameters and field performances; in this way, tests' results would not be used at all.

Some research has been done in this field, but there is the need to improve the analysis of the performances of cold mixes.

2.4. STANDARDS

Although cold mix asphalts are widely used all across the world, there is not a common standard regarding their production and use.

Some regulations were found for different states in the US and some other indications are present in South Africa and few European countries.

In Europe, within the Road Surface Treatments sector, only surface dressing and slurry surfacings are affected by CE Marking because they are now regulated by harmonized Product Standards (hENs). Other surface treatments are either covered by HAPAS (Highway Authorities Product Approval Scheme) or are proprietary.

Therefore many treatments are unaffected by CE marking in a technical sense although, if some authorities decided to only purchase CE marked products, this would then become a commercial issue for these providers (Robinson, 2014).

Almost no requirements for material properties were found in the European standards. There are some test methods listed in a few standards or technical specifications but no values are given as the requirements; sometimes there are only some broad limits for particle size distribution of aggregate grading (ERA-NET ROAD, 2012).

Below are listed some information gained from various countries, related to potholes definitions, repair materials and techniques.

AUSTRIA

Some technical specifications for cold asphalt mixtures are present, in which there are requirements for binder, aggregate and filler. Those specifications are quite general, no value for tested characteristics are given (Österreichisches Normungsinstitut (Austrian Standards Institute), 2011).

CZECH REPUBLIC

A catalogue of distress of flexible pavements contain both a general description of different distresses and some technical requirements for pothole repair procedures and materials. They suggest using hot asphalt in suitable weather conditions, while cold mixes for winter conditions (Czech Ministry of Transport, 2010).

DENMARK

A reminder describes the procedure for selection of test trial and products; the trial was divided into 25 test fields. The reference material was defined as the one that the Danish Road Directorate normally uses for repairing of potholes.

The report describes the establishment of weather and traffic monitoring station and the results of the first measurements and inspections (Danish Road Directorate and Danish Road Institute, 2009).

GERMANY

The guidelines in this country suggest bonding the patch to the surrounding road by using a polymer-modified bitumen, a joint sealing band or a joint sealer. They require to patch the pothole only in dry weather conditions and to use the same thickness of the one of normal road constructions.

To improve the compactability of the cold mixes, they suggest using small grains and low viscosity binder (Forschungsgesellschaft für Straßen- und Verkehrswesen- Arbeitsgruppe Asphaltbauweisen, 2009).

NORWAY

They only have a standard definition for pothole, as anything wider than 100 mm for a road and 30 mm for a bike lane. In practice a risk assessment is applied before repair (ERA-NET ROAD, 2012).

SLOVAKIA

In this country is present a catalogue of repair techniques for distress basic type, in which there is a short description of repair procedures. Two main groups of repair techniques are identified according to durability and reliability; the repair methods are chosen depending on the type of pothole (Slovak Ministry of Transport, 2011).

SLOVENIA

The technical specification for public roads divides the patching procedures depending on the weather conditions. In harsh winter conditions no preparation of pothole is required and the throw and roll procedure can be used; in particular, with low temperature cold mix asphalt should be used, instead of hot mixes.

In more favorable conditions the pothole should be cleaned and a bond coat must be applied; in this way a more durable repair can be obtained.

For potholes deeper than 40 mm they require to apply the asphalt in more layers, each one compacted separately (Ministry of Transport - Agency Slovene Roads, 2005).

SWITZERLAND

Some guidelines provide instruction and catalogues for a visual conditioning survey and evaluation of road conditions

In particular in the city of Basel it is suggested that in cold winter temperatures potholes should be filled with cold asphalt mixtures as a temporarily solution, while a real maintenance program should be performed in most comfortable environmental situations (Bau- und Verkehrsdepartement des Kantons Basel-Stadt, 2010).

UNITED KINGDOM

In UK they perform both a first assessment, with laboratory testing and product trial, and a certification performed by the British Board of Agrement (British Board of Agrément, 2010).

The BAA certificate includes HAPAS requirements, technical specification, design data, installation procedures and technical investigations.

SOUTH AFRICA

In this country a guide describes a quality control system for potholes repair; a controlled quality-assurance program must be followed and implemented, each stage should be checked (CSIR Council for Scientific and Industrial Research, 2010).

USA

The Army Corps of Engineers describes a field evaluation of pothole repair materials, then different materials were subjected to laboratory and field evaluation.

They say that open-graded cold mixes have higher workability and that mixtures with denser or well-graded aggregates with harder binders tend to have a higher Marshall stability. However, the Marshall stability test is not a good indicator of performance because it is not an appropriate test for open graded mixtures (US Army Corps of Engineers, 2005).

The Virginia Department of Transportation gives a list of approved proprietary cold asphalt mixes for patching applications, after an evaluation process that consists in both laboratory and field tests.

The authors identified as the primary distresses in cold mix asphalt the bleeding, rutting and dishing, debonding, raveling, pushing and shoving (Virginia Department of Transportation, 2009).

OTHER RECOMMENDATIONS

The Federal Highway Administration prepares a field guide to suggest that the mix should be placed in thin lifts and thoroughly compacted, with the top lift compacted to leave the patch slightly above the level of the surrounding pavement. In this way, traffic will compact the patch and make it flush with the surrounding pavement (Bergstralh-Shaw-Newman, 1996).

A research made by NCHRP reports the need for technical developments in patching practices, highlighting the need to have rational ways to compare different patching materials. This document says that until now engineering judgment is still the primary consideration when selecting the type of maintenance activity (McDaniel et al., 2014).

2.5. PERFORMANCE REQUIREMENTS

From different researches, it results that the most important properties that a cold mix asphalt for patching application should have are (Abela Munyagi, 2006; Maher et al., 2001):

STABILITY

It is required to allow the patch to resist horizontal and vertical displacement due to traffic; it can be related to different characteristics of the mixture. It depends on the grading, it increases with a rough and angular surface texture and it is influenced by the same properties that contribute to the compactability of the mix.

STICKINESS

Property needed so the patch can adhere to the sides of the pothole and to the underlying pavement; it is influenced by the temperature of the mixture and the binder. Usually the adhesion of hot mixtures is great when they are still hot, whereas cold-mixtures do not have adequate stickiness.

DURABILITY

It can be expressed as the resistance to disintegration due to traffic and weathering forces; usually is not very high in the case of cold mix asphalt. It is influenced by the type, viscosity and quantity of binder.

RESISTANCE TO WATER ACTION

It is required to keep the binder from stripping off the aggregate in presence of water, it is affected by the binder and aggregate types.
A low water resistance can be caused by a poor compaction or a not adequate water drainage of the pavement. To improve this property, anti-stripping additives are often used.

SKID RESISTANCE

This characteristic should be similar to the one of the pavement in which the patch is placed, in particular for long and large patches.

A low value can be caused by aggregates that are easily polished and an excessive binder content.

FREEZE-THAW RESISTANCE

This property is intended as the ability of the mixtures to resist the weakening effect of cyclic thermal expansion and contraction due to freeze and thaw cycles. It is one of the factors that contributes to premature failure in cold areas.

WORKABILITY

It is necessary during handling operations to enable the material to be easily shoveled, spread and shaped. It is heavily influenced by temperature, that controls the hardness of the bituminous binder. To improve this property, low viscosity binders should be used.

STORAGEABILITY

The mixtures should remain workable when stockpiled for a long period, without hardening excessively or having the binder drain off the aggregates. It is influenced both by the quality of materials and by the packaging type; this because exposition to air reduce the stocking performance.

2.5.1. PERFORMANCE RATING

Some of this properties were analyzed and combined together during a study for the Virginia DOT, in which Prowell and Franklin developed a performance rating system that uses a measurement of the workability, a parameter related to the survivability of the patches and some visual evaluations regarding raveling, edge disintegration, bleeding, dishing, pushing and shoving (Prowell & Franklin, 1995).

The equation is the following:

$$Perf.\ rate = Sur \cdot \frac{[0{,}171\ W + 0{,}177\ R + 0{,}156\ E + 0{,}144\ B + 0{,}180\ D + 0{,}204\ PS]}{4{,}0} \cdot 100 \qquad (1.1)$$

Where:

- W: workability evaluation rating;
- R: raveling evaluation rating;
- E: edge disintegration evaluation rating;
- B: bleeding evaluation rating;
- D: dishing evaluation rating;
- PS: pushing and shoving evaluation rating;
- Sur: survivability, which equation is:

$$Sur = \frac{suviving\ number\ of\ patches\ of\ the\ material}{originalnumber\ of\ patches\ of\ the\ material} \qquad (1.2)$$

Workability is the workers' evaluation of how difficult they felt the products were to place and compact.

Raveling is the loss of aggregate from the surface of the patch, evaluated as the size of particles that were being lost.

Edge disintegration was measured as the percentage of cracking at the edge of the patch for each quadrant.

Bleeding is considered as the flushing of the asphalt binder to the surface of the patch; the rating is the percentage of the surface that was flushed, based on visual observation.

Dishing is the further compaction of the patch under traffic loads, derived from material instability and inadequate compaction during the placement; the ratings were determined from the depth measurements.

Pushing and shoving is the vertical or horizontal movement of the patch material in the pothole.

Some types of inadequate performance and their probable causes were found in the literature and are listed in the _Table 2.2_ (Anderson, Thomas, Siddiqui, & Krivohlavek, 1988):

Problem or Symptom of Failure	Probable Causes—Failure Mechanisms
In Stockpile	
Hard to work	Binder too stiff; too many fines in aggregate, dirty aggregate; mix too coarse or too fine
Binder drains to bottom of pile	Binder too soft; stockpiled or mixed at high temperature
Loss of coating in stockpile	Stripping; inadequate coating during mixing; cold or wet aggregate
Lumps—premature hardening	Binder cures prematurely
Mix too stiff in cold weather	Binder too stiff for climate; temperature susceptibility of binder too great; too many fines in aggregate, dirty aggregate; mix too coarse or fine
During Placement	
Too hard to shovel	Binder too stiff; too many fines, dirty aggregate; mix too coarse or too fine
Softens excessively upon heating (when used with hot box)	Binder too soft
Hard to compact (appears "tender" during compaction)	Insufficient mix stability; too much binder; insufficient voids in mineral aggregate; poor aggregate interlock; binder too soft
Hard to compact (appears stiff during compaction)	Binder too stiff; excess fines; improper gradation; harshmix—aggregate surface texture and shape
In Service	
Pushing, shoving	Poor compaction; binder too soft; too much binder; tack material contaminates mix; binder highly temperature susceptible, causes mix to soften in hot weather; inservice curing rate too slow; moisture damage-stripping; poor aggregate interlock; insufficient voids in mineral aggregate
Dishing	Poor compaction; mixture compacts under traffic
Raveling	Poor compaction; binder too soft; poor cohesion in mix; poor aggregate interlock; moisture damage—stripping; absorption of binder by aggregate; excessive fines, dirty aggregate; aggregate gradation too fine or too coarse
Freeze-thaw deterioration	Mix too permeable; poor cohesion in mix; moisture damage-stripping
Poor skid resistance	Excessive binder; aggregate not skid resistant; gradation too dense
Shrinkage or lack of adhesion to sides of hole	Poor adhesion; no tack used, or mix not self-tacking; poor hole preparation
Note: In some instances items appear as both symptoms and causes. It is difficult to separate the symptoms from the causes in some cases.	

Table 2.2: Problems and Failure Mechanisms in Cold-Mix Patching Materials - Anderson, Thomas, Siddiqui, & Krivohlavek, 1988

2.6. TECHNIQUES AND REPAIR METHODS

There are four different pothole repair methods that have been used by many maintenance agencies. These methods are well described by the Manual of Practice made by the Federal Highway Administration and are defined as: throw-and-roll, edge seal, semi-permanent and spray injection (Wilson P & Romine R, 2001).

THROW AND ROLL

This is one of the oldest method for pothole repair, it consists in filling the pothole with loose material and compacting it with truck tires. After the maintenance crew leaves the site, the road is immediately open to traffic.

This method is fast, easy and doesn't require expensive equipment, for these reasons it is widely used.

It is an evolution of the traditional *throw and go* method, in which no compaction is performed. The extra time required to compact the patches does not affect the productivity, but it will increase the quality of the repair and extend its life.

An important practice that should be respected to improve the patches life and performances is to leave a crown of asphalt above the surface to allows a further compaction made by traffic (Nazzal, Kim, & Abbas, 2014).

Figure 2.3: Throw-and-roll procedure, material placing - Wilson P & Romine R, 2001

Figure 2.4: Throw-and-roll procedure, patch compaction - Wilson P & Romine R, 2001

EDGE SEAL

This method is an improvement of the throw and roll, in this case the compacted patch is left to dry for one day and then a ribbon of asphaltic tack material is placed on the patch's perimeter. A thin layer of sand is placed over the tack material to prevent tracking by vehicle tires.

A disadvantage of this method is that the maintenance crew must return two times at the same site, to allow the drying of the patching material; as a benefit this procedure limits the amount of water that penetrates through the edges of the patches and can glue together pieces of the surrounding pavement, improving the support.
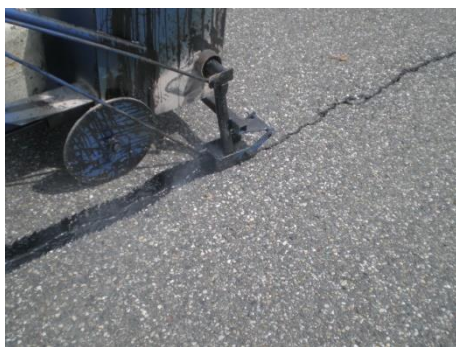
Figure 2.5: Edge sealing procedure,
Huizenga Enterprises

Figure 2.6: Edge sealing procedure,
AsphaltPro

SEMI-PERMANENT REPAIR

This method is one of the best for repairing potholes, it can be considered as a partial-depth repair, but it requires more time than the others procedure and more expensive machinery.

It consists in the removal of all the debris and water from the pothole, then the sides of the patch are squared up with a jackhammer or a pavement saw. After this preparation the mixtures can be placed and compacted using a single drum vibratory roller or a vibratory plate; the compacting device should be smaller than the single patch area.

Although this method as a very low productivity rate compared to the others, it results in the longest life of the repair, thanks to the greater compaction and since it improves the surrounding support of the patches (Nazzal et al., 2014).

Figure 2.7: Semi-permanent procedure, edge cutting - Wilson P & Romine R, 2001

Figure 2.8: Semi-permanent procedure, compaction - Wilson P & Romine R, 2001

SPRAY INJECTION PATCHING

This procedure requires the higher equipment costs but it has a high productivity and the lower material costs, compared to the other techniques.

It consists in removing water and debris from the pothole, spraying a tack coat of binder on the sides and bottom of the pothole, blowing asphalt and aggregate into the pothole and covering the patched area with a layer of aggregate. This method does not require any compaction after the covering.

The mix of aggregate and emulsion can be varied depending on the size and location of the pothole, so this method is quite flexible. However, a wrong mix design can adversely affect the longevity of the patches.

Compared to other methods, spray injection is more versatile since it can be used also to repair cracks and ruts; moreover it can be used in different weather conditions (Nazzal et al., 2014).

Figure 2.9: Spray-injection device, truck and trailer unit - Wilson P & Romine R, 2001

Figure 2.10: Spray-injection device, truck mounted unit - Michal Maňas

2.7. EFFECT OF WEATHER

Pothole patching can be performed during various weather conditions; it is generally used either as an emergency repair under harsh conditions or as routine maintenance.
Pothole repairs conducted during the cold, wet winter and spring months have in general a short life. The climatic conditions have an even stronger effect on cold-mix patching materials, they usually can withstand only a few cycles of freeze-thaw and they do not provide a permanent solution for winter patching (Maher et al., 2001).

Winter patching operations generally take place during period of snow melt, when maintenance crews do not perform the winter service. Because winter patching occurs when more winter conditions are expected, the patching materials are subjected to more stress, owing to repeated cycling between very cold and warm conditions. The aggregates should be high quality, crushed with few fines; binder should be emulsified with at least anti-stripping additive. The mixture must be workable at low temperatures.

2. Literature review

Spring patching differs from winter operation in that climatic conditions do not stress the patches to the same degree because freeze-thaw cycles should have finished, so most of the conditions that soften the underlying support have already passed. Any material acceptable for winter patching is generally acceptable for spring patching; but the differences in workability over wide temperature ranges should be considered. Materials that are workable at very low temperatures tend to be very sticky and hard to use at higher temperatures (ERA-NET ROAD, 2012).

2.8. PATCHING COSTS

A patching operation is affected by three main costs of material, labor and equipment; there can also be some user-delay costs associated with pothole patching operations, as well as associated to lane-closure time (Wilson P & Romine R, 2001).

MATERIALS

The cost most commonly associated with pothole patching is the one of materials, but usually this is one of the least significant contributors to the overall cost.

The material used for patching influences the cost of the overall operation due to differences in mixtures' performance. More expensive materials that are placed with less effort and last longer can reduce the cost of the initial patching effort, as well as the amount of repatching needed.

LABOR

For the throw-and-roll technique, the labor consists of the two workers who do the actual patching, plus traffic control.

One of the two workers shovels the material from the truck into the pothole, and the other drives the truck over the section to compact the patch.

The edge seal procedure requires the same two workers and traffic control as the throw-and-roll procedure, but requires an extra pass to place the tack and sand materials.

The semi-permanent patching operation has proven to be the most efficient when four workers are used, along with the appropriate traffic control.

This procedure can be accomplished using more or fewer workers, but the experience of many agencies has found four workers to be optimum.

The single-unit spray-injection device requires a single operator. Two operators are recommended when using the trailer-unit equipment (one to operate the vehicle and one to place the material). In both cases, traffic control is required.

EQUIPMENT

For the throw-and-roll, edge seal, and semi-permanent methods, shovels, rakes, or other hand tools are needed for placing the material.

For the throw-and-roll and edge seal methods, the only major equipment costs are for the truck carrying the material and the traffic control vehicles and signs.

For the semi-permanent repair method, the necessary equipment varies from agency to agency. In general, it includes a material and equipment truck, an edge-straightening device and a compaction one, a traffic control vehicle and signs.

The only equipment needed for spray injection is the spray-injection device and the traffic control trucks and signs.

COST-EFFECTIVENESS EVALUATION

The Manual of Practice presents a worksheet for the calculation of the cost-effectiveness of the overall patching operation. This evaluation should be performed by the administrations either for current operations or for a proposed patching operation, using different materials or procedures, in order to choose the best one (Wilson P & Romine R, 2001).

3. TESTING: BASIC PROPERTIES, COMPOSITION AND COMPACTION CHARACTERISTICS

3.1. INTRODUCTION

This chapter describes the starting analysis of seven commercial Cold Mix Asphalt used for patching problems in Italy. All the basic properties of the materials were obtained from laboratory tests, due to the lack of information from the respective suppliers.

The analysis consists of the check of the stocking quality, the determination of the composition, both the binder content and the particle size distribution, the theoretical maximum density and the density of extracted aggregates.

The final step of this phase is the study of the compaction characteristics, obtained with the Gyratory Shear Compactor (GSC). The results were averaged from three samples for each material, compacted until 180 rounds.

3.2. MATERIALS

This study analyses seven proprietary cold mix products; they are produced by private companies that test the local aggregates, design the mixes and monitor production to ensure the quality of the product. When using proprietary materials that are already mixed, some acceptance testing must be done before purchasing the material (Wilson P & Romine R, 2001).

All the products are available in the Italian market, four of them are sealed in bags, two in buckets and one is a loose material.

The products tested, their commercial name and the manufacturers are shown in the *Table 3.1*Table 3.1: Materials; henceforth, the materials will be referred with code from M1 to M7.

Code	Commercial name	Producer
M1	Asfaltival Special	Valli Zabban (FI)
M2	Asfaltival 2.0 Revolution	Valli Zabban (FI)
M3	RoadPav	M.A.GE (RO)
M4	ProntoSint	Sintexcal (FE)
M5	Bitem	Bitem (MO)
M6	Bitux	Bitux (TO)
M7	BlackTop	Insta Service (BG)

Table 3.1: Materials

The products are described as follows:

Asfaltival Special: it is a bagged material produced with a mix of selected aggregates, the binder is composed with bitumen, vegetal oils, plasticizers and additives that increase the workability. It is available in two different size, 0/10mm and 0/5mm.

This mixture is produced by Valli Zabban, an Italian company originally founded in 1928; its headquarter is located in Florence but the bituminous mixtures are produced in a factory near Arezzo.

Figure 3.1: M1 - packaging

Asfaltival 2.0 Revolution: it is a bagged product made with a mix of sands and basalt, with a SBS modified bitumens as binder, that contains powder of SBR/NR from end-of-life tires. It is available only in one size, 0/8mm.

It is produced by Valli Zabban, the same company that make Asfaltival Special.

Figure 3.2: M2 - packaging

RoadPav: it is a cold mix asphalt that, due to a chemical process, hardens in contact with water; for this reason, it can be used also in presence of rain and snow. It is available in bucket and in three different sizes: 0/4mm, 0/8mm, 0/11mm.

This product is commercialized by M.A.GE., a company based in Rome.

Figure 3.3: M3 - packaging

ProntoSint: it is a bagged cold mix asphalt used for urgent intervention; the binder is composed of cationic emulsion with non-toxic vegetal additives.

The mix is produced by Sintexcal spa, a society born in 1986 in Ferrara that has different production site all across center and north Italy.

Figure 3.4: M4 - packaging

Bitem: it is a product available both in bags and as a loose material; it uses bitumen emulsion and vegetal solvents as binder. It is available in 0/8mm size.

This mixture takes the name from its producer, Bitem srl, a company specialized in bitumen and emulsion whose headquarter is in Modena.

Figure 3.5: M5 - packaging

Bitux: it is a loose material taken directly at the production site; for this study it was provided in open paper bags.

This CMA is produced by Bitux spa, an historical company in Piedmont, founded in 1950. Its activities concern both the design and the production of materials used in infrastructures construction.
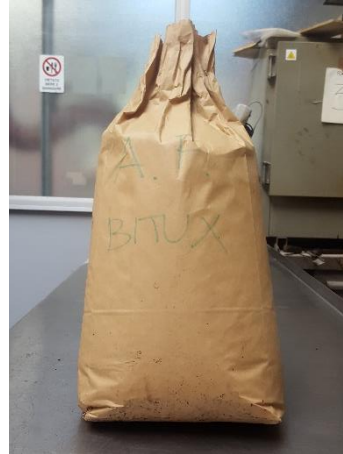
Figure 3.6: M6 - packaging

BlackTop: it is a cold mix asphalt sealed in buckets, made mainly with basalt aggregates; the binder is composed of a patented bitumen emulsion produced in England. It is available in three different sizes: 0/3mm, 0/5mm, 0/8mm; the one with the green top, used in this study, is the one with bigger aggregates.

BlackTop is commercialized in Italy by Insta Service Srl, a company based in Bergamo.

Figure 3.7: M7 - packaging

3.3. STOCKING QUALITY

This is the first step after the arrival of the materials and consists on a visual check of the stocking quality.

Storageability is fundamental to maintain the original properties of workability and durability; a storage life of at least six months is desired to ensure workability during installation.

In general, there are three packaging possibilities: loose material, bags and buckets.

LOOSE MATERIAL

In this case the cold mix asphalt is produced in bulk, stockpiled and then sold directly at the production site, without any kind of packaging. The storage time must be short, in order to avoid the hardening of the material in contact with air.

This kind of packaging is the one used for M6.

BAGS

The CMA is produced and then packaged into bags to make the material easier to handle in the field. The stocking time is longer, due to a protection from air contact; it goes from ten months to more than two years, depending on the kind of bags. In this study, two of four materials that use this kind of packaging arrived with some holes, as can be seen in *Figure 3.8*, probably due to low plastic quality used for bags and careless transportation. To assess the ability to store the bagged materials, a drop test was developed by the Texas DOT to drop the bags and determine if the bag split (Rosales-Herrera & Prozzi, 2007). Materials M1, M2, M4 and M5 use this kind of packaging.

Figure 3.8: Holed bag

BUCKETS

This kind of packaging is the most expensive but the one with the better quality; buckets have a higher resistance to puncture than bags, in this way the materials can maintain their properties for a longer time.

Buckets are also easier to handle than bags and they can be closed after a partial use, reducing the waste of unused material in case of small interventions.

For materials that contain additives that react with air moisture, the buckets can be sealed (*Figure 3.9*) and de-aerated with a vacuum system; in the case of M3 RoadPav, air is substituted with nitrogen.

This kind of packaging is used for M3 and M7.

Figure 3.9: Sealing membrane

3.4. COMPOSITION

3.4.1. BINDER CONTENT

The test used to determine the binder content is the ignition method, according to the (UNI EN 12697-39, 2004). This method consists in the separation of the bitumen and all the others volatile substances from the aggregates and is an alternative to the traditional method of extraction using solvents.

The remaining aggregates will be used in the determination of the aggregate gradation and specific gravity.

TEST METHOD

The Asphalt Binder Analyzer, also known as Carbolite (_Figure 3.10_), is a high precision apparatus combining an ignition oven with a continuous weighing system that monitors the loss of weight of the asphalt sample and automatically determines, at the end of the test, the binder content and percentage. An independently controlled auxiliary afterburner chamber significantly reduces the furnace emissions.

An highly efficient heating system with afterburner for total combustion of fumes to minimize emissions is installed in accordance with CE requirements.

Figure 3.10: Carbolite machine

TEST DESCRIPTION

The test procedure starts spreading more than 1200 grams of loose material in the sample basket keeping the material away from the edges; the basket is divided into two levels to guarantee a bigger ignition surface.

Once the basket is ready, it is inserted inside the chamber, that reaches a temperature of 540°C, to burn every flammable substance. The toxic fumes produced during the test are highly reduced by the afterburner, that has a temperature greater than 900°C

During the test, the machine monitors the temperature and the weight changes; the test ends when there are no more changes in weight.

Figure 3.11: Material before test   *Figure 3.12: Material after test*

With a comparison between the weight of the sample before and after the test it is possible to determine the binder content, both related to the mixture (3.1) and aggregates (3.2).

This evaluation must be done with the material at the same condition, to avoid error and changes on the weight due to the high temperature. To cool the sample, the basket should remain some hours outside the machine and inside a safety cover.

The equations used are:

$$\%B_{mixture} = \frac{\left(Net\ W_{ante} - Net\ W_{post}\right)}{Net\ W_{ante}} \tag{3.1}$$

$$\%B_{aggregates} = \frac{\left(Net\ W_{ante} - Net\ W_{post}\right)}{Net\ W_{post}} \tag{3.2}$$

Results

The binder content related to the mixture varies from 5.54% to 8.41%, while the one related to the aggregates varies from 5.86% to 9.18%; in this value all the volatile substances are included. The results are summarized in the _Table 3.2_.

	Material	$\%B_{mixture}$ [%]	$\%B_{aggregates}$ [%]
M1	Asfaltival Special	8.41	9.18
M2	Asfaltival 2.0 Revolution	5.98	6.36
M3	RoadPav	7.63	8.26
M4	ProntoSint	6.40	6.84
M5	Bitem	5.54	5.86
M6	Bitux	5.55	5.88
M7	BlackTop	5.89	6.26

Table 3.2: Binder content

3.4.2. PARTICLE SIZE DISTRIBUTION

The particle size distribution of the extracted aggregates is obtained using the clean material derived from the ignition test. The test was performed according to the (UNI EN 12697-2, 2003).

TEST METHOD

This test consist in the determination of the aggregates gradation by means of sieving and weighting; it is performed with a sieve shaker that is activated by electromagnetic impulses and has a triple vibrating action (vertical, lateral and rotational); the vibration continues for 15 minutes.

In this study ten UNI sieves were used, which openings, in mm, are: 12.5, 10.0, 8.0, 6.3, 4.0, 2.0, 1.0, 0.5, 0.25, 0.063.

Figure 3.13: Aggregates before test
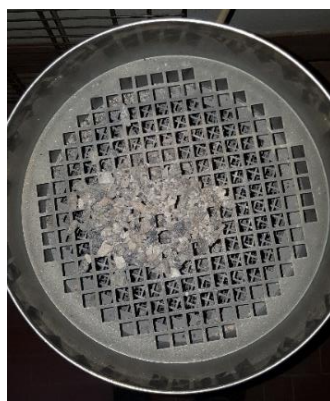
Figure 3.14: Test preparation

Figure 3.15: Shaker machine

TEST DESCRIPTION

The first operation required in this test is the washing of the aggregates, using a sieve with an opening of 0.063mm, to remove the filler. This is important in order to have better results after the sieve shaking, because the filler can remain attached to the aggregates' surface, overestimating the weight of the retained. The weight loss of this phase will be considered as a part of the total filler content.

Before starting the test, the material must be dried, this phase is performed in an oven at a constant temperature of $105 \pm 5°C$, according to the UNI EN 1097.

After the drying, the material must be cooled until environmental temperature.

Figure 3.16: M2 aggregates   *Figure 3.17: M6 aggregates*   *Figure 3.18: M7 aggregates*

After this, the aggregates are ready for the test and are located at the top of the sieves pile.

At the end of the test, each sieve is weighted to measure the retained for each opening; from this value is possible to obtain the progressive passing and build the particle size distribution curves.

The equations used are:

- Partial retained [%]:

$$r_i = 100 \cdot \frac{m_i}{m_{tot}} \tag{3.3}$$

- Progressive retained [%]:

$$R_i = \sum_{j=0}^{i} r_j \tag{3.4}$$

- Progressive passing [%]:

$$P_i = 100 - R_i \tag{3.5}$$

Results

The different curves for the seven materials are shown in the following figures, together with the related tables of retained and passing.

M1 Asfaltival Special				
Sieve [mm]	Retained [g]	Partial retained [%]	Progressive retained [%]	Progressive passing [%]
12.5	0.0	0.0	0.0	100.0
10.0	0.0	0.0	0.0	100.0
8.0	37.8	3.2	3.2	96.8
6.3	174.8	14.7	17.8	82.2
4.0	424.5	35.6	53.4	46.6
2.0	332.1	27.8	81.3	18.7
1.0	97.6	8.2	89.5	10.5
0.5	36.9	3.1	92.5	7.5
0.25	22.1	1.9	94.4	5.6
0.063	28.1	2.4	96.8	3.2
Filler	38.7	3.2	100.0	-
total	1193.0			

Table 3.3: M1 - Progressive passing
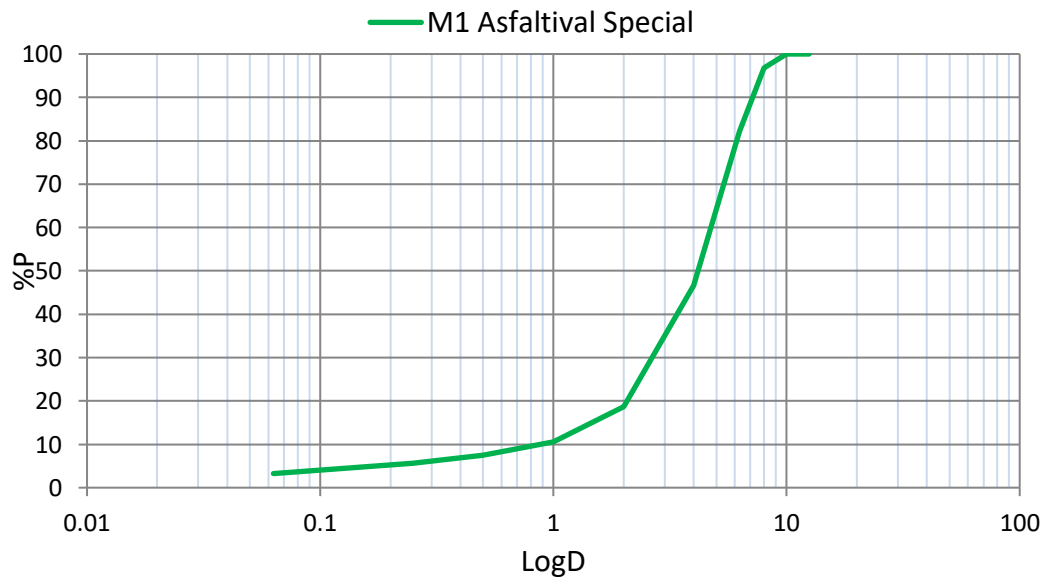
Graph 3.1: M1 - Particle size distribution

M2 Asfaltival 2.0 Revolution

Sieve [mm]	Retained [g]	Partial retained [%]	Progressive retained [%]	Progressive passing [%]
12.5	0.0	0.0	0.0	100.0
10.0	0.0	0.0	0.0	100.0
8.0	25.4	2.1	2.1	97.9
6.3	176.2	14.4	16.5	83.5
4.0	502.3	41.0	57.4	42.6
2.0	292.4	23.9	81.3	18.7
1.0	73.2	6.0	87.3	12.7
0.5	38.9	3.2	90.5	9.5
0.25	27.9	2.3	92.7	7.3
0.063	38.2	3.1	95.9	4.1
Filler	50.8	4.1	100.0	-
total	1225.3			

Table 3.4: M2 - Progressive passing
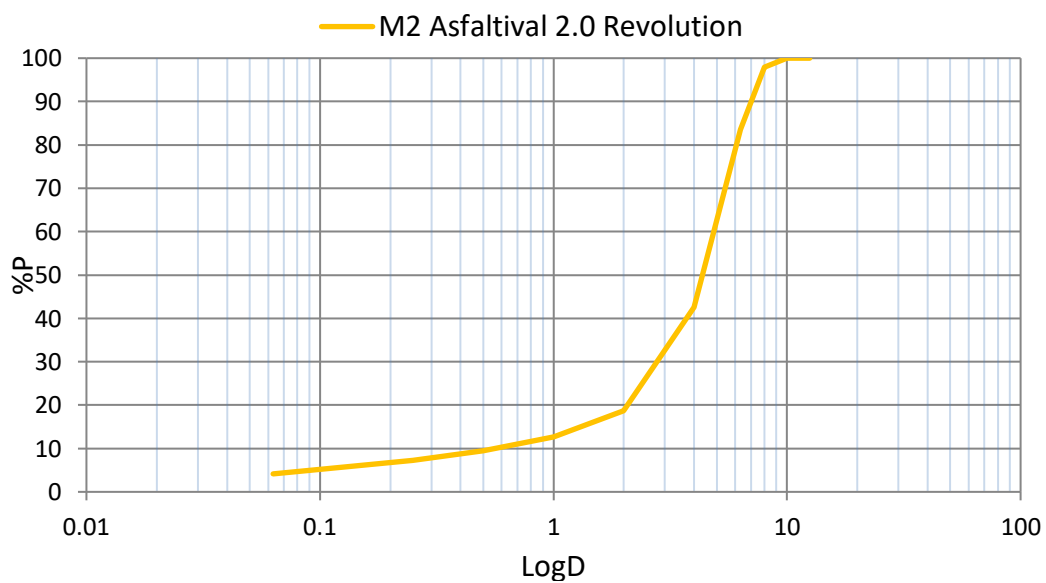
Graph 3.2: M2 - Particle size distribution

M3 RoadPav

Sieve [mm]	Retained [g]	Partial retained [%]	Progressive retained [%]	Progressive passing [%]
12.5	0.0	0.0	0.0	100.0
10.0	0.0	0.0	0.0	100.0
8.0	40.4	3.4	3.4	96.6
6.3	123.3	10.4	13.8	86.2
4.0	276.8	23.3	37.1	62.9
2.0	222.6	18.7	55.8	44.2
1.0	284.7	24.0	79.8	20.2
0.5	113.7	9.6	89.3	10.7
0.25	38.6	3.2	92.6	7.4
0.063	38.4	3.2	95.8	4.2
Filler	49.7	4.2	100.0	-
total	1188.2			

Table 3.5: M3 - Progressive passing
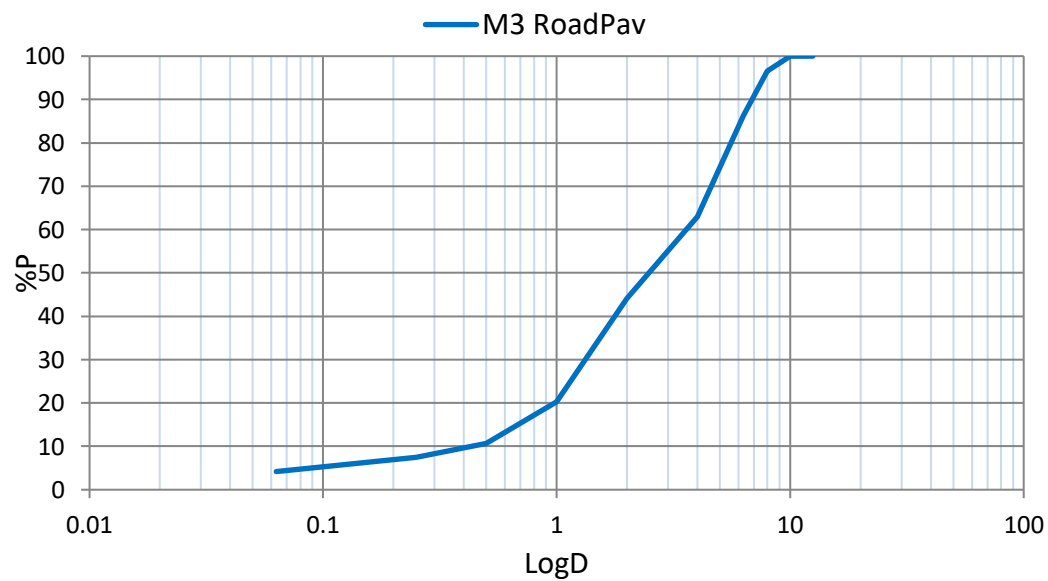
Graph 3.3: M3 - Particle size distribution

M4 ProntoSint

Sieve [mm]	Retained [g]	Partial retained [%]	Progressive retained [%]	Progressive passing [%]
12.5	0.0	0.0	0.0	100.0
10.0	0.0	0.0	0.0	100.0
8.0	0.0	0.0	0.0	100.0
6.3	9.4	0.8	0.8	99.2
4.0	379.5	32.3	33.1	66.9
2.0	695.7	59.1	92.2	7.8
1.0	45.1	3.8	96.0	4.0
0.5	7.0	0.6	96.6	3.4
0.25	3.0	0.3	96.9	3.1
0.063	5.0	0.4	97.3	2.7
Filler	32.0	2.7	100.0	-
total	1176.7			

Table 3.6: M4 - Progressive passing
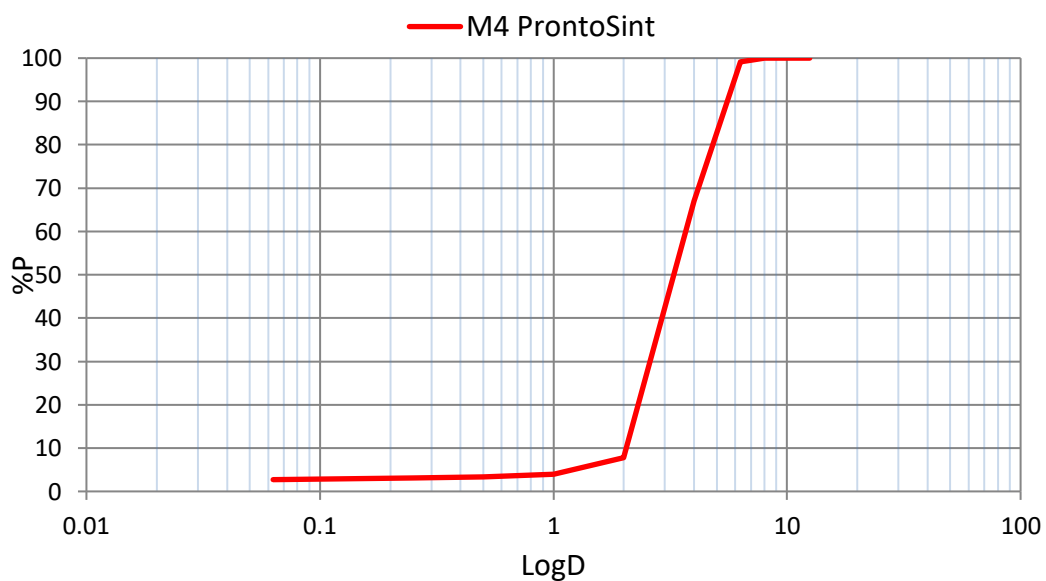
Graph 3.4: M4 - Particle size distribution

3.   Testing: basic properties

M5 Bitem

Sieve [mm]	Retained [g]	Partial retained [%]	Progressive retained [%]	Progressive passing [%]
12.5	0.0	0.0	0.0	100.0
10.0	0.0	0.0	0.0	100.0
8.0	0.0	0.0	0.0	100.0
6.3	19.3	1.7	1.7	98.3
4.0	428.6	36.8	38.5	61.5
2.0	594.4	51.1	89.6	10.4
1.0	75.4	6.5	96.0	4.0
0.5	7.6	0.7	96.7	3.3
0.25	3.0	0.3	96.9	3.1
0.063	3.9	0.3	97.3	2.7
Filler	31.6	2.7	100.0	-
total	1163.8			

Table 3.7: M5 - Progressive passing
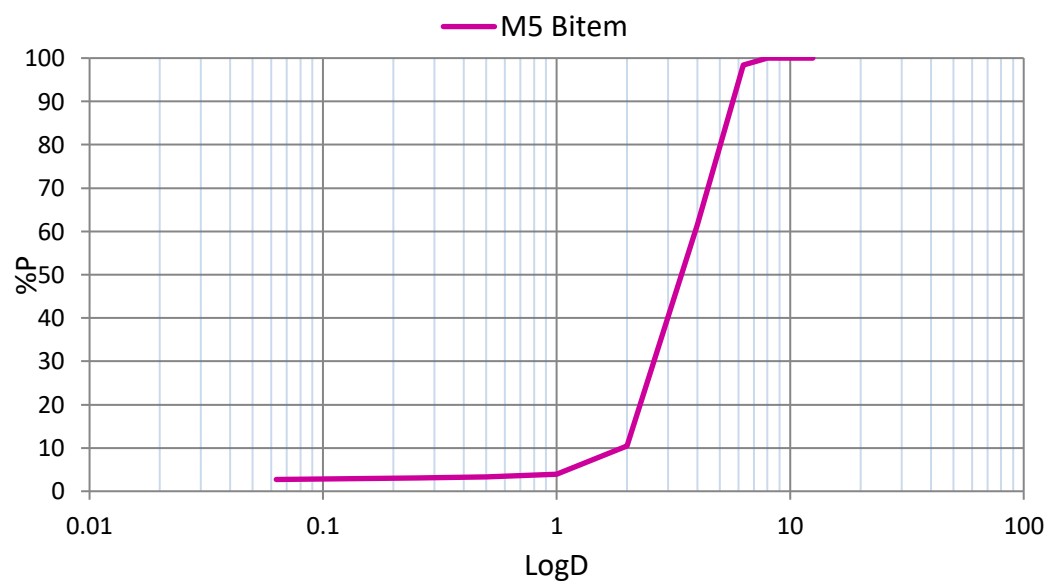
Graph 3.5: M5 - Particle size distribution

46

Sieve [mm]	Retained [g]	Partial retained [%]	Progressive retained [%]	Progressive passing [%]
		M6 Bitux		
12.5	0.0	0.0	0.0	100.0
10.0	2.7	0.2	0.2	99.8
8.0	27.7	2.3	2.6	97.4
6.3	207.6	17.6	20.1	79.9
4.0	500.3	42.3	62.5	37.5
2.0	176.9	15.0	77.4	22.6
1.0	60.1	5.1	82.5	17.5
0.5	50.7	4.3	86.8	13.2
0.25	50.4	4.3	91.1	8.9
0.063	58.9	5.0	96.0	4.0
Filler	46.8	4.0	100.0	-
total	1182.1			

Table 3.8: M6 - Progressive passing
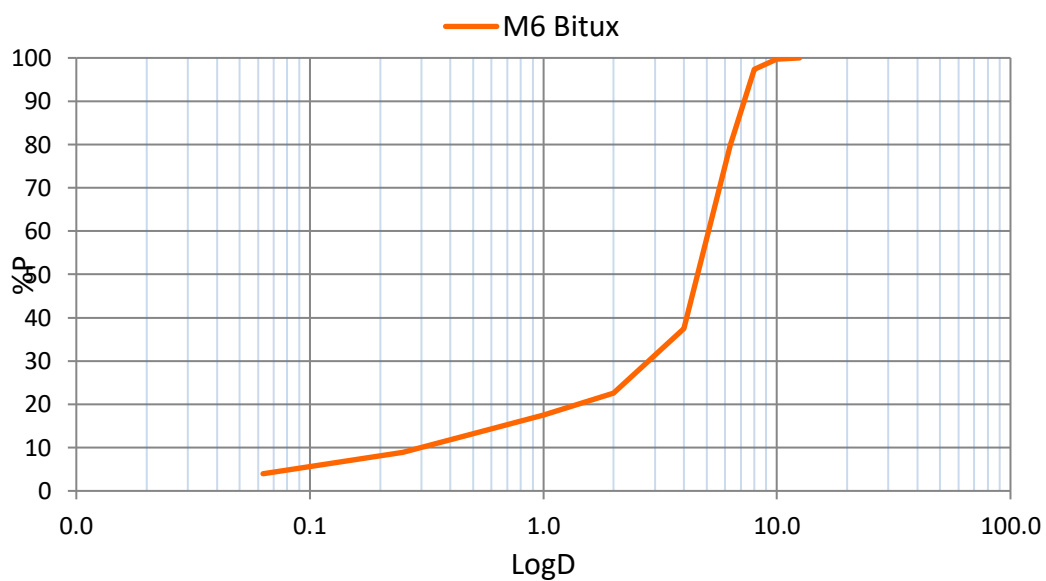
Graph 3.6: M6 - Particle size distribution

M7 BlackTop

Sieve [mm]	Retained [g]	Partial retained [%]	Progressive retained [%]	Progressive passing [%]
12.5	0.0	0.0	0.0	100.0
10.0	64.2	4.9	4.9	95.1
8.0	201.5	15.3	20.1	79.9
6.3	190.5	14.4	34.5	65.5
4.0	340.5	25.8	60.3	39.7
2.0	280.6	21.2	81.6	18.4
1.0	184.7	14.0	95.6	4.4
0.5	21.7	1.6	97.2	2.8
0.25	3.6	0.3	97.5	2.5
0.063	3.5	0.3	97.7	2.3
Filler	29.8	2.3	100.0	-
total	1320.6			

Table 3.9: M7 - Progressive passing
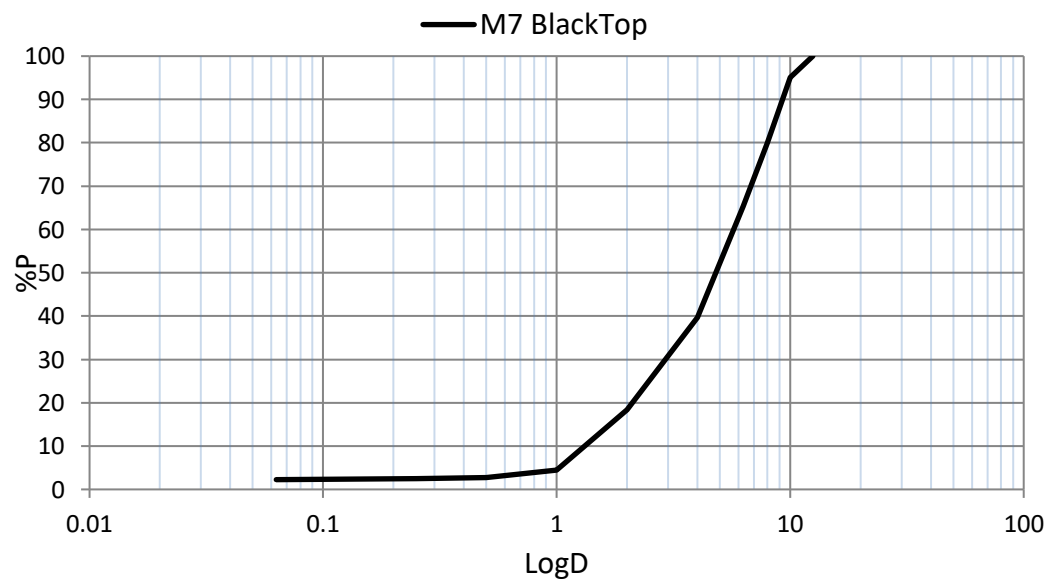
Graph 3.7: M7 - Particle size distribution

3. Testing: basic properties

The first characteristics that can be analyzed are the maximum diameter of the particles (D_M), corresponding to the dimension of the first sieve that has a retained, and the maximum nominal diameter ($D_{N,M}$), that is the dimension that corresponds to the 90% of passing.

From a visual analysis of the curves it's possible to distinguish three different classes of materials: M3 and M6 are characterized by a continuous curve, M4, M5 and M7 have a discontinuous gradation, the other materials are placed in-between.

This is reflected by the uniformity coefficient C_u, that is the ratio between the diameter of particles that correspond to the 60% of passing and the diameter of the 10% of passing.

A low value of this coefficient means that the material is uniform, so most of the particles have the same dimension; in this way the curve results discontinuous.

These three parameters are reported in the following *Table 3.10*:

	Material	D_M	$D_{N,M}$	C_U
M1	Asfaltival Special	8.00	7.21	5.34
M2	Asfaltival 2.0 Revolution	8.00	7.06	8.70
M3	RoadPav	8.00	6.92	8.21
M4	ProntoSint	6.30	5.64	1.82
M5	Bitem	6.30	5.78	2.04
M6	Bitux	10.00	7.28	16.73
M7	BlackTop	10.00	9.33	4.16

Table 3.10: Maximum diameter, maximum nominal diameter, uniformity coefficient

From these results it can be seen that, although Blacktop is sold as a mixture with a biggest dimension of 8 mm, it has a maximum diameter of 10 mm.

M6 is the material with the higher uniformity coefficient, with a value of 16.73, while the lower ones are M4 and M5, with a value around 2.

The maximum diameter influences the application range, bigger materials should not be used to repair shallow holes.

Another possible analysis is the division of the aggregates in the mixtures in three different classes:

- Gravel: dimension bigger than 2 mm;
- Sand: dimension between 2 and 0.063 mm;
- Filler: dimension smaller than 0.063 mm.

The behavior of the materials depends on the quantity of each class, the biggest particles determine the lytic skeleton of the mix, while the smaller ones fill the voids, increasing the strength of the mix.

These elements should be correctly balanced, because a mix with a high percentage of gravel will no compact under load, while a high percentage of filler, combined with bitumen, will create a paste around the bigger particles and avoiding their contact, making the mix acting like a fluid.

	Material	Gravel [%]	Sand [%]	Filler [%]
M1	Asfaltival Special	81.3	15.5	3.2
M2	Asfaltival 2.0 Revolution	81.3	14.5	4.1
M3	RoadPav	55.8	40.0	4.2
M4	ProntoSint	92.2	5.1	2.7
M5	Bitem	89.6	7.7	2.7
M6	Bitux	77.4	18.6	4.0
M7	BlackTop	81.6	16.2	2.3

Table 3.11: Aggregate classes

From the *Table 3.11* it can be seen that M4 and M5 are the ones characterized by the bigger amount of gravel, they can be defined like monogranular materials; this, as seen also in the uniformity coefficient, reflects the particle size distribution, that is discontinuous.

M1, M2 and M7 are similar, they have a high percentage of gravel but they are more balanced compared to the previous ones, with an amount of sand around 15%.

M6 is similar to the last ones, but it has a smaller quantity of bigger aggregates with a higher amount of smaller particles.

M3 is the most uniform material, with almost a half of the mixture composed by gravel, 40% of sand and the highest content of filler.

3.5. BASIC VOLUMETRIC

3.5.1. THEORETICAL MAXIMUM DENSITY AND DENSITY OF EXTRACTED AGGREGATES

The Theoretical Maximum Density (TMD) is the density of the mixture excluding air voids and it is determined using a sample of loose material and calculating the volume of water it displaces, according to the (UNI EN 12697-5, 2003).

The density of extracted aggregates is the specific gravity of the skeleton of the material, it is determined from the aggregates obtained from the ignition test. This test is performed according to the (UNI EN 1097-6, 2013).

TEST METHOD

The test uses a vacuum system that removes the air inside a pycnometer, where is placed a sample of loose material covered with distilled water.

The volume of the sample was calculated using the volumetric procedure, measuring the water's displacement caused by the material in the pycnometer.

TEST DESCRIPTION

For this test, a loose sample of material is placed inside a pycnometer, previously weighted with specific top, and the total mass is recorded. The sample is covered with distilled water and then the air inside the material's voids is removed by applying a vacuum to the pycnometer.

Occasionally the pycnometer is shaken by hand to facilitate the air removal.

When the air flow stops, the vacuum is slowly released and the pycnometer is covered with is top and it is filled with previously deaerated water.

To obtain the density, the mass of the completely filled container is registered; an important parameter is the water temperature, measured with a digital thermometer.

For each material, two different measures with two different pycnometers were taken, to reduce the fluctuation of the results.

3. Testing: basic properties

Figure 3.19: Vacuum system

Figure 3.20: Pycnometers and tops

The equation used is:

$$\rho_{mv} = \frac{m_2 - m_1}{1000 \cdot V_P - (m_3 - m_2)/\rho_w} \tag{3.6}$$

Where:

- ρ_{mv}: density of the sample [kg/m³];
- m_1: mass of the pycnometer and the top [g];
- m_2: mass of the pycnometer and the top, filled with the sample [g];
- m_3: mass of the pycnometer and the top, filled with the sample and water [g];
- V_P: volume of the pycnometer and the top [m³];
- ρ_w: density of the water at test temperature [kg/m³].

RESULTS

The results of this test are shown in _Table 3.12_; the TMD ranges from 2400 kg/m^3 for M3 to 2648 kg/m^3 for M7. These values will be used to determine the weight of the material required to determine the compaction curves.

Regarding the density of the extracted aggregates (MVA), the mean value stands around 2700 kg/m^3, with only one big difference: M7 has a density of 2946 kg/m^3.

	Material	TMD [kg/m^3]	MVA [kg/m^3]
M1	Asfaltival Special	2412	2735
M2	Asfaltival 2.0 Revolution	2466	2720
M3	RoadPav	2400	2732
M4	ProntoSint	2447	2697
M5	Bitem	2513	2765
M6	Bitux	2548	2794
M7	BlackTop	2684	2946

Table 3.12: Theoretical Maximum Density and Density of extracted aggregates

After the TMD test, lots of bitumen and other substances remain attached to the pycnometers; it confirms the high percentage of binder and other unknown additives inside the mixtures, as viewed on paragraph 3.4.1: _Binder content_.

Figure 3.21: TMD test

Figure 3.22: Pycnometer after TMD test

Figure 3.23: MVA test

3.6. COMPACTION

To understand the attitude to be compacted of a bituminous mixture, it's important to analyze the compaction characteristics. They can be obtained with two different techniques:

- Marshall compactor;
- Gyratory Shear Compactor (GSC).

In this study the GSC is used, since it better simulates the action of the steamrollers during the construction phase; moreover, it allows to evaluate the density during the test.

The machine can work both fixing the number of rounds and fixing the final height of the specimen.

This phase was performed according to the (UNI EN 12697-31, 2004).

TEST METHOD

The machine consists of a rigid body, a load element and a system that measure and record the sample height.

The compaction is achieved by the simultaneous action of a static compression equal to 600 kPa, and of the shearing action resulting of the motion of the centerline from the test piece. The mould has an inclination angle of 1.25° in order to generate a conical revolution surface; this rotation creates in the specimen some shear forces that, combined with the static force, allows to reach the optimal densification, with a continuous rearrangement of the particles (Santagata, Canestrari, & Pasquini, 2005).

The sample compaction procedure is schematized on the *Figure 3.25* (Riviera, Bellopede, Marini, & Bassani, 2014).

Figure 3.24: GSC machine
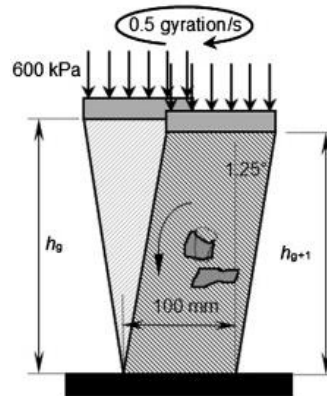
Figure 3.25: GSC sample compaction

In the specific case of M3, that requires water to be activated, it was necessary to introduce a special holed plate at the bottom, to avoid the accumulation of water inside the mould.

The complete equipment is shown in the *Figure 3.26*: the mould, the bottom holed plate (left), the top plate (center) and the standard bottom plate (right).

Figure 3.26: GSC equipment

Another particularity of M3 is that, during compaction, it produces a sort of gel (*Figure 3.27* and *Figure 3.28*) that covers the sample creating a closed surface.

The test is performed with the material at a temperature between 20 and 25°C.

Figure 3.27: M3 – Gel production

Figure 3.28: M3 – Gel production

TEST DESCRIPTION

At first the total mass required for each sample was evaluated from the TMD, according to the following equation:

$$M = 10^{-9} \cdot \pi \cdot \frac{D^2}{4} \cdot h_{min} \cdot \rho_M \tag{3.7}$$

In which:

- M: the mass of the mixture to be introduced in the mould [kg];
- D: the internal diameter of the mould [mm];
- h_{min}: the minimum height of compacted specimen, corresponding to a zero percentage of voids [mm];
- ρ_M: the maximum density of the mixture [kg/m³].

The bituminous mixture is placed in a cylindrical mould, with an inner diameter of 100mm, and this is inserted inside the GSC. After 180 rounds, at a constant speed of 30 rpm, the sample is extruded.

The machine can record the height of the specimen at each round, from this data is possible to calculate the volume of the sample, its density and so the compaction and the voids content.

Representing the compaction related to the number of round in a graph is possible to obtain the compaction curve.

In particular this study focuses on the compaction after two specific number of rounds:

- 50 rounds, to analyze the low compaction characteristics, related to the material after its placing on site;
- 180 rounds, to examine the high compaction characteristics, referred to the material after the compaction due to the traffic load.
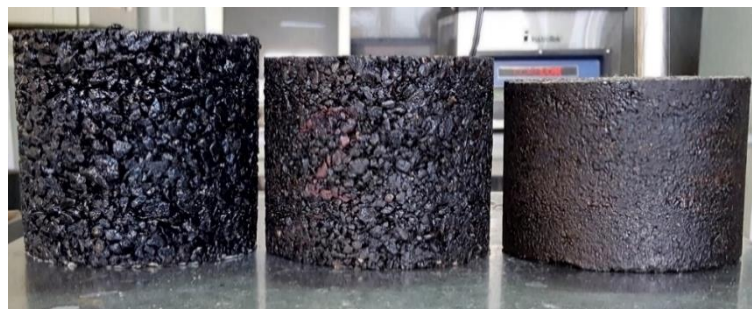
Figure 3.29: M5-M2-M3: samples at 180 rounds

RESULTS

The final compaction curves of the material are plotted in the following *Graph 3.1*; in these curves the starting point represent the auto densification while the slope of the curve is the workability of the material.
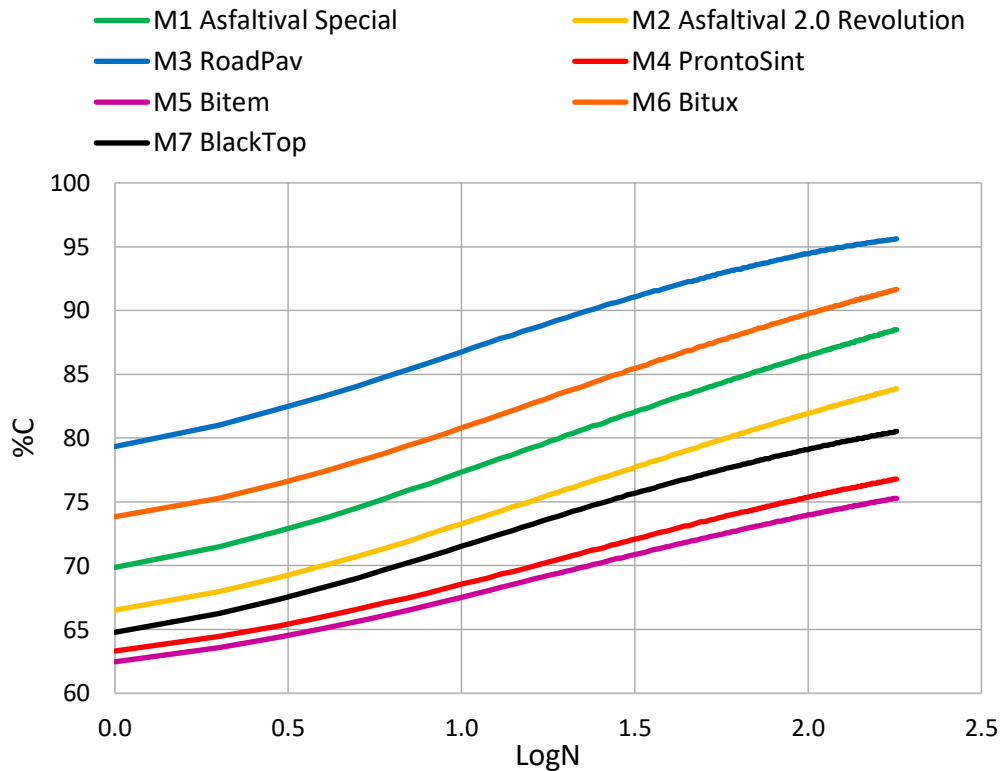
Graph 3.8: Compaction curves

From a visual analysis it is possible to say that the slopes of the different curves are similar, with a light difference in the final part, where M3 and M7 tend to reach a plateau, while the others continue to increase.

The main difference is the starting point, each mix is different and this heavily affect the compaction characteristics.

In particular, M3 has the highest starting point, about 80%, and it reaches a final compaction near 96%; this reflects the better compaction quality of this mix compared to the others.

Materials M4 and M5 are characterized by a similar behavior, with the lowest starting point; M7 has an initial compaction value comparable to the worst ones, but it has a higher slope so it reaches better final characteristics.

3. Testing: basic properties

The compaction characteristics can be compared to the particle size distribution; with references to _Table 3.11: Aggregate classes_, it is possible to see that materials with a more uniform composition will compact more than the others.

In particular M3, that has the lower gravel percentage, has the lowest voids content thanks to the higher quantity of smaller aggregates; on the opposite side, M4 and M5 are composed almost only by gravel; this implies low compaction characteristics and a high void content of the mixtures.

The following tables summarize the voids content (_Table 3.13_) and the density (_Table 3.14_) of the specimen after 10, 50, 100 and 180 rounds in the GSC. Due to the impossibility of placing the samples into water and taking the real density and void content, all the results refers to geometric measurements.

In this phase the study focused on four different compaction levels, that refers to different state of the materials:

- 10 rounds: material poured in the patch and subjected only to its own weight, without any type of mechanical compaction;
- 50 rounds: patch subjected to a light compaction by the workers, before its opening to the traffic;
- 100 rounds: level that is comparable with hot mix asphalt compaction analysis;
- 180 rounds: material after the compaction due to traffic loads.

	Material	%v [%]			
		10 rounds	_50 rounds_	_100 rounds_	_180 rounds_
M1	Asfaltival Special	22.7	16.1	13.5	11.5
M2	Asfaltival 2.0 Revolution	26.7	20.5	18.1	16.1
M3	RoadPav	13.2	7.5	5.6	4.4
M4	ProntoSint	31.5	26.6	24.6	23.2
M5	Bitem	32.5	27.8	26.0	24.7
M6	Bitux	19.2	12.8	10.3	8.3
M7	BlackTop	28.5	22.8	20.9	19.5

Table 3.13: Voids content

	Material	MV [kg/m³]			
		10 rounds	*50 rounds*	*100 rounds*	*180 rounds*
M1	Asfaltival Special	1865	2023	2085	2134
M2	Asfaltival 2.0 Revolution	1807	1959	2020	2068
M3	RoadPav	2082	2220	2266	2295
M4	ProntoSint	1677	1797	1845	1879
M5	Bitem	1697	1813	1859	1891
M6	Bitux	2059	2222	2287	2336
M7	BlackTop	1919	2071	2123	2162

Table 3.14: Density

It's evident that most of the materials have poor compaction quality, in fact the voids content is very high compared to the average content in a hot mix asphalt. In particular, both M4 and M5 have a voids content after 180 rounds greater than 20%; while only two materials, M3 and M6, reach a value lower than 10%.

There is also a big difference in the beginning of the compaction, with some materials (M4 and M5) that have a starting void content greater than 30%, while others (M3 and M6) lower than 20%.

To better understand the behavior of the materials it is possible to introduce some differences between the values of the void contents; in particular the following parameters are analyzed:

- $\Delta\%_{10-50}$: the relative difference between the void content after 10 rounds and the one after 50 rounds, divided by the first value; this reflects the sensibility of the material to the compaction energy.

- $\Delta\%_{50-180}$: the relative difference between the voids at 50 and 180 rounds, divided to the first ones; they reflect the densification of the materials due to traffic loads.

- Δ_{50-180}: the absolute difference between the voids at 50 rounds and the ones after 180 rounds; it reflects the compaction of the material after the opening of the road to the traffic and the volume reduction during its life.

	Material	$\Delta\%_{10-50}$ [-]	$\Delta\%_{50-180}$ [-]	Δ_{50-180} [-]
M1	Asfaltival Special	29.07	28.57	4.60
M2	Asfaltival 2.0 Revolution	23.30	21.46	4.40
M3	RoadPav	43.53	41.37	3.09
M4	ProntoSint	15.54	12.63	3.36
M5	Bitem	14.40	11.15	3.10
M6	Bitux	33.38	34.82	4.45
M7	BlackTop	19.98	14.47	3.30

Table 3.15: Voids indices

Materials M3 and M6 have a high $\Delta\%_{10-50}$, this means that they require the lower compaction energy, respect to the other mixtures; the materials that need higher energy are M4 and M5.

This index can give a suggestion regarding the compaction techniques: if low energy is required, a manual compaction can be performed, while if the mixtures requires more energy, some mechanical instruments should be used.

Regarding the second index, a high value suggest that the mechanical properties should increase during material's life, due to the reduction of voids content under traffic load. A low value indicates that the characteristics of the mixtures should remain stable, without any effect of the applied stresses.

Materials M3 and M6 belong to the first category, while materials M4, M5 and M7 belongs to the second one; the others have a behavior somewhere between these two classes.

The last difference indicates the volume reduction of the patch volume under loads, it can be used as an operational index. It gives indications about the quantity of materials to place in the pothole, in order to avoid the creation of a shallow depression on the road surface due to post compaction, as it is possible to see in *Figure 3.30*.

Figure 3.30: Volume reduction due to post compaction

Mixtures M1, M2 and M6 have the highest value, this means that more material must be placed to obtain the same final results of the other mixes.

Both the relative differences give indications about the compaction quality of the mixes, as seen in the compaction curves. A high value in these parameters reflects high compaction characteristics; placing the material in descending order replicates the disposition of the compaction curves of the materials in the _Graph 3.8: Compaction curves_.

3.7. SUMMARY

This chapter gives an initial approach to the analysis of the seven materials, it provides information about their composition, basic volumetric properties and compaction characteristics.

Starting from the stocking quality, it reflects the overall characteristics of the mixes; in particular M4 and M5, that have the poorest bags, result to be the ones with the worst compaction properties. The presence of holes can be considered as a negative factor that influences the durability of the material during the storage period.

To avoid a loss of quality due to contact with air, other producers use better quality bags (M1 and M2) or plastic buckets (M3 and M7); this last one is the best option, that allows a great storage period of different months.

Regarding the binder content analysis, the results are quite different; this can be caused by the kind of materials, that, to be workable at low temperature, require a high presence of other volatile substances that can't be identified and studied.

These additives should have a role in increasing the mechanical characteristics of the mixtures, thanks to some chemical reaction.

The density of the mixes is similar, with the exception of M7 that has a specific gravity quite higher than the others. This can be seen also in the density of the extracted aggregates, that has the same differences of the TMD.

Although the density of the aggregates is similar, they have a different nature; this can be seen from a visual analysis.

The main results of this chapter regard the compaction properties of the mixtures, that are used both to analyses the characteristics of the materials and to obtain the samples to test in the following chapters.

The compaction curves have a starting point that ranges from about 60% to about 80%, while the final point ranges from 75% to 95%, this means that, although the analyzed mixtures are all cold mix asphalts, produced for the same applications, their behavior can be quite different.

Analyzing the differences in the voids content at different stages, it is possible to obtain some index that can gives suggestions related to the operational procedures, such as the required energy to compact the mix and the necessary amount of material. These index gives also information about the possible mechanical behavior of the mixes.

The compaction curve will be also deeply investigated with analytical models in chapter 6: _Modelling_.

4. TESTING: LOW COMPACTION STRENGTH

4.1. INTRODUCTION

This chapter describes the analysis of the low compaction characteristics of the seven materials; the aim of this part is to evaluate the behavior of the mixtures in the first phase of their life.

The samples were realized with a density obtained from the compaction curve, referring to 50 rounds in the GSC.

The analysis is divided into two main parts: the first consists on the evaluation of the Indirect Tensile Strength on three samples obtained from the GSC, after four different curing time; the second on the estimation of the California Bearing Ratio, on two specimens compacted with the Proctor procedure, after one day of conditioning.

4.2. INDIRECT TENSILE STRENGTH

The Indirect Tensile Strength (ITS) is a test that provides a braking parameter of the material; it is obtained by loading the specimen diametrically across the circular cross section. The material rupture happens due to the traction along the direction perpendicular to the load one (Poisson effect).

This test was performed according to (UNI EN 12697-23, 2006).

4. Testing: low compaction strength

TEST METHOD

For this test, the compacted specimen is inserted inside a press (*Figure 4.1*), in which the load increases with a constant deformation speed of 50 ± 2 mm/min of the vertical ram, until the breakage of the sample.

The machine records three different parameters: the traction, the strain and the load applied; from this last one it is possible to calculate the tensile strength.

Figure 4.1: ITS static press machine

Figure 4.2: Sample for ITS test

TEST DESCRIPTION

The specimens for this test were prepared compacting the material with the GSC until the final chosen height of 70mm, using a precise amount of material derived from the compaction curves. The target density was the same of the material after 50 rounds in the GSC.

All specimens were cured inside a climate cell, at a fixed temperature of 20°C, for one, three, seven and twenty-eight days. In this way, it's possible to analyses the evolution of the tensile strength inside the material. For each curing time, three samples were made.

At the beginning of the study, different curing temperature were tested, but it was discovered that this process does not affect the materials' resistance.

4. Testing: low compaction strength

Due to the weakness of the samples, it was necessary to use a confinement during the curing period, to avoid the collapse of the specimens before the test (*Figure 4.3*).

Figure 4.3: Collapsed sample

After the conditioning, the materials were tested: the specimens were placed in the compression testing machine between the loading strips, and loaded diametrically along the direction of the cylinder axis, with a constant speed of displacement until they break. The ITS can be evaluated using the following equation:

$$ITS = \frac{2 \cdot P}{\pi \cdot d \cdot t} \qquad (4.1)$$

In which:

- ITS: Indirect Tensile Strength [GPa];
- P: maximum applied load [kN];
- d: diameter of the specimen [mm];
- t: thickness of the specimen [mm].

RESULTS

Due to the low resistance of this kind of materials, lots of specimens collapsed during the placing on the machine (*Figure 4.5*); in other cases, the tensile strength was so low that the machine wasn't able to record it or it gives some unreliable result, for this reason it was chosen a threshold value of 0.100 kPa under which the test was considered failed.

| Figure 4.4: M3 - ITS run test | Figure 4.5: M4 - ITS test failure |

Only three materials, M3, M6 and M7, give readable results for each curing time, in this case it was possible to plot the different values of the tensile strength.

The results are summarized in the following tables; because of the low value, the measurement unit was changed from GPa to kPa.

		Curing time [d]	Load [kN]	Deformation [mm]	Traction [mm]	σ_t [kPa]
M1	Asfaltival Special	1		collapsed		n.a.
		3		collapsed		n.a.
		7		collapsed		n.a.
		28		collapsed		n.a.

Table 4.1: M1 - ITS results

4. Testing: low compaction strength

		Curing time [d]	Load [kN]	Deformation [mm]	Traction [mm]	σ_t [kPa]
M2	Asfaltival 2.0 Revolution	1		collapsed		n.a.
		3		collapsed		n.a.
		7		collapsed		n.a.
		28		collapsed		n.a.

Table 4.2: M2 - ITS results

M1 and M2 gives some readable results, all characterized by a high variability and always lower than the threshold value. The maximum resistance is hundreds of times lower than the average required for a standard HMA.

		Curing time [d]	Load [kN]	Deformation [mm]	Traction [mm]	σ_t [kPa]
M3	RoadPav	1	4.028	2.657	0.546	366.4
		3	4.645	2.194	0.647	422.4
		7	4.591	2.777	0.944	417.5
		28	4.913	2.487	0.355	446.8

Table 4.3: M3 - ITS results
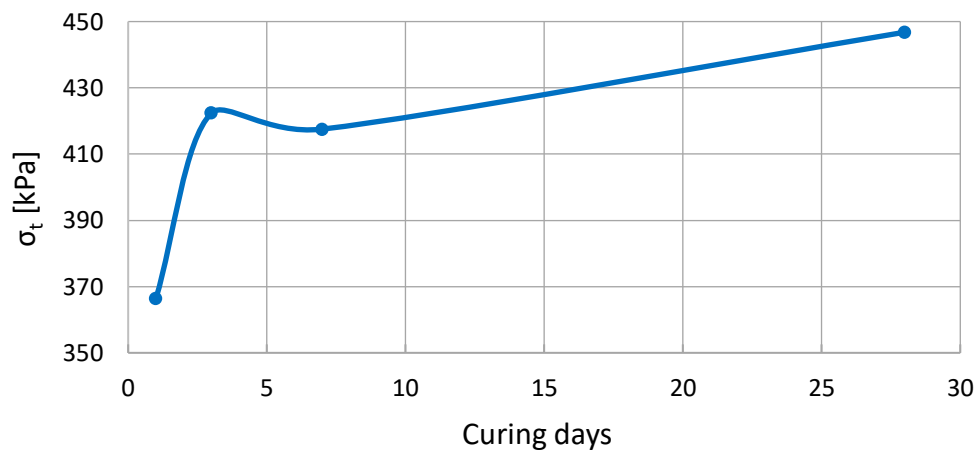
Graph 4.1: M3 - ITS trend

M3 has a good resistance, this material has great performances in its early life, with a high increase of resistance in the first three days, then it continues to harden but with a lower speed; this can be caused by the evaporation of the water in the first life.

4.   Testing: low compaction strength

		Curing time [d]	Load [kN]	Deformation [mm]	Traction [mm]	σ_t [kPa]
		1		collapsed		n.a.
M4	ProntoSint	3		collapsed		n.a.
		7		collapsed		n.a.
		28		collapsed		n.a.

Table 4.4: M4 - ITS results

		Curing time [d]	Load [kN]	Deformation [mm]	Traction [mm]	σ_t [kPa]
		1		collapsed		n.a.
M5	Bitem	3		collapsed		n.a.
		7		collapsed		n.a.
		28		collapsed		n.a.

Table 4.5: M5 - ITS results

For both M4 and M5 it was impossible to perform this test, all the specimens collapsed under their own weight after the removal of the confining element, even after 28 days of curing.

		Curing time [d]	Load [kN]	Deformation [mm]	Traction [mm]	σ_t [kPa]
		1	0.282	1.362	0.601	25.6
M6	Bitux	3	0.305	1.415	0.544	27.7
		7	0.295	1.400	0.559	26.8
		28	0.254	1.158	0.678	23.1

Table 4.6: M6 - ITS results
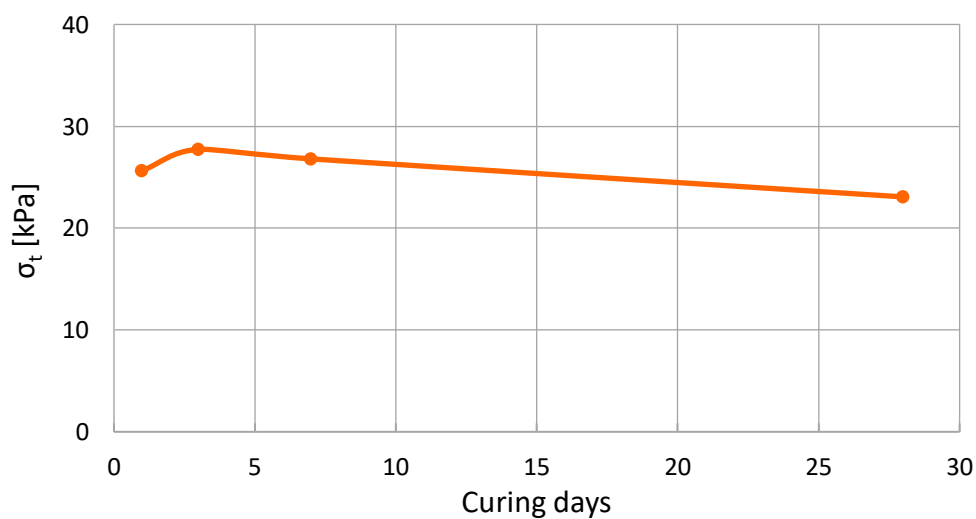
Graph 4.2: M6 - ITS trend

		Curing time [d]	Load [kN]	Deformation [mm]	Traction [mm]	σ_t [kPa]
		1	0.254	1.158	0.678	23.1
M7	BlackTop	3	0.322	1.862	0.975	29.3
		7	0.744	2.213	1.074	67.6
		28	2.805	2.015	0.368	255.1

Table 4.7: M7 - ITS results
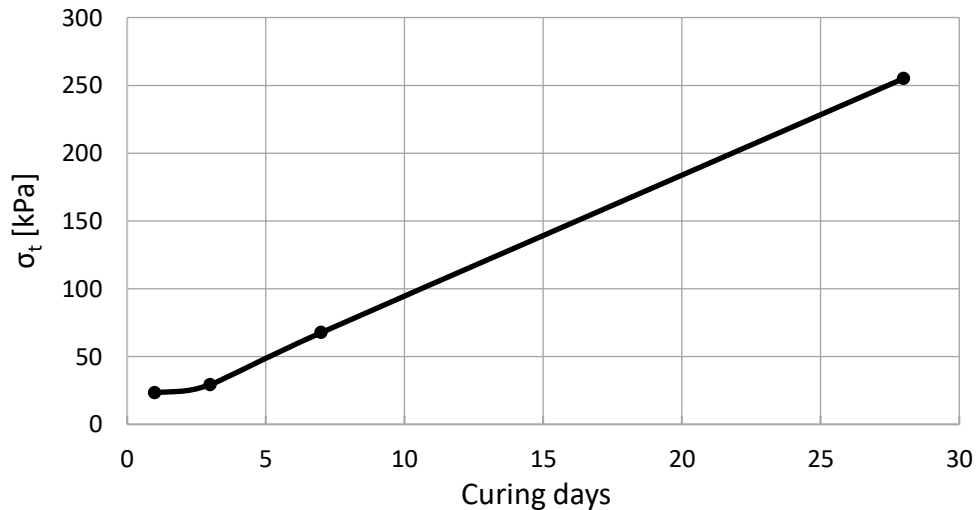
Graph 4.3: M7 - ITS trend

M6 and M7 give some results for every curing time, but they have a different behavior: M6 has a constant resistance, around a value of 26kPa, so for this material the curing has no effect and its properties do not change in time. Moreover, there is a low decrease after 28 days, this can mean that this material suffers of a sort of softening that lowers the resistance.

M7 has a more progressive increase of the resistance, starting from 23.1 kPa after one day and reaching 255 kPa after four weeks, meaning that the curing time has a great effect.

This result is significant because, although M7 is one of the materials with the highest voids content, as shown in the *Table 3.13: Voids content* of chapter 3, it has a great indirect tensile strength, compared to most of the other materials.

This resistance probably derives from some chemical reaction due to the presence of additives. In particular, as it can be seen from the graph, the material starts to harden after 3 days of curing, meaning that these reactions require some time to be activated.

In an overall view, M3 is the mix that has the higher resistance, anyway its tensile strength is lower than the average one of a HMA.

In order to make a classification of the materials, M3 can be considered as a high quality one, M6 and M7 as middle quality mixes, while the others can be assumed as low-quality materials.

4.3.   CALIFORNIA BEARING RATIO

The California Bearing Ratio (CBR) test is a simple test that compares the bearing capacity of a material with the one of a standard well-graded crashed stone. It was developed by the California Division of Highways in around 1930.

Although it is primarily intended for evaluating the strength of cohesive material, it was used in this research due to the lateral confining requested by the test procedure. This allows to obtain results for every material, even the ones that collapsed during the ITS test.

This test was done according to the (UNI EN 13286-47, 2006).

The specimens were compacted using the modified Proctor procedure, according to the (UNI EN 13286-2, 2010).

TEST METHOD

The modified Proctor compaction is done in 5 different layers; this compaction method has a constant energy for volume unit of 269 N/cm^2, obtained from the equation:

$$E = \frac{W_{rammer} \cdot h \cdot n_{hl} \cdot n_l}{V_{mould}}$$

(4.2)

Where, according to the modified standard procedure:

- W_{rammer}: weight of the rammer, 4.535 kg;
- h: falling height, 45.7 cm;
- n_{hl}: number of hits per layer, 56;
- n_l: number of layers, 5;
- V_{mould}: volume of the mould.

The mould used has a diameter of 152.4 mm and a height of 116.4 mm.

4. Testing: low compaction strength

The scheme used to compact each layer is the *Figure 4.6*:
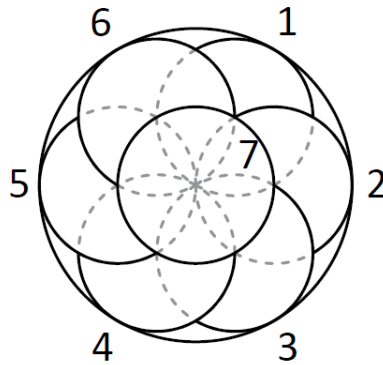
Figure 4.6: Modified Proctor compaction scheme

The CBR test is performed applying a load to a small penetration piston, at a constant rate of 1.3 mm (0.05'') per minute and recording the total load at penetration ranging from 0.64 (0.025 in.) up to 7.62 mm (0.300 in.)

Figure 4.7: Proctor compactor

Figure 4.8: CBR static press machine

TEST DESCRIPTION

The samples were realized using an amount of material derived from the volume of the mould and the density after 50 rounds in the GSC.

The specimens were compacted in five sequential layers, each one with a mass equal to one fifth of the previously calculated one.

The compaction was performed with the Proctor procedure, at first the total specimen is realized with a height of 140 mm, then the upper part of the mould can be removed and the specimen is shaved, to reach its final height of 116.4 mm. In this way the surface results smoother and regular.

For each material two sample were made, each one was subjected to a curing period of one day at 20°C.

Figure 4.9: Sample after Proctor compaction

Figure 4.10: Sample before CBR test

After the conditioning, the CBR test is performed without the confining weight on the upper surface of the samples as the standard requires; this because the CMA are used for surfaces applications, so it would be wrong to apply a weight on the top.
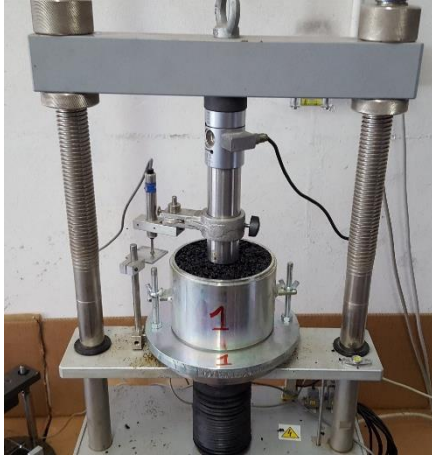
Figure 4.11: CBR test runs

Figure 4.12: Sample after CBR test

The CBR value is obtained comparing the material resistance on the piston and the standard unit load for the reference Californian well graded crushed stone, for two fixed penetration depths: 2.54 mm and 5.08 mm.

The used equation is the following:

$$CBR = 100 \cdot \frac{p}{p_s}$$ (4.3)

Where:

- CBR: California Bearing Ratio [%];
- p: resistance of material [MPa];
- p_s: standard unit load:
    - 6.9 MPa (1000 psi) for 2.54 mm (0.1") penetration;
    - 10.3 MPa (1500 psi) for 5.08 mm (0.2") penetration.

From this equation two different results are obtained, the final CBR value is the highest of the two.

RESULTS

Analyzing the volume of the sample and its mass, it is possible to evaluate the obtained density; this can be compared to the target one, in order to understand the ability of the material to be compacted by bowl.

Regarding the CBR value, they range from 26.4% of M6 to 62.2% for M3; the results are expressed in the *Table 4.8*:

	Material	MV_{obj} [kg/m^3]	MV [kg/m^3]	%v [%]	CBR [%]
M1	Asfaltival Special	2023	2063	14.5	59.3
M2	Asfaltival 2.0 Revolution	1959	1990	19.3	60.1
M3	RoadPav	2220	2189	8.8	62.2
M4	ProntoSint	1797	1903	22.2	37.7
M5	Bitem	1813	1912	23.9	37.8
M6	Bitux	2222	2154	15.5	26.4
M7	BlackTop	2071	1912	28.8	42.0

Table 4.8: CBR results

Four materials out of seven reach a density similar to the target one, with a difference lower than 40 kg/m^3, while M4, M5 and M7 have differences in the order of 100 kg/m^3. This reflects the particle size distribution of the materials, the ones characterized by a discontinuous curve have more difficulties to be compacted.

In general, it is possible to say that the harder is the surface, the higher is the CBR rating; this can mean that materials M1, M2 and M3, that are characterized by the higher CBR values, will deform less under traffic loads.

M4 and M5 have a very similar CBR so, also in this case, the two mixes have a similar behavior.

Even if the CBR is a test for soil, it was useful to perform on CMA because from the results it is possible to recognize two different classes of materials, one with a CBR around or lower than 40%, one with a ratio around or higher than 60%.

4.4. SUMMARY

This chapter shows that most of the tested materials have a poor resistance after low compaction, this means that, in the first part of their life, the patches will probably be subjected to a fast deterioration.

Regarding the ITS test, a problem occurs during the preparation of the specimen, when some samples collapsed and so a confining element must be introduced.

Generally, the mixes have no indirect strength even after the 28 days of curing, with only three out of seven materials gives some readable results.

M3 showed a fast increasing in the resistance in the first days, then it remains stable around a value greater than 400 kPa.

M6 has a constant resistance of around 26 kPa, so there are no curing effects for this material.

M7 has a resistance that continues to increase in time, in particular after 3 days of curing, starting from a value of 23.1 kPa after one day and reaching a maximum resistance of 255 kPa.

In general, the ITS reflects the compaction quality of the materials analyzed in chapter 3, with the exception of M7 for which some chemical reactions that increase the resistance were supposed.

The CBR was used because of its confining element that is present also during the test, this allows to obtain results for all the materials.

A great variation in the CBR value was observed, with values that ranges from 26.4% of M6 to 62.2% for M3.

In conclusion, it is possible to say that the material with the highest resistance after a low compaction is M3.

5. TESTING: HIGH COMPACTION STRENGTH

5.1. INTRODUCTION

After the analysis of low compaction characteristics, the study focuses on the high compaction strength of the mixtures, to examine their real behavior when subjected to the traffic.

In this phase the specimens have a target density equal to the one after 180 rounds in the GSC.

The first step is the evaluation of the resilient modulus using a Nottingham Asphalt Tester on three slender sample obtained from the GSC, after two different curing time.

The second step consists on the estimation of the rutting resistance, using a wheel tracking machine on two compacted slabs, after one day of conditioning.

5.2. RESILIENT MODULUS AND QUICK SHEAR

The resilient modulus is a parameter that reflects the mechanical behavior of the material: the deformation response of loaded materials can be divided into two components, one recoverable (resilient) and one residual (permanent).

In addition to the value of the resilient modulus, it is possible to simulate the behavior of the material with some models.

The test is performed according to the (AASHTO T307, 1999).

The quick shear is performed after the evaluation of the resilient modulus, applying a constant deformation rate. This in order to obtain the maximum stress that the material can support.

TEST METHOD

The Nottingham Asphalt Tester (NAT), in (*Figure 5.1*) is composed of a load system, a pneumatic unit, a control and data recording system and a climatic chamber to control the temperature.

5. Testing: high compaction strength

The deformation of the specimen is measured with two Linear Variable Differential Transducers (LVDT) that have an accuracy of 250μm.

Thanks to a specific software, it's possible to control all the parameters required for the test, such as the load period, the load value and the confining pressure, inside the triaxial cell (*Figure 5.2*).

Figure 5.1: Nottingham
Asphalt Tester (NAT)

Figure 5.2: Triaxial cell

For this specific study the test protocol used was the one realized for subgrades, that has the following characteristics, summarized in the *Figure 5.3*:

Sequence No.	Confining pressure kPa	Max axial stress kPa	Cyclic stress kPa	Contact stress kPa	No. load applications
0	41,4	27,6	24,8	2,8	500
1	41,4	13,8	12,4	1,4	100
2	41,4	27,6	24,8	2,8	100
3	41,4	41,4	37,3	4,1	100
4	41,4	55,2	49,7	5,5	100
5	41,4	68,9	62,0	6,9	100
6	27,6	13,8	12,4	1,4	100
7	27,6	27,6	24,8	2,8	100
8	27,6	41,4	37,3	4,1	100
9	27,6	55,2	49,7	5,5	100
10	27,6	68,9	62,0	6,9	100
11	13,8	13,8	12,4	1,4	100
12	13,8	27,6	24,8	2,8	100
13	13,8	41,4	37,3	4,1	100
14	13,8	55,2	49,7	5,5	100
15	13,8	68,9	62,0	6,9	100

Figure 5.3: Subgrade protocol

5. Testing: high compaction strength

This protocol consists in a first 500 assessment cycles, followed by 15 sequences of 100 cycles, combining three different confining pressures with five different deviatoric stresses. Each cycle is composed by a loading period of 0.1 s and a resting period of 0.9 s.

To obtain the confining pressure, the specimen must be covered with a rubber membrane and sealed inside the triaxial cell with some O-rings; moreover, to transfer the load, at the top and at the bottom there are two rigid plates.

After this test, the specimen is subjected to a constant deformation rate until its rupture, in this way it is possible to evaluate the shear resistance.

Both the evaluation of the resilient modulus and the quick shear test are performed at a constant temperature of 20°C, controlled with the climatic chamber.

SPECIMEN PRODUCTION

In order to obtain a slender sample using the GSC, with a height of 200 mm, characterized by a constant density, different procedures were tried. The best solution is to make the specimen in three different layers, the first with a height of 70 mm and the other two with a height of 65 mm.

The specimens were made with a target density equal to the one after 180 rounds in the GSC.

Figure 5.4: M3 - slender sample

Figure 5.5: M5 - collapsed sample

5.   Testing: high compaction strength

Due to the weakness of the majority of the materials (_Figure 5.5_), it was necessary to modify the procedure to perform the test. The best option was to freeze the specimen, inside the mould, for about 25 minutes; then they were extruded directly inside the membrane (_Figure 5.6_), in order to have a lateral confining during the curing time.
For this study there were realized four specimens for two different curing time, one and twenty-eight days at 20°C.

This frozen procedure worked well, but some specimen of materials M4 and M5 collapsed under only their own weight before twenty-eight days (_Figure 5.7_).

Figure 5.6: M1 - frozen sample

Figure 5.7: M5 - collapsed frozen sample

5. Testing: high compaction strength

RESULTS

The results of the resilient modulus and the quick shear are shown in the four following tables, one for each curing time:

Curing time [d]		Material	M_R min [MPa]	M_R max [MPa]	M_R mean [MPa]
	M1	Asfaltival Special	79.6	155.8	119.6
	M2	Asfaltival 2.0 Revolution	62.3	135.0	100.2
	M3	RoadPav	182.0	317.0	264.8
1	M4	ProntoSint	73.0	148.4	109.9
	M5	Bitem	88.4	182.3	132.1
	M6	Bitux	119.5	218.8	166.0
	M7	BlackTop	145.8	265.1	208.1

Table 5.1: Resilient modulus, 1 day

Curing time [d]		Material	M_R min [MPa]	M_R max [MPa]	M_R mean [MPa]
	M1	Asfaltival Special	66.0	134.6	100.5
	M2	Asfaltival 2.0 Revolution	60.9	127.4	94.9
	M3	RoadPav	173.3	338.2	263.9
28	M4	ProntoSint	70.2	140.0	102.9
	M5	Bitem	78.1	138.9	110.1
	M6	Bitux	108.3	186.9	147.5
	M7	BlackTop	168.1	297.8	241.6

Table 5.2: Resilient modulus, 28 days

Curing time [d]		Material	Strain [%]	Load [kN]	Stress [kPa]
	M1	Asfaltival Special	2.6	3.6	452.9
	M2	Asfaltival 2.0 Revolution	2.3	3.3	423.6
	M3	RoadPav	1.2	8.6	1091.8
1	M4	ProntoSint	1.8	1.8	232.9
	M5	Bitem	2.4	2.1	271.2
	M6	Bitux	1.9	3.6	458.6
	M7	BlackTop	2.1	3.5	445.6

Table 5.3: Quick shear, 1 day

5.   Testing: high compaction strength

Curing time [d]		Material	Strain [%]	Load [kN]	Stress [kPa]
28	M1	Asfaltival Special	2.6	2.9	364.1
	M2	Asfaltival 2.0 Revolution	2.2	3.2	405.4
	M3	RoadPav	1.0	8.5	1082.0
	M4	ProntoSint	1.8	1.6	209.2
	M5	Bitem	1.7	1.6	207.2
	M6	Bitux	1.8	3.3	419.2
	M7	BlackTop	2.1	5.8	738.5

Table 5.4: Quick shear, 28 days

A first analysis can be done regarding the mean value of the resilient modulus, that ranges from 94.9 MPa for M2 after twenty-eight days to 264.8 MPa for M3 after one day.

It is evident that the mean resilient modulus remains almost constant in the time, with the exception of M7, whose value goes from 163.7 MPa to 241.6 MPa after twenty-eight days.

Regarding the shear resistance, there is a high variation for the different materials; moreover, the results of M3 are not representing the real resistance of the mixture, but only the maximum value that the machine can reach (1 GPa).

From this test it is possible to recognize 3 different classes of materials:

1. Materials with low resistance, lower than 300 kPa: M4 and M5;

2. Materials with medium resistance, from 300 kPa to 500 kPa: M1, M2, M6 and M7 in its early life;

3. Materials with high resistance, greater than 500 kPa: M3 and M7 after a curing period.

As in the case of the ITS, M7 gives some interesting results because, although its high voids content, it reaches a very high shear resistance after 28 days. This can be caused by some chemical reaction that increase the material's strength.

Also the resilient modulus increases in time, starting from a mean value of 163.7 MPa and reaching a value of 241.6 MPa, that is similar to the one of M3.

M7 is also the only one for which the curing time has a great effect; for most of the others mixes the resilient modulus remain almost constant in time, while the shear resistance is subjected to a low decrease, probably caused by the softening of the compacted materials.

A more detailed analysis of the resilient modulus can be done using some predictive model, that express the effects of the confinement in terms of minor principal stress, bulk stress and deviatoric stress.

The Uzan equation was developed as a combination of bulk and deviator stress models in an effort to improve the predicted response of M_R test results by including both axial and shear effects. The model defines the resilient modulus as (Uzan, 1985):

$$M_R = k_1 \cdot \sigma_{atm} \cdot \left(\frac{\theta}{\sigma_{atm}}\right)^{k_2} \cdot \left(\frac{\sigma_d}{\sigma_{atm}}\right)^{k_3} \qquad (5.1)$$

Where:

- k_1, k_2, k_3: material constants;
- θ: bulk stress ($\sigma_1 + \sigma_2 + \sigma_3$);
- σ_d: deviatoric stress;
- σ_{atm}: atmospheric pressure.

The materials' constants for the different mixtures and the two curing times are shown in the following tables:

Curing time [d]		Material	K_1 [-]	K_2 [-]	K_3 [-]	RMS [-]
	M1	Asfaltival Special	1025.61	0.84	-0.22	14.77
	M2	Asfaltival 2.0 Revolution	809.30	0.97	-0.28	11.88
	M3	RoadPav	3021.11	0.30	0.09	18.74
1	M4	ProntoSint	835.77	0.87	-0.33	20.72
	M5	Bitem	1010.45	0.89	-0.32	19.56
	M6	Bitux	1348.42	0.73	-0.26	20.87
	M7	BlackTop	1734.47	0.76	-0.24	30.69

Table 5.5: Uzan model, 1 day

5.   Testing: high compaction strength

Curing time [d]		Material	K_1 [-]	K_2 [-]	K_3 [-]	RMS [-]
28	M1	Asfaltival Special	822.16	0.88	-0.26	13.63
	M2	Asfaltival 2.0 Revolution	823.91	0.84	-0.21	10.91
	M3	RoadPav	2637.58	0.61	-0.06	16.78
	M4	ProntoSint	870.72	0.75	-0.22	14.38
	M5	Bitem	961.41	0.67	-0.19	14.33
	M6	Bitux	1239.49	0.68	-0.22	18.04
	M7	BlackTop	2286.96	0.59	-0.11	16.05

Table 5.6: Uzan model, 28 days

It is evident that the model predicts in a better way the behavior of the materials after twenty-eight days of conditioning, but the average RMS is still high to consider these results acceptable.

Another model is the one proposed by the National Cooperative Highway Research Program (NCHRP) project 1-28A (Andrei et al, 2004); it is a version of Uzan model for use in the Mechanistic-Empirical Pavement Design Guide (MEPDG) in the US (Mazari, Abdallah, Garibay, & Nazarian, 2016).

This model was later slightly modified (Ooi, Archilla, & Sandefur, 2004) because in this way it is more appropriate for estimating the responses of the modulus-based devices (Nazarian et al., 2014):

$$M_R = k_1 \cdot \sigma_{atm} \cdot \left(\frac{\theta}{\sigma_{atm}} + 1 \right)^{k_2} \cdot \left(\frac{\tau_{oct}}{\sigma_{atm}} + 1 \right)^{k_3} \qquad (5.2)$$

Where:

- k_1, k_2, k_3: material constants;
- θ: bulk stress ($\sigma_1 + \sigma_2 + \sigma_3$);
- τ_{oct}: octahedral stress;
- σ_{atm}: atmospheric pressure.

5. Testing: high compaction strength

The results are summarized in the two following tables:

Curing time [d]		Material	K_1 [-]	K_2 [-]	K_3 [-]	RMS [-]
1	M1	Asfaltival Special	471.56	1.88	-1.87	9.47
	M2	Asfaltival 2.0 Revolution	357.00	2.17	-2.44	12.99
	M3	RoadPav	1536.38	0.65	0.71	31.18
	M4	ProntoSint	466.97	1.99	-2.81	20.50
	M5	Bitem	549.92	2.03	-2.83	14.50
	M6	Bitux	793.39	1.66	-2.19	22.03
	M7	BlackTop	930.14	1.74	-2.06	20.79

Table 5.7: MEPDG model, 1 day

Curing time [d]		Material	K_1 [-]	K_2 [-]	K_3 [-]	RMS [-]
28	M1	Asfaltival Special	394.39	1.98	-2.24	13.21
	M2	Asfaltival 2.0 Revolution	368.29	1.86	-1.68	15.09
	M3	RoadPav	1199.00	1.33	-0.49	27.15
	M4	ProntoSint	466.01	1.64	-1.74	21.21
	M5	Bitem	522.13	1.53	-1.57	13.21
	M6	Bitux	728.21	1.55	-1.90	16.79
	M7	BlackTop	1184.33	1.32	-0.94	17.11

Table 5.8: MEPDG model, 28 days

A third model was developed to take into account both confining and deviatoric stresses (Puppala, Mohammad, & Allen, 1997):

$$M_R = k_1 \cdot \sigma_{atm} \cdot \left(\frac{\sigma_3}{\sigma_{atm}}\right)^{k_2} \cdot \left(\frac{\cdot \sigma_d}{\sigma_{atm}}\right)^{k_3} \qquad (5.3)$$

Where:

- k_1, k_2, k_3: material constants;
- σ_3: confining pressure;
- σ_d: deviatoric stress;
- σ_{atm}: atmospheric pressure.

5. Testing: high compaction strength

The parameters founded with this model are showed in the following tables:

Curing time [d]		Material	K_1 [-]	K_2 [-]	K_3 [-]	RMS [-]
1	M1	Asfaltival Special	2473.73	0.49	0.06	18.82
	M2	Asfaltival 2.0 Revolution	2217.19	0.57	0.03	23.26
	M3	RoadPav	4117.07	0.16	0.20	32.68
	M4	ProntoSint	2135.43	0.53	-0.05	16.79
	M5	Bitem	2587.21	0.54	-0.04	23.77
	M6	Bitux	2909.46	0.43	-0.02	34.59
	M7	BlackTop	3882.88	0.45	0.01	34.07

Table 5.9: Puppala model, 1 day

Curing time [d]		Material	K_1 [-]	K_2 [-]	K_3 [-]	RMS [-]
28	M1	Asfaltival Special	2065.58	0.52	0.02	21.19
	M2	Asfaltival 2.0 Revolution	1965.60	0.48	0.07	23.43
	M3	RoadPav	4955.49	0.34	0.15	39.43
	M4	ProntoSint	1879.77	0.42	0.03	27.95
	M5	Bitem	1966.88	0.40	0.04	17.06
	M6	Bitux	2532.84	0.40	0.00	27.95
	M7	BlackTop	4253.73	0.34	0.09	29.52

Table 5.10: Puppala model, 28 days

From these tables is possible to say that all the three models don't represent correctly the behavior of the materials; the Root Mean Square (RMS) error is generally high, with only one value lower than ten, in the case of MEPDG model simulating M2 after one day of curing.

There is not also one single model that behaves better, in fact, after a curing time of one day, one material is better represented by Puppala model, three by MEPDG model and four by Uzan model; after 28 days, three mixtures are simulated better by MEPDG and 4 by Uzan. Moreover, for M4, M6 and M7 the model that simulates better the behavior change in time.

To check the accuracy of the models, it is possible to represent the comparison of the calculated and the real resilient modulus in two graphs:

- a graph with the resilient modulus on the vertical axis, and the bulk stress on the horizontal one, that reports both the measured and the calculated moduli;
- a graph with the calculated modulus on the vertical axis and the measured one on the horizontal axis; in this case it is possible to calculate the coefficient of determination (R^2), the proportion of the variance in the dependent variable that is predictable from the independent variable.

As an example, the following graphs represent the results of Uzan model for M3, Puppala model for M4 and MEPDG model for M5.
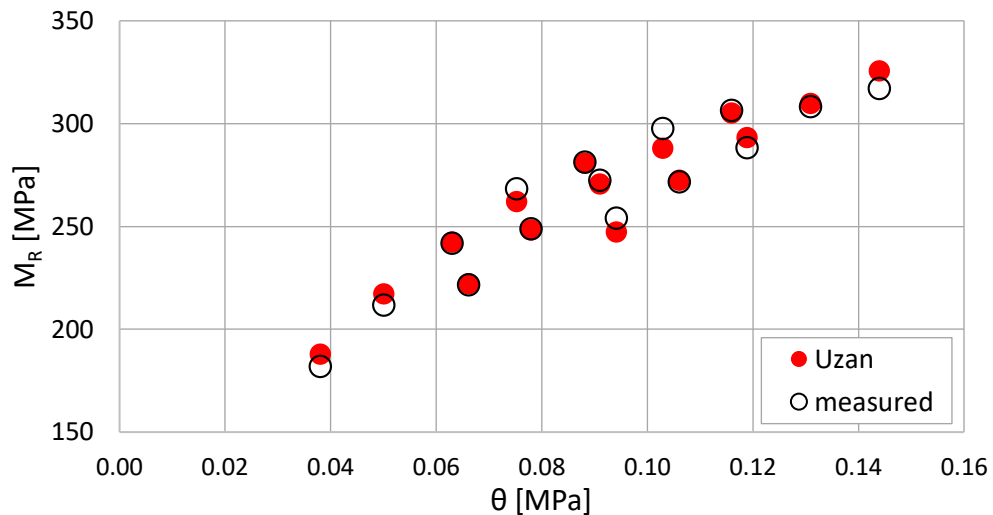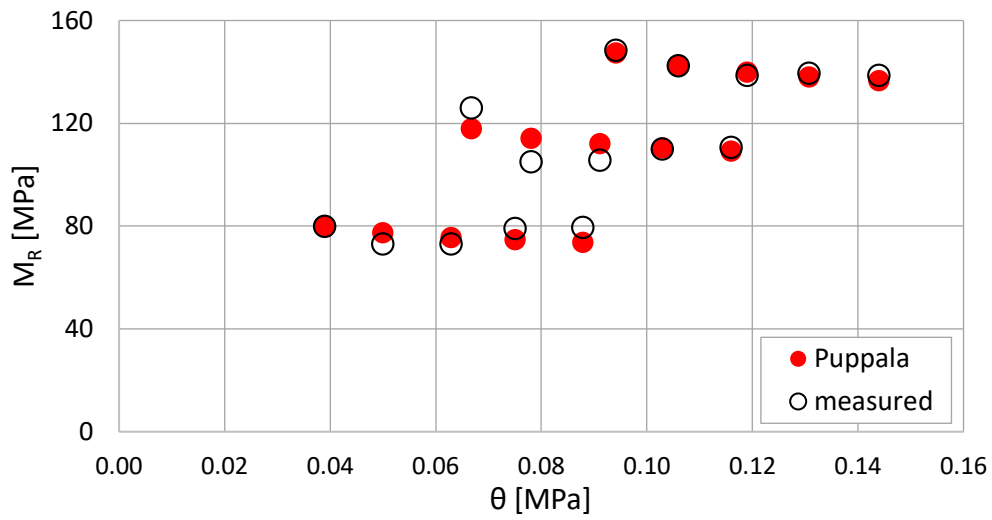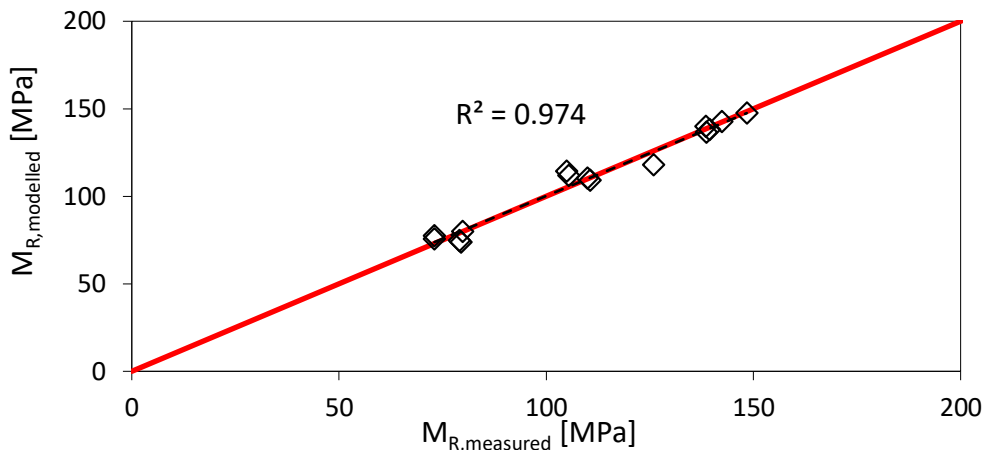

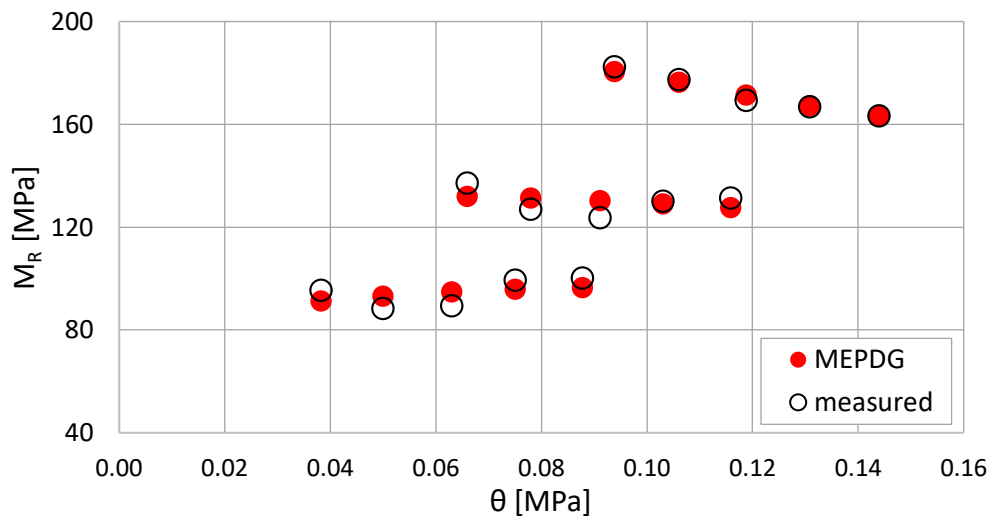Graph 5.1: M3 - Uzan model
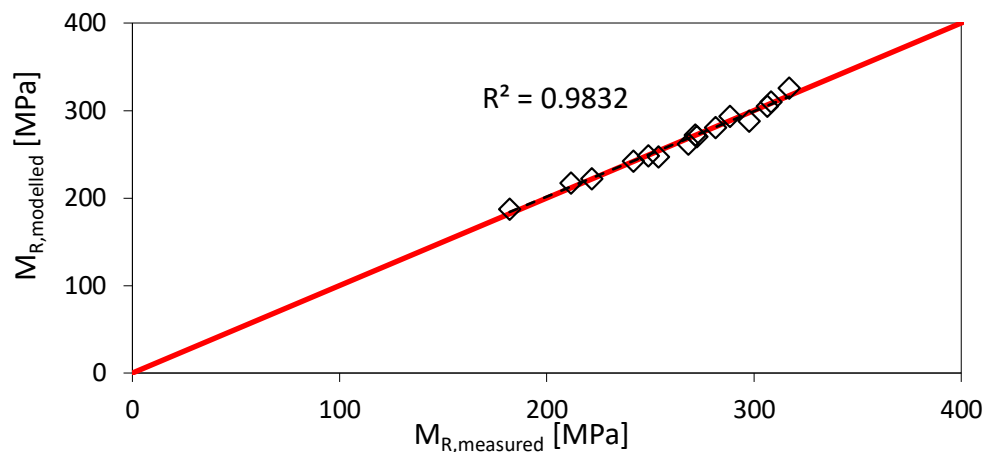
Graph 5.2: M3 - Uzan model, R^2

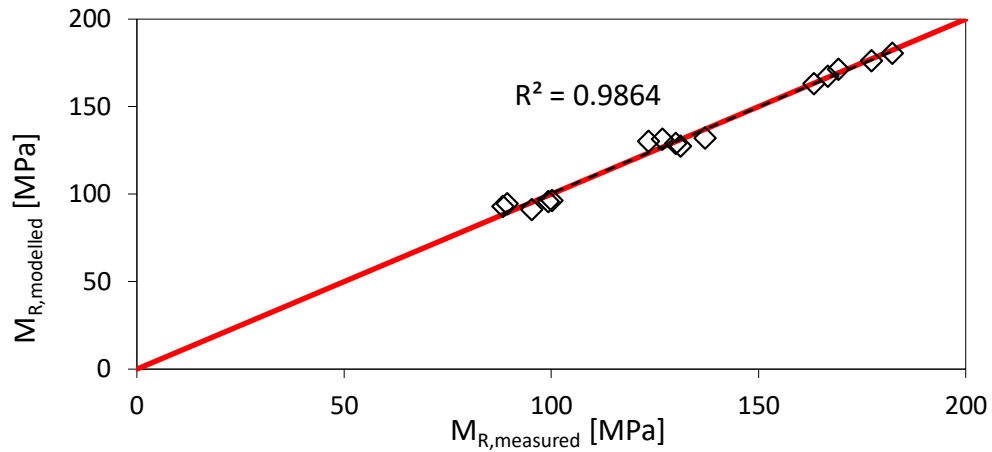# 5. Testing: high compaction strength

Graph 5.3: M4 - Puppala model

$R^2 = 0.974$

Graph 5.4: M4 - Puppala model, R^2

Graph 5.5: M5 - MEPDG model

Graph 5.6: M5 - MEPDG model, R^2

Analyzing the distance between the calculated points and the measured ones, or calculating the distance between the obtained points in the second graphs and its bisector, it is possible to have an idea of the accuracy of the model.

Another correlation possible is the one between CBR and resilient modulus; there are different equations available in literature, one of the more efficient is the correlation made from Uzan (Dione, Fall, Berthaud, Benboudjema, & Michou, 2015):

$$M_R = 91.226 + 0.017 \cdot CBR^2 \qquad\qquad (5.4)$$

Due to the fact that the CBR was evaluated after one day of conditioning, the estimation of the resilient modulus was compared with only the real modulus with the same curing time. The predicted modulus and the percentage errors are shown in the following table:

	Material	M_R [MPa]	$M_{R,predicted}$ [MPa]	Error [%]
M1	Asfaltival Special	119.6	151.1	26.4
M2	Asfaltival 2.0 Revolution	121.8	152.6	25.3
M3	RoadPav	264.8	157.0	40.7
M4	ProntoSint	109.9	115.4	5.0
M5	Bitem	132.1	115.5	12.6
M6	Bitux	166.0	103.0	37.9
M7	BlackTop	208.1	121.2	41.7

Table 5.11: Predicted resilient modulus

It is evident that the average error is quite high, this probably because the predictive model was developed for unbound materials, starting from the CBR of limestones.

An interesting result is the low error of materials M4 and M5, that are the mixtures with the lowest resistance performance in the previous test; so, with references to this analysis, their behavior can be assumed as the one of unbound materials.

One of the reason of the high error is that CBR and resilient modulus are significantly different in nature: the modulus is determined from a dynamic load test and depends on the state of stress, the CBR corresponds to a force measurement results from a monotonous test.

5.3. WHEEL TRACKING TEST

Rutting is one of the main failure modes in pavements; the wheel tracking test was performed to understand the rutting resistance of the seven materials. In this test a compacted slab is subjected to a load given by different passages of a tire.

The slab is compacted following the (UNI EN 12697-33, 2004), while the rutting test is performed according to the (UNI EN 12697-22, 2004).

SLAB PREPARATION

To prepare the slab, a given mass of the mixture is compacted in a rectangular mould under a load applied at first by one wheel with pneumatic tire, then with a smooth steel roller.

The mass is calculated from the density of the material after 180 rounds in the GSC and from the final desired volume of the slab.

The mould used have interior dimensions of: 500 mm for the long edge, 180 mm for the short side, 50 mm in height.

At first the mould is fixed to the machine, which has a movable plate that is used to control the height of the specimen; then the material is poured and the compaction can take place.

The device used for the initial compaction is a wheel equipped with threadless tires with a diameter of 400 mm and a contact width of 80 mm.

Figure 5.8: Roller compactor

5.   Testing: high compaction strength

The compaction is performed in two main phases, an initial assessment one, in which the tire pressure is 0.1 MPa and the load applied is 1 kN; a second one in which the pressure is 0.6 MPa and the load is 5 kN.

When the material is well compacted, a smooth steel roller is used to regulate and to smooth the surface, applying a load of 5 kN; this roller is applied over the tires, which maintain a pressure of 0.6 MPa.

For each material two slabs are made, then they are conditioned for one day at the temperature of 20°C.

A positive aspect of this test is the presence of a lateral confinement: although is not representative of the real situation, because it is smooth and doesn't allows a lateral interlock, it reduces the possibility of collapse of the material, as happened for the ITS test.

During this phase, some materials were not able to compact and they continued to flow also after a great number of compacting cycles (*Figure 5.10*).

Figure 5.9: Slab well compacted

Figure 5.10: Slab compaction problem

TEST DESCRIPTION

The susceptibility of the mixtures to deform is evaluated by measuring the rut depth formed by repeated passes of a loaded wheel at a fixed temperature.

The testing machine is composed of a temperature chamber, in which there are two table that can carry one slab each.

The slabs are loaded by a wheel fitted with a pneumatic tire without tread pattern, with a track width of 80 ± 5 mm and a pressure of 600 kPa.

The two specimens are pushed against the wheel with a pressure of 5000 $\pm$ 50 N and the tire is moved back and forth in linear path with a frequency of travel of 1.0 $\pm$ 1 Hz.

Figure 5.11: Wheel tracking machine   Figure 5.12: Slab positioning

Before starting the test, the density and voids content of the slabs are evaluated, by measuring the mass and taking 15 height measures; these are taken with an electronic caliper in specific points, that will also be used to evaluate the rut depth during the test.
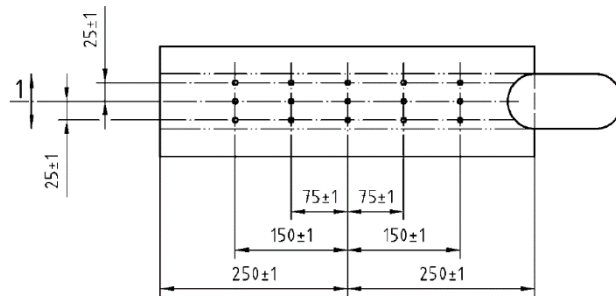

Figure 5.13: Measurement points, UNI EN 12697-22

The first phase of the test consists in 1˙000 settling cycles at environmental temperature; then the temperature is raised up to 40°C, it is measured with a sensor inside one of the two slabs.

The test is interrupted at the desired number of load cycles and the 15 heights are recorded, for this study after 0, 100, 300, 1˙000, 3˙000, 10˙000, 30˙000 cycles.

RESULTS

Because of the low resistance of the materials, only M3 completed the test with all the 30˙000 cycles, one slab of M7 resisted until the first 1˙000 testing cycles while all the others collapsed before the first 1˙000 settling cycles.
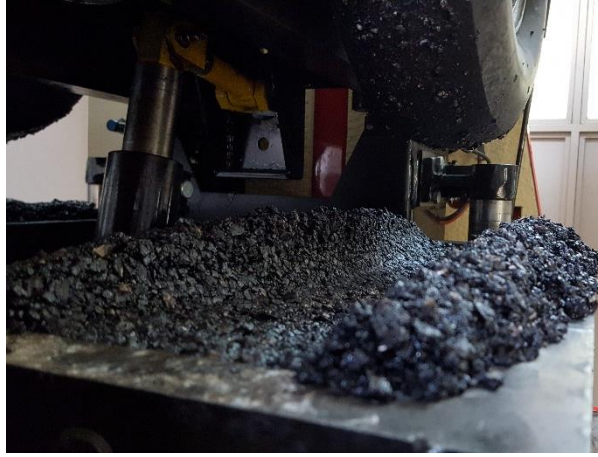

Figure 5.14: M3 - after test

Figure 5.15: M1 - collapsed slab

This problem was already noted during the compaction phase, when some materials continued to flow under the pressure of the tire, even after lots of compacting cycles.

The rutting depth is expressed as a percentage of the slab thickness and it is given as a function of the number of wheel passes:

$$P = 100 \cdot \sum_{j=1}^{15} \frac{(r_{ij} - r_{0j})}{15 \cdot h} \qquad (5.5)$$

In which:

- r_{ij}: rut depth from the reference point [mm];
- r_{0j}: height from the reference point [mm];
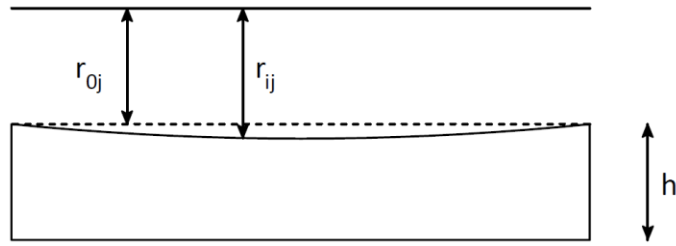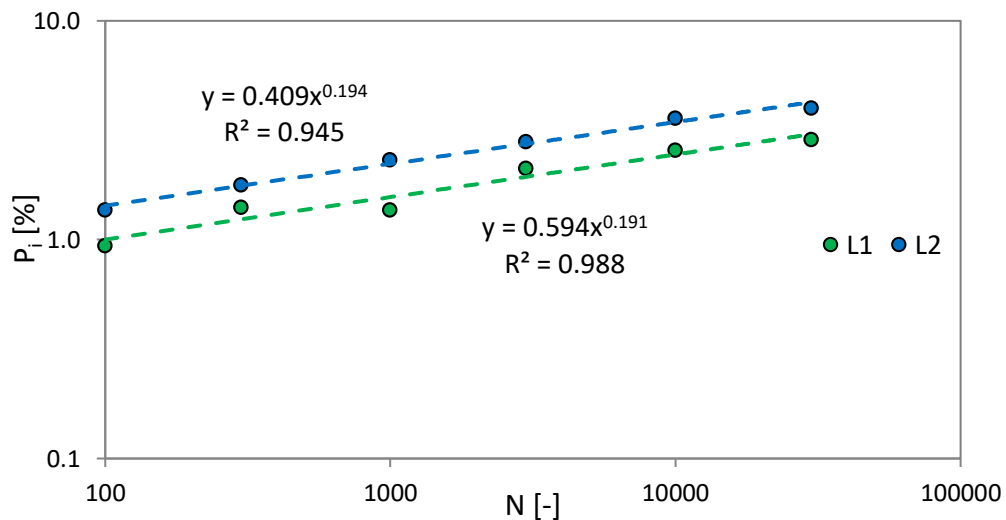- h: thickness of the slab [mm].

Figure 5.16: Reference heights

Then the depth at the different cycles can be represented in a bi-logarithmic graph; the results of M3 are shown in the following table and graph:

ID slab	v_{geo} [%]	P_i [%]					
		100	*300*	*1000*	*3000*	*10000*	*30000*
M3_L1	10.0	0.9	1.4	1.4	2.1	2.6	2.9
M3_L2	10.7	1.4	1.8	2.3	2.8	3.6	4.0
mean	10.3	1.2	1.6	1.8	2.5	3.1	3.4

Table 5.12: M3 - Rutting values

Graph 5.7: M3 - Rutting trend

The first result that can be analyzed is the voids content of the slab, that in average is equal to 10.3%, much greater than the objective void content of 4.4%; this means that this material can't be compacted well with this method, although its performances during the test are very good, compared to the other materials.

The rut depth obtained is very low also after 30˙000 cycles, so this material has a high resistance to rutting already after only one day; the results are comparable with the ones of a hot mix asphalt for a surface course:

| Material	v_{geo} [%]	P_i [%]					
		100	300	1000	3000	10000	30000
M3	10.3	1.2	1.6	1.8	2.5	3.1	3.4
HMA	7.27	-	-	1.5	1.9	2.4	2.8
difference	3.06	-	-	0.4	0.6	0.7	0.6

Table 5.13: Rutting comparison

Analyzing the absolute difference, it is very low after the first thousand cycles, then increases until a level of 0.65%; moreover, the behavior of the two material is quite similar, since the relative difference between the rut depth after 1000 cycles and the one at the end of the test is about 90% for both the mixes.

From this data it is possible to say that M3 will rut in a similar way of a standard hot mix asphalt under traffic load.

Regarding M7, the results are summarized in the following table and graph:

Material	v_{geo} [%]	P_i [%]					
		100	300	1000	3000	10000	30000
M7	22.9	1.1	3.1	collapsed			

Table 5.14: M7 - Rutting values

$$y = 0.012x^{0.973}$$
$$R^2 = 1.000$$
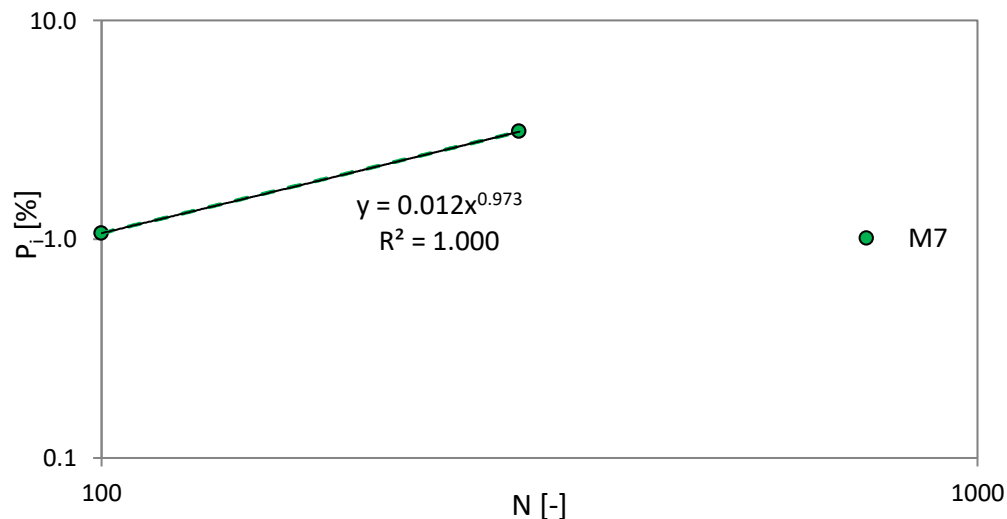
Graph 5.8: M7 - Rutting trend

This material still has a very high void content after the compaction and it gives readable measures only after 100 and 300 cycles. Moreover, the rut depth of M7 after 300 cycles is bigger than the one of M3 after 10˙000 cycles.

5.4. SUMMARY

Based on the results on this chapter, it has been shown that the majority of the products have low resistance also after a high compaction, only M3 shows good results in both the test performed.

During the resilient modulus evaluation and the quick shear test, some of the specimen of M4 and M5 couldn't resist for 28 days, even if they were confined with the plastic membrane.

These mixes have the lowest shear resistance, compared to the other tested mixtures.

These products also show no resistance to rutting, in fact they can't resist to the first settling cycles and no results could be recorded from the wheel tracking test.

In conclusion, they can be defined as the worst ones regarding the high compaction properties.

Materials M1, M2, M6 and M7 gives similar results from the quick shear test after one day of curing, but they behave differently after twenty-eight days, when M7 shown an increase in the shear resistance while for the others there is a small decrease.

Regarding rutting, only M7 has a low resistance, the other materials collapses before the setting cycles.

For these reasons these four mixes can be defined as middle quality regarding high compaction properties.

Material M3 has very good performances related to shear resistance, where it reaches the maximum load that the machine can apply without collapsing, both after one and twenty-eight days of curing.

It was also the only one that resists to all the 30'000 cycles in the wheel tracking test, showing good results with low depth rut, comparable to a standard hot mix asphalt for surface course.

In conclusion, this product is the best one when talking about high compaction properties.

6. MODELLING

6.1. INTRODUCTION

The objective of this chapter is to find a model that can simulate the compaction characteristics of the materials; to do this, different analytical models were analyzed to find the better solution.

The obtained algorithms try to predict the compaction curves of the mixtures, minimizing the difference with the real ones obtained from the GSC in the paragraph 3.6: *Compaction*.

A constitutive model is a mathematical simplification of a quite complex physical behavior, the main aim is to choose a model that is sufficiently accurate, but not too complex and computationally expensive.

The study started from the basic viscoelastic models, but, due to the behavior of the materials when the load is removed, it was necessary to introduce a plastic element, to simulate their permanent deformation at the end.

To understand the behavior of the models, the study started from the analysis of basic types of load, then, to simulate the action given by the GSC, an haversine load was applied.

After the analytical studies, the models were implemented in MATLAB, a multi-paradigm numerical computing environment that, using an optimization algorithm, finds the best fitting solution changing the parameter of the models.

6.2. THEORETICAL BASIS

All the models analyzed are a composition of three simple linear theories: the elastic, the viscous and the plastic. All these theories are perfect idealization and doesn't reflect the real behavior of the materials (Haddad, 1995).

The behavior of the models can be analyzed with the creep and recovery test: the time-dependent response of a material after rapid initial loading up to constant (nominal) stress is denoted creep.

The time-dependent stress change after rapid loading, while the strain is held constant, is denoted relaxation. The relaxation behavior is thus complementary to the creep behavior.

LINEAR ELASTIC THEORY

The linear elastic theory is the simplest way to create a model, it consists only of a linear spring with stiffness modulus E. The constitutive equation is:
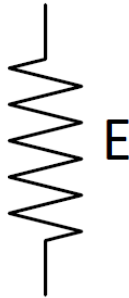
$$\sigma(t) = E \cdot \varepsilon \qquad (6.1)$$

Figure 6.1: Spring

The behavior of this element can be studied with a creep and recovery test (*Figure 6.2* and *Figure 6.3*): the reaction to an applied load σ_0 is:

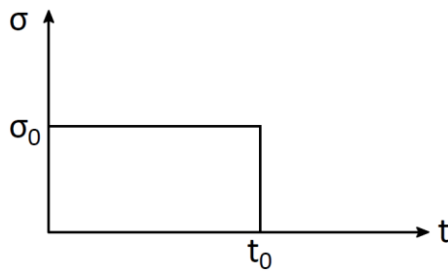$$\varepsilon_0 = \frac{\sigma_0}{E} \tag{6.2}$$

Figure 6.2: Creep and recovery test -
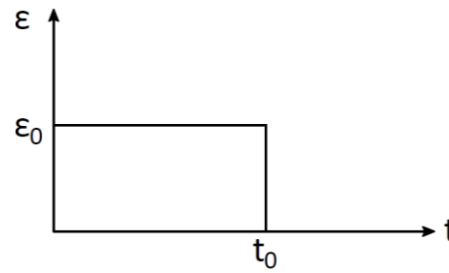*Spring, stress*
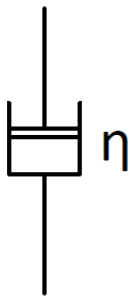

Figure 6.3: Creep and recovery test -
Spring, strain

It's evident that the response of the material is immediate with any load change, and this is not very representative of the behavior of any real material.

LINEAR VISCOUS THEORY

Viscosity is the property of a fluid which opposes the relative motion between two surfaces of the fluid that are moving at different velocities. A velocity gradient is thus established and it can be verified that it is related to the applied shear by a constant η, the viscosity of the fluid.

$$\frac{dv}{dy} = \frac{1}{\eta}\tau \tag{6.3}$$

The linear viscous theory starts from this concept and studies a dashpot, that is a piston moving in a fluid with a certain viscosity. For this element the behavior is:

$$\sigma(t) = \eta \cdot \dot{\varepsilon} \tag{6.4}$$

Figure 6.4: Dashpot

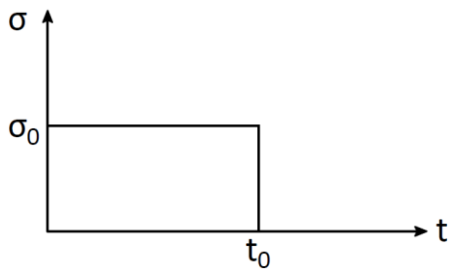The answer of this element to a creep and recovery test is the following:

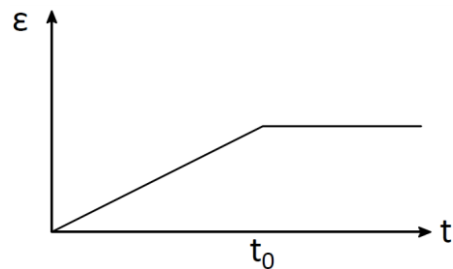Figure 6.5: Creep and recovery test - Dashpot, stress

Figure 6.6: Creep and recovery test - Dashpot, strain

There is no instantaneous deformation, the slope of the creep line is σ_0/η and there is a permanent strain.

VISCOELASTIC THEORY

The viscoelastic theory regards the combination of the viscous and elastic linear theories; there are two main models the Maxwell and the Voight one.

Maxwell model

This model is composed by a spring, with elasticity modulus E, and a dashpot, with viscosity coefficient η, connected in series. In this way the two elements will have the same stress, equal to the applied one, while the total deformation of the model is given by the sum of the strain of the two components.

The scheme and the constitutive equation are:
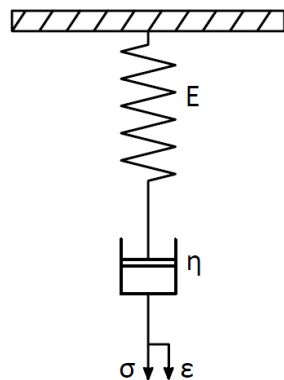
$$\sigma(t) = \dot{\varepsilon} \cdot \eta + \frac{\eta}{E} \cdot \dot{\sigma} \qquad (6.5)$$

Figure 6.7: Maxwell model

The behavior of this model can be studied with both the creep and the relaxation test. Regarding the creep test (*Figure 6.8* and *Figure 6.9*), when the load is applied the dashpot acts like a rigid body, while the spring reacts immediately; during the period in which the load is constant, the deformation of the model is given only by the viscous element.

When the load is removed, the spring returns to the initial position while the dashpot maintains its deformation, so at the end there will be a permanent strain.
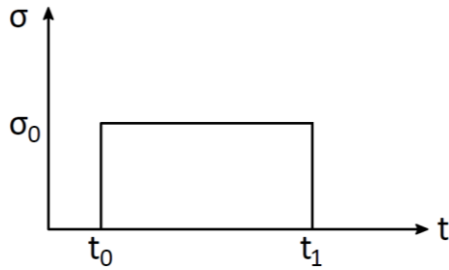

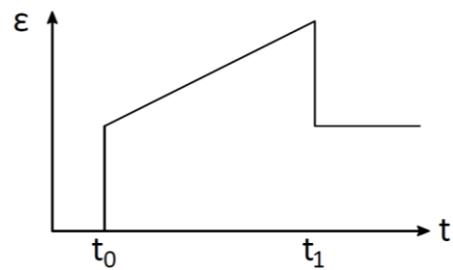Figure 6.8: Creep and recovery test - Maxwell model, stress

Figure 6.9: Creep and recovery test - Maxwell model, strain

Concerning the relaxation test (_Figure 6.10_ and _Figure 6.11_), in the moment when the deformation is applied the system's modulus is only the elasticity modulus of the spring, then the dashpot starts to deform while the spring contracts.
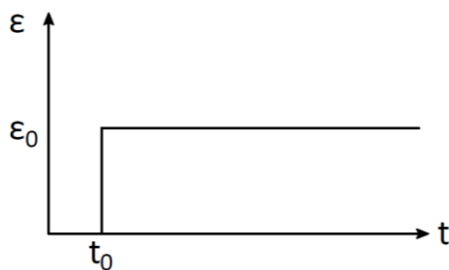

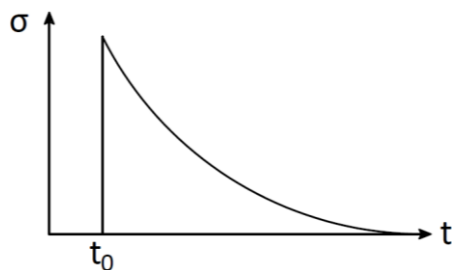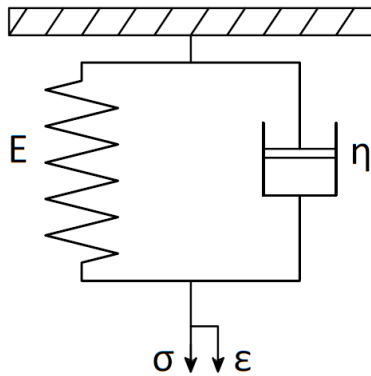Figure 6.10: Relaxation test - Maxwell model, strain

Figure 6.11: Relaxation test - Maxwell model, stress

Voight model

This model is the combination of a spring and a dashpot in parallel: the strain of the spring is the same as the one of the dashpot, while the total stress is the sum of the ones of the two elements.

The model is schematized as:

$$\sigma(t) = E \cdot \varepsilon + \eta \cdot \dot{\varepsilon} \tag{6.6}$$

Figure 6.12: Voight model

During the creep and recovery test (*Figure 6.13* and *Figure 6.14*), applying a load to the model, the spring tries to stretch immediately but is blocked by the dashpot, so all the stress is taken by the viscous element. The system starts to deform with a slope depending on the viscosity of the dashpot.

When the load is removed, the spring starts to contract and again the dashpot holds it back; after a given time, depending on the parameters of the model, the system will return to its original position.
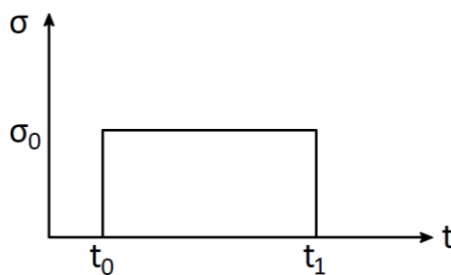

*Figure 6.13: Creep and recovery test -
Voight model, stress*

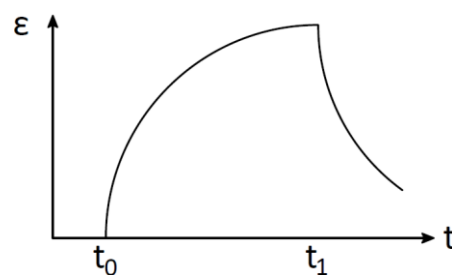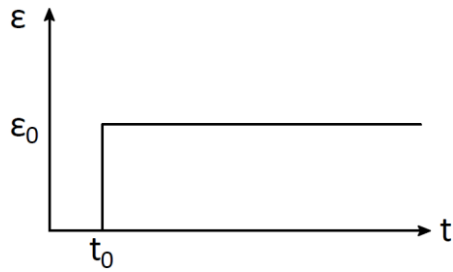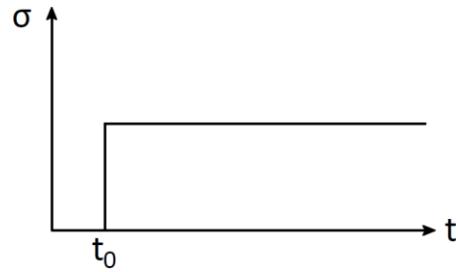*Figure 6.14: Creep and recovery test -
Voight model, strain*

6.   Modelling

This model doesn't react well to the relaxation test (*Figure 6.15* and *Figure 6.16*), in particular, to apply the initial deformation it's necessary an infinite instantaneous force.

Figure 6.15: Relaxation test - Voight model, strain
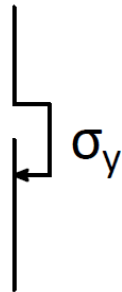
Figure 6.16: Relaxation test - Voight model, stress

PLASTIC THEORY

Plasticity can be considered the property of materials that can have their shape easily changed by the application of appropriately directed forces, and retain their new shape upon removal of such forces(Lubliner, 2006).

It can be idealized as a slider with a certain yielding strength σ_y; its constitutive law is:

$$\sigma(t) \le \sigma_y \tag{6.7}$$

Figure 6.17: Slider

When a load is applied, this element starts to deform only if the stress is bigger than the yielding stress, and the strain continues to increase until the stress lowers:
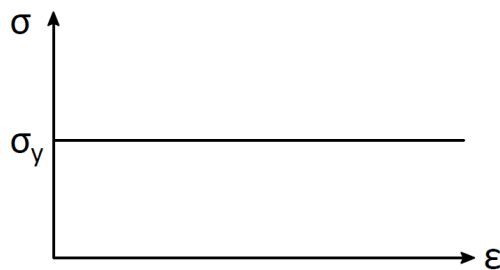
Figure 6.18: Plastic behavior

This result is a perfect idealization of materials, usually it is present at least a starting elastic behavior.

ELASTIC – PERFECTLY PLASTIC THEORY

To improve the plastic theory, it's possible to attach a spring in series with the dashpot, in this way the model will have a more progressive behavior.
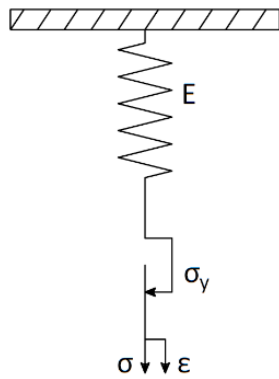
Figure 6.19: Elastic-plastic
model

$$\sigma(t) = E \cdot \varepsilon \leq \sigma_y \qquad (6.8)$$

When the load is applied the system starts to deform with an elastic behavior until the achieving of the yielding stress, after which there is a plastic deformation.
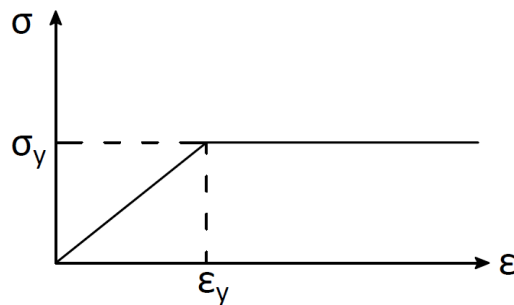
Figure 6.20: Elastic-plastic behavior

6.3. ANALYTICAL MODELS

Starting from the basic theories, it's possible to create complex arrangements then solve the mathematical equations and compare the results with the real measures.

In this paragraph will be analyzed different models that were implemented to improve the solution, reducing the difference with the real compaction curves obtained with the GSC.

ANTI-ZENER

This model is composed by a Voight model linked with a dashpot in series.

Figure 6.21: Anti-Zener model

The model is characterized by the following functions:

$$\sigma = \sigma_1 = \sigma_2 \tag{6.9}$$

$$\varepsilon = \varepsilon_1 + \varepsilon_2 \tag{6.10}$$

6. Modelling

These are the basic equations that control the model, deriving and combining them it is possible to obtain the constitutive law of the system.

$$\dot{\varepsilon} = \dot{\varepsilon}_1 + \dot{\varepsilon}_2 \tag{6.11}$$

$$\dot{\varepsilon}_2 = \frac{\sigma}{\eta_2} \tag{6.12}$$

$$\dot{\varepsilon}_1 = \frac{1}{\eta_1}(\sigma - \varepsilon_1 \cdot E_1) \tag{6.13}$$

$$\dot{\varepsilon}_1 = \frac{1}{\eta_1}(\sigma - \varepsilon_1 \cdot E_1) \tag{6.14}$$

$$\varepsilon_1 = \varepsilon - \varepsilon_2 = \varepsilon - \frac{1}{\eta_2} \cdot \int \sigma \, dt \tag{6.15}$$
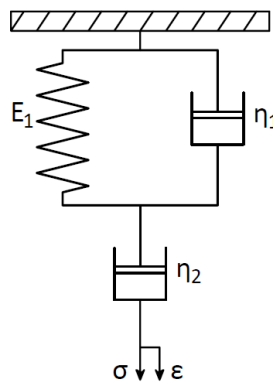
Substituting equation (6.12) and (6.13) into (6.11):

$$\dot{\varepsilon} = \frac{1}{\eta_1}(\sigma - \varepsilon_1 \cdot E_1) + \frac{\sigma}{\eta_2} \tag{6.16}$$

Using equation (6.15) into (6.16):

$$\dot{\varepsilon} = \frac{1}{\eta_1}\left(\sigma - \varepsilon \cdot E_1 + \frac{E_1}{\eta_2} \cdot \int \sigma \, dt\right) + \frac{\sigma}{\eta_2} \tag{6.17}$$

From which:

$$\dot{\varepsilon} + \frac{\varepsilon \cdot E_1}{\eta_1} = \sigma \cdot \left(\frac{1}{\eta_1} + \frac{1}{\eta_2}\right) + \frac{E_1}{\eta_1 \cdot \eta_2} \cdot \int \sigma \, dt \tag{6.18}$$

Considering $\tau_1 = \eta_1/E_1$

$$\dot{\varepsilon} + \frac{1}{\tau_1} \cdot \varepsilon = \sigma \cdot \left(\frac{\eta_1 + \eta_2}{\eta_1 \cdot \eta_2}\right) + \frac{1}{\tau_1 \cdot \eta_2} \cdot \int \sigma \, dt \tag{6.19}$$

Taking the derivative:

$$\ddot{\varepsilon} + \frac{1}{\tau_1} \cdot \dot{\varepsilon} = \dot{\sigma} \cdot \left(\frac{\eta_1 + \eta_2}{\eta_1 \cdot \eta_2}\right) + \frac{1}{\tau_1 \cdot \eta_2} \cdot \sigma \tag{6.20}$$

This is the constitutive equation of the Anti-Zener model, it can be written in the common form as:

$$\ddot{\varepsilon} + a \cdot \dot{\varepsilon} + b \cdot \varepsilon = g \cdot \dot{\sigma} + h \cdot \sigma \qquad (6.21)$$

Where:

- $a = \dfrac{1}{\tau_1}$ \qquad\qquad\qquad\qquad (6.22)

- $b = 0$ \qquad\qquad\qquad\qquad (6.23)

- $g = \dfrac{\eta_1 + \eta_2}{\eta_1 \cdot \eta_2}$ \qquad\qquad\qquad\qquad (6.24)

- $h = \dfrac{1}{\tau_1 \cdot \eta_2}$ \qquad\qquad\qquad\qquad (6.25)

The constitutive equation in the common form can be solved using analytical or numerical methods. The implementation in MATLAB of this model will be discussed in the following paragraph.

ANTI-ZENER PLUS SPRING

This model is an evolution of the previous one, it is composed by an Anti-Zener model connected with a spring in parallel.
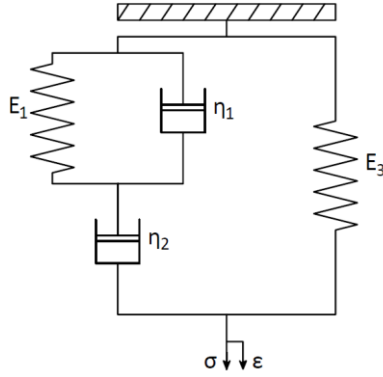
Figure 6.22: Anti-Zener plus spring

model

This model is characterized by the following fundamental laws:

$$\sigma = \sigma_{AZ} + \sigma_3 \qquad (6.26)$$

$$\varepsilon = \varepsilon_{AZ} = \varepsilon_3 \qquad (6.27)$$

In which the subscript AZ corresponds to the stress and strain in the Anti-Zener model. By using a procedure similar to the one seen in the previous model, it is possible to obtain the following constitutive law, expressed in common form:

$$\ddot{\varepsilon} + a \cdot \dot{\varepsilon} + b \cdot \varepsilon = g \cdot \dot{\sigma} + h \cdot \sigma \qquad (6.28)$$

In which:

- $a = \dfrac{1}{\tau_1} + E_3 \cdot \left(\dfrac{\eta_1 + \eta_2}{\eta_1 \cdot \eta_2} \right)$ (6.29)

- $b = \dfrac{E_3}{\tau_1 \cdot \eta_2}$ (6.30)

- $g = \dfrac{\eta_1 + \eta_2}{\eta_1 \cdot \eta_2}$ (6.31)

- $h = \dfrac{1}{\tau_1 \cdot \eta_2}$ (6.32)

ANTI-ZENER PLUS SLIDER

This model is similar to the previous one, but instead of a spring there is a slider linked in parallel with an Anti-Zener.
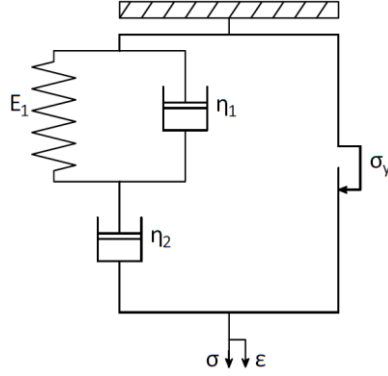
Figure 6.23: Anti-Zener plus slider

model

Also in this case, starting from the basic constitutive law, it is possible to obtain a generalized equation in common form, which is:

$$\ddot{\varepsilon} + a \cdot \dot{\varepsilon} + b \cdot \varepsilon = g \cdot \dot{\sigma} + h \cdot \left(\sigma - \sigma_y \right) \tag{6.33}$$

Where:

- $a = \dfrac{1}{\tau_1}$ (6.34)

- $b = 0$ (6.35)

- $g = \dfrac{\eta_1 + \eta_2}{\eta_1 \cdot \eta_2}$ (6.36)

- $h = \dfrac{1}{\tau_1 \cdot \eta_2}$ (6.37)

In this it is important to highlight that the model doesn't deform until the stress inside the slider reaches the yielding stress, so whenever there is:

$$\sigma - \sigma_{AZ} < \sigma_y \tag{6.38}$$

The system acts like a rigid body.

Bingham

The Bingham model is the simplest elastoviscoplastic model, it is composed by a spring, a dashpot and a slider all in parallel.
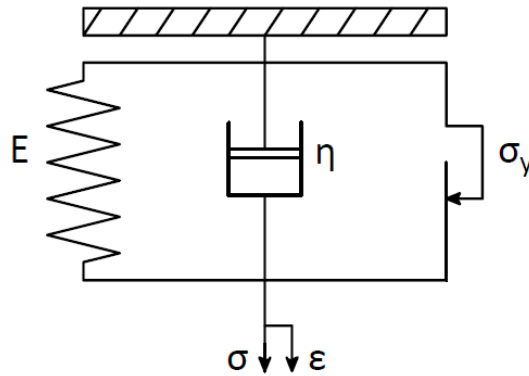
Figure 6.24: Bingham model

The constitutive laws of the elements are:

$$\sigma_{sp} = E_1 \cdot \varepsilon \tag{6.39}$$

$$\sigma_d = \eta \cdot \dot{\varepsilon} \tag{6.40}$$

$$\sigma_{sl} \leq \sigma_y \tag{6.41}$$

In which the subscripts mean:

- sp: spring element;
- d: dashpot element;
- sl: slider element.

The total stress is:

$$\sigma = \sigma_{sp} + \sigma_d + \sigma_{sl} \tag{6.42}$$

The generalized equation is:

$$\dot{\varepsilon} + \frac{1}{\tau_1}\varepsilon = \frac{\sigma - \sigma_y}{\eta_1} \qquad (6.43)$$

Also in this case, the system acts like a rigid body until the stress inside the slider is lower than the yielding stress.

The behavior of the model is:

- $\ddot{\varepsilon} = 0$ $\qquad\qquad |\sigma_{sl}| = |\sigma - E_1 \cdot \varepsilon| \leq \sigma_y$ $\qquad (6.44)$

- $\ddot{\varepsilon} > 0$ $\qquad\qquad \sigma_{sl} = \sigma - E_1 \cdot \varepsilon - \eta \cdot \dot{\varepsilon} = \sigma_y$ $\qquad (6.45)$

BINGHAM PLUS SPRING

This model is an implementation of the simple Bingham system, with the addition of a spring in series.
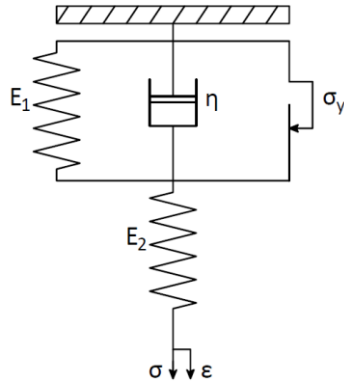
Figure 6.25: Bingham plus spring

model

The generalized equation is:

$$\dot{\varepsilon} + \frac{1}{\tau_1}\varepsilon_B = \frac{\sigma - \sigma_y}{\eta_1} + \frac{\dot{\sigma}}{E_2} \qquad (6.46)$$

In which the subscript B corresponds to the stress and strain in the Bingham model.

This system has a double behavior: since the stress is equal in both the elements, until the applied load is lower than the yielding stress of the slider, there is only the response of the spring, while for higher stresses also the Bingham element starts to work.

BINGHAM AND VOIGHT

This model is composed by a Bingham model linked with a Voight in series.
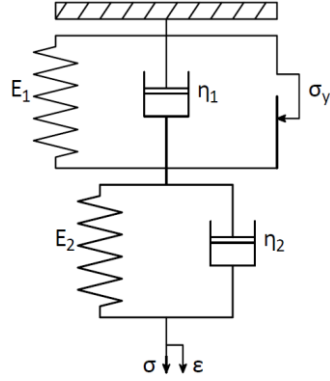
Figure 6.26: Bingham and Voight

model

The fundamental laws of this model are:

$$\sigma = \sigma_B = \sigma_V \tag{6.47}$$

$$\varepsilon = \varepsilon_B + \varepsilon_V \tag{6.48}$$

Combining and deriving them, the result is the following generalized equation:

$$\dot{\varepsilon} + \frac{1}{\tau_1}\varepsilon_B + \frac{1}{\tau_2}\varepsilon_V = \left(\frac{1}{\eta_1} + \frac{1}{\eta_2}\right)\sigma - \frac{\sigma_y}{\eta_1} \tag{6.49}$$

BINGHAM AND MAXWELL

This system is similar to the last one, but there is a Maxwell model instead of a Voight one, connected in series with a Bingham.
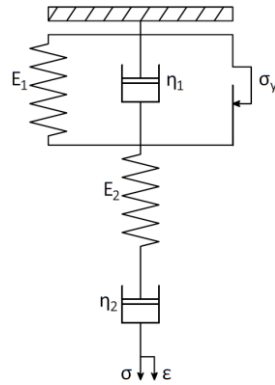
Figure 6.27: Bingham and

Maxwell model

Following the same procedure as the previous models, it's possible to obtain the following generalized equation:

$$\dot{\varepsilon} + \frac{1}{\tau_1}\varepsilon_B = \frac{\dot{\sigma}}{E_2} + \frac{\sigma}{\eta_2} + \frac{\sigma - \sigma_y}{\eta_1} \tag{6.50}$$

6.4. MATLAB COMPUTATION

MATLAB (MATrix LABoratory) is a multi-paradigm numerical computing environment and proprietary programming language developed by MathWorks.

This software is used in this study matrix manipulations, implementation of algorithms and plotting of functions and data.

The analysis starts with the implementation of the generalized equation in the computing environment, then, to calibrate the model and to check the accuracy of the code, some simple load types were simulated.

The model analyzed with this type of loads was the Anti-Zener, because it was possible to make a comparison between the numerical solution and the analytical one and verify the correctness of the simulation.

At first a constant rate load was used, which can be described with the following equation:

$$\sigma(t) = A \cdot t \qquad\qquad (6.51)$$

Graphically it is represented as:
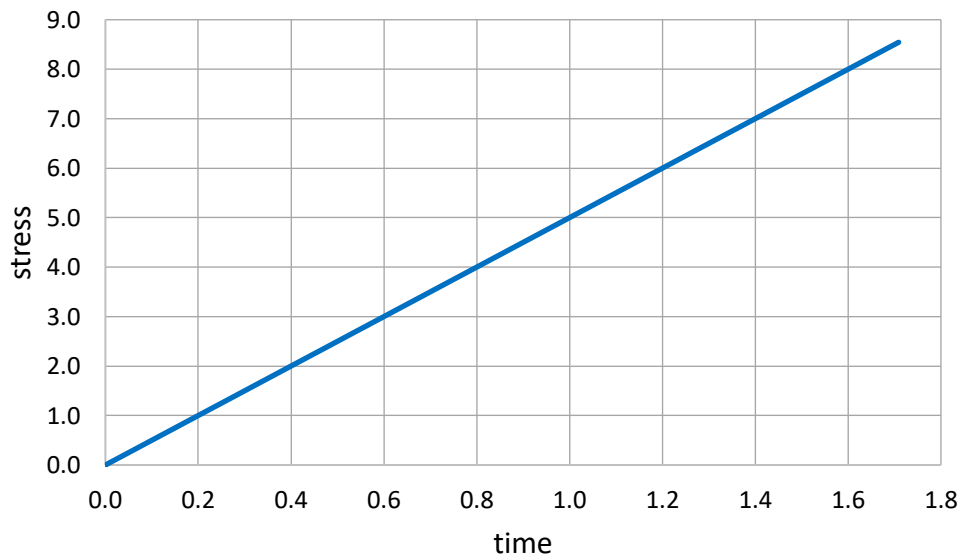
Graph 6.1: Constant rate load, stress
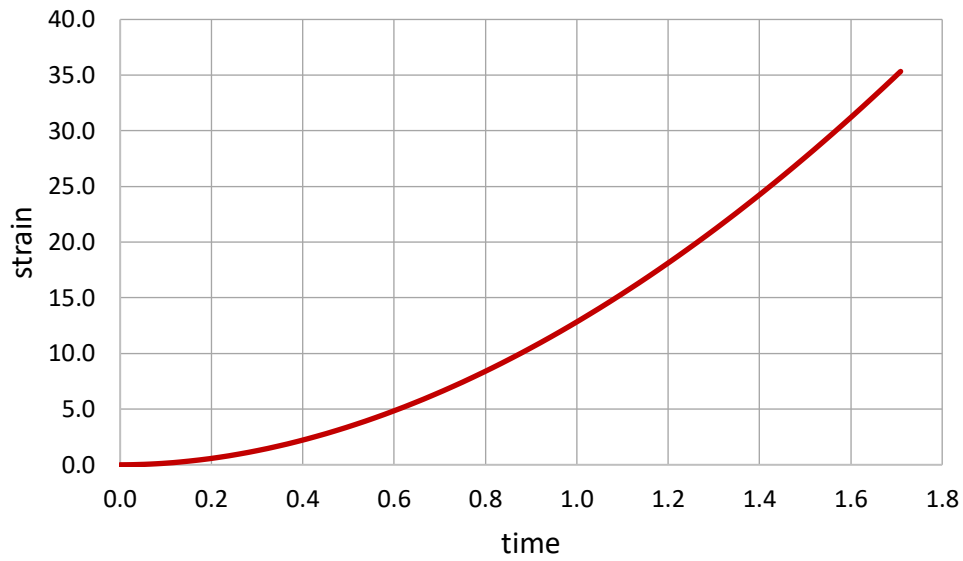
Graph 6.2: Constant rate load, strain

The following step was to increase the complexity of the load, using a sinusoidal one and then a haversine one, which has a sinusoidal shape until a certain time, then it stops; this is more simulative of the assumed GSC load.

The general equation for the sinusoidal load is:

$$\sigma(t) = A \cdot sin(2\pi f t + \phi) + D \qquad (6.52)$$

While for the haversine load is:

$$\begin{cases} t < t_{hav} & \sigma(t) = A \cdot sin(2\pi f t + \phi) + D \\ t \geq t_{hav} & \sigma(t) = 0 \end{cases} \qquad (6.53)$$

Graphically they can be described as:
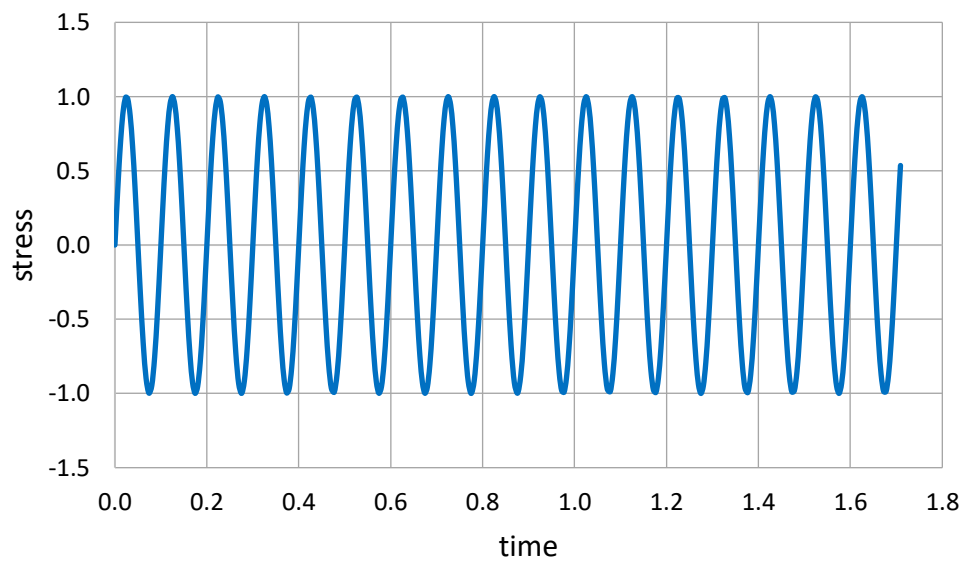
Graph 6.3: Sinusoidal load, stress
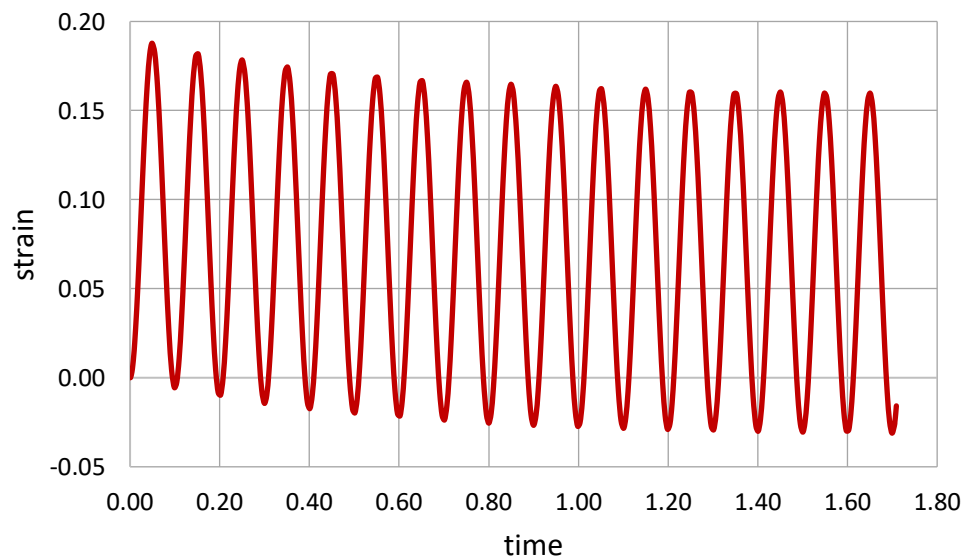
Graph 6.4: Sinusoidal load, strain
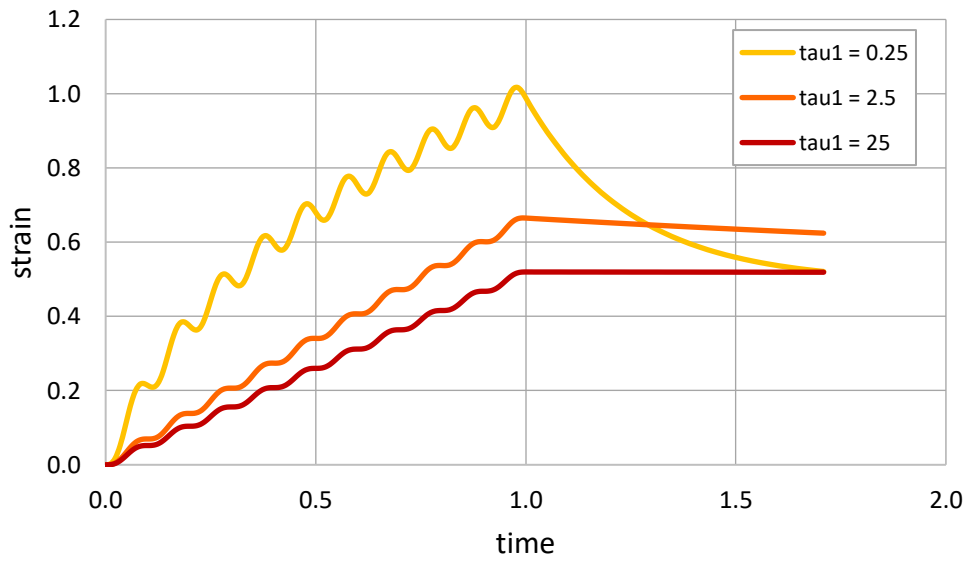
Graph 6.5: Haversine load, strain
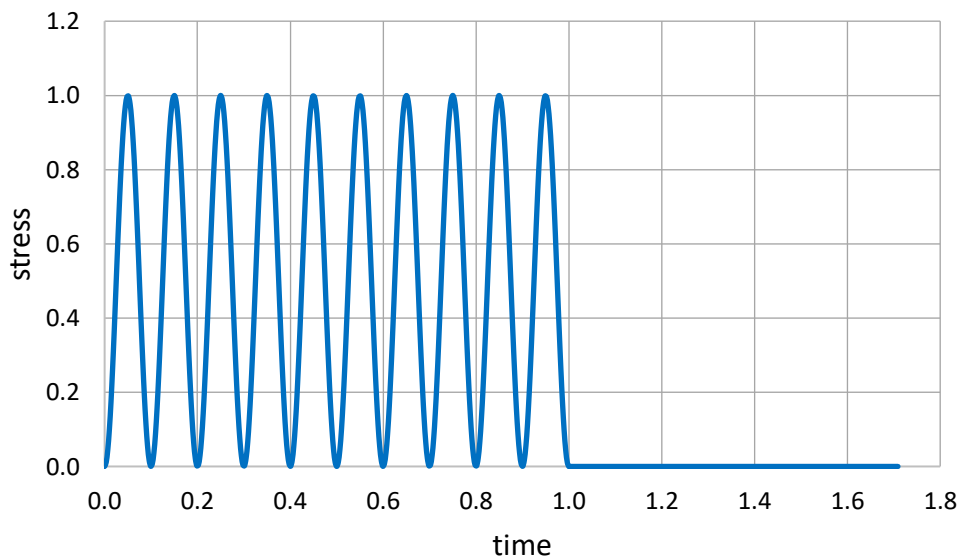
Graph 6.6: Haversine load, stress

Also in this case, regarding the sinusoidal load, it was possible to compare the numerical solution with the analytical one, to check the accuracy of the code. In the case of haversine load, different parameters were tried, to start to understand their influence in the model.

6.   Modelling

The last step was to create a simulative load of the GSC, in this study it was assumed as a haversine load, whose sinusoidal part oscillates between 585 and 600 kPa, with a frequency of 0.5 Hz. The load last 360 s to simulate the 180 rounds of the compaction curves.

$$\sigma(t) = A \cdot sin(2\pi ft + \phi) + D \qquad (6.54)$$

In which:

- *A:* 7.5 kPa;
- *f:* 0.5 Hz;
- *ϕ:* -π/2;
- *D:* 592.5 kPa.
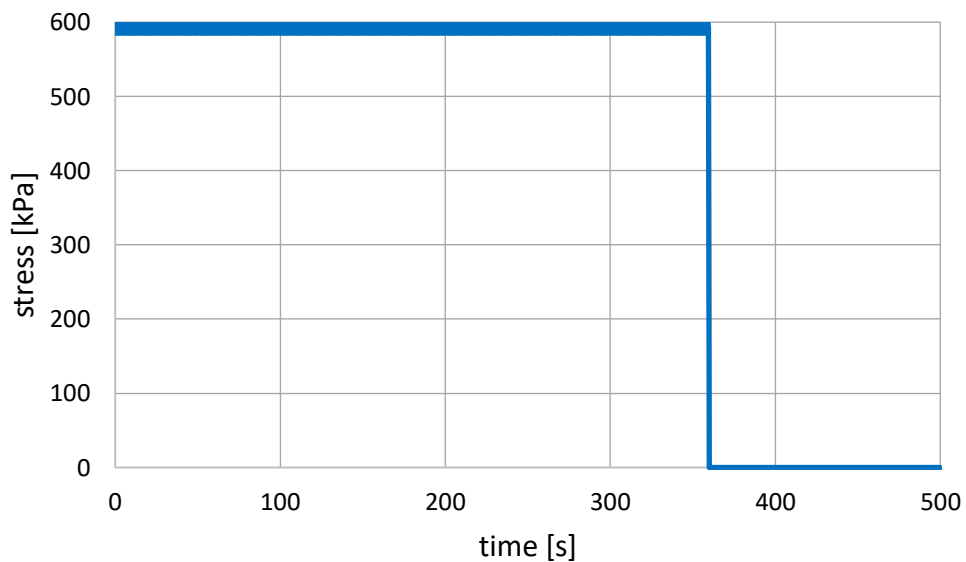
Graph 6.7: GSC load, stress

Once defined the load type, it was possible to start the simulation of the various models presented in the previous paragraph.

The objective of this part was to obtain a set of parameters that describe the model, in a way to minimize the distance between the simulated compaction curve and the real one.

6.   Modelling

To do this, the genetic algorithm was used: this method was invented by John Holland in the 1960s and allows to move from one population of element to a new one, using a "natural selection" together with some bio-inspired operators, such as mutation, crossover and inversion (Mitchell, 1996).

Using this method, at each population a certain number of sets of parameters is created, then the distance from the real curve is calculated and the best solution is saved; starting from this population, a new one is generated, until reaching some stopping criteria, defined by the users.

This method was chosen because its advantages, with respect to other optimization algorithm, is that it has greater probability to find the global minimum, instead of focusing on a local one.

The study started with the comparison of six of the models analyzed in the previous paragraph, comparing them to the compaction curve of M3, in order to choose the best ones.

In the following pages, the simulated compaction curves and the related parameters of the models are shown.

ANTI-ZENER MODEL

Model	M3 RoadPav					
	E_1	E_2	η_1	η_2	σ_y	RMS
Anti-Zener	41	-	612	5056746	-	2.89

Table 6.1: M3 - Anti-Zener model
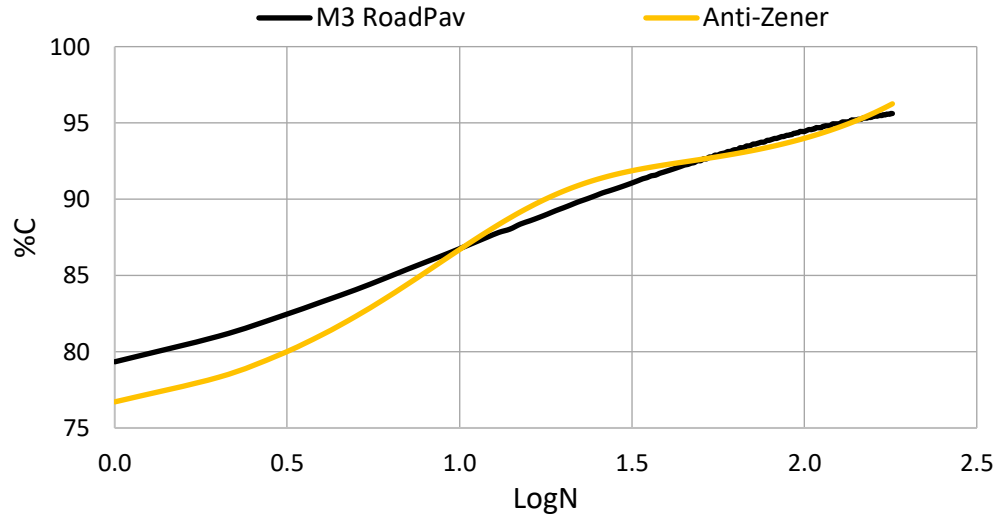
Graph 6.8: M3 - Anti-Zener model

ANTI-ZENER PLUS SLIDER MODEL

Model	M3 RoadPav					
	E_1	E_2	η_1	η_2	σ_y	RMS
Anti-Zener plus slider	110	-	496	527609	577	5.44

Table 6.2: M3 - Anti-Zener plus slider model
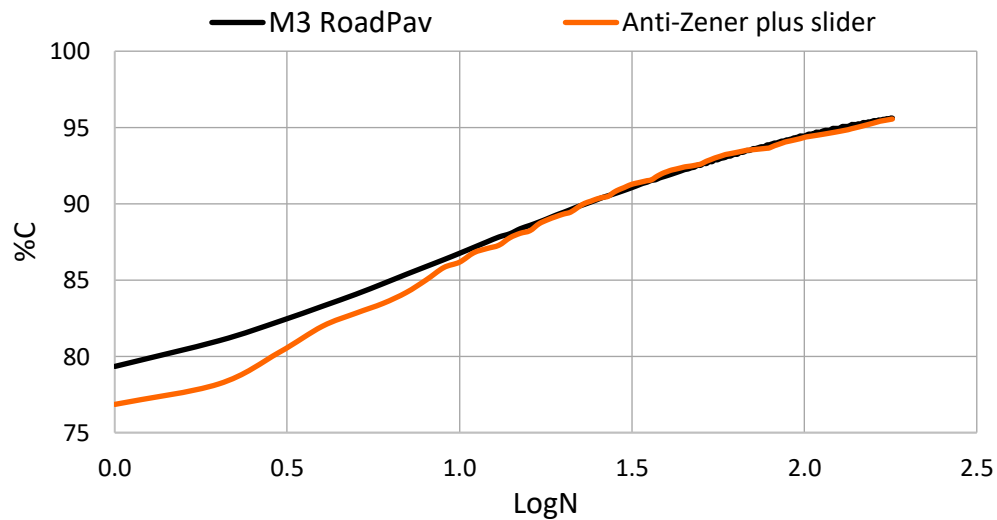
Graph 6.9: M3 - Anti-Zener plus slider model

BINGHAM MODEL

Model	M3 RoadPav					
	E_1	E_2	η_1	η_2	σ_y	RMS
Bingham	125	-	886	-	573	8.74

Table 6.3: M3 - Bingham model
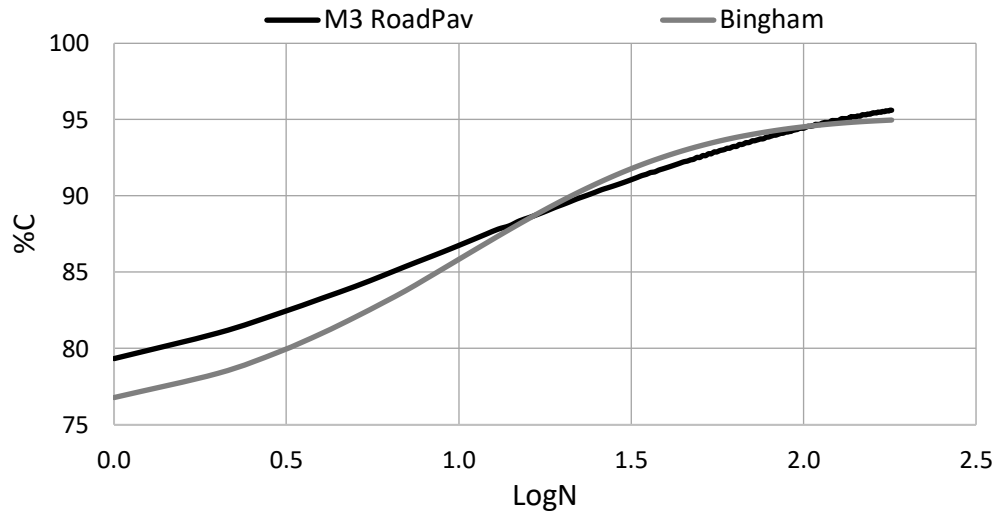
Graph 6.10: M3 - Bingham model

BINGHAM PLUS SPRING MODEL

Model	M3 RoadPav					
	E_1	E_2	η_1	η_2	σ_y	RMS
Bingham plus spring	163	107399	1337	-	566	8.78

Table 6.4: M3 - Bingham plus spring model
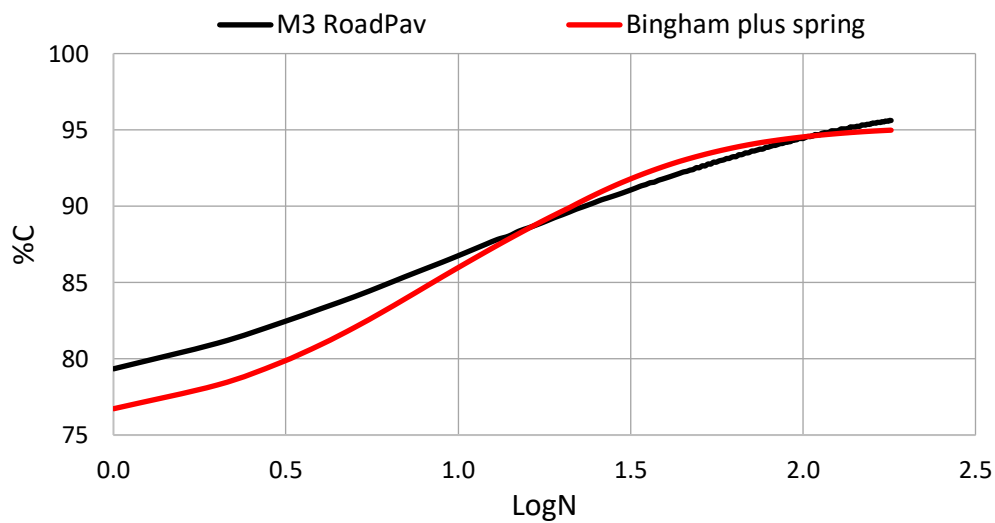
Graph 6.11: M3 - Bingham plus spring model

BINGHAM PLUS VOIGHT MODEL

Model	M3 RoadPav					
	E_1	E_2	η_1	η_2	σ_y	RMS
Bingham plus Voight	6444	3315	6903318	46989	579	8.33

Table 6.5: M3 - Bingham plus Voight model
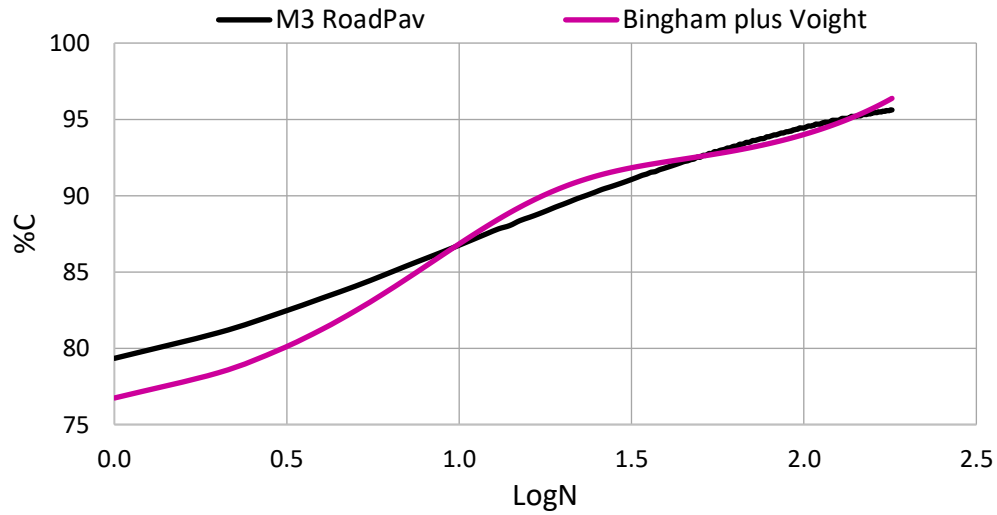
Graph 6.12: M3 - Bingham plus Voight model

BINGHAM PLUS MAXWELL MODEL

Model	M3 RoadPav					
	E_1	E_2	η_1	η_2	σ_y	RMS
Bingham plus Maxwell	152	9758819	1065	5775154	572	4.78

Table 6.6: M3 - Bingham plus Maxwell model
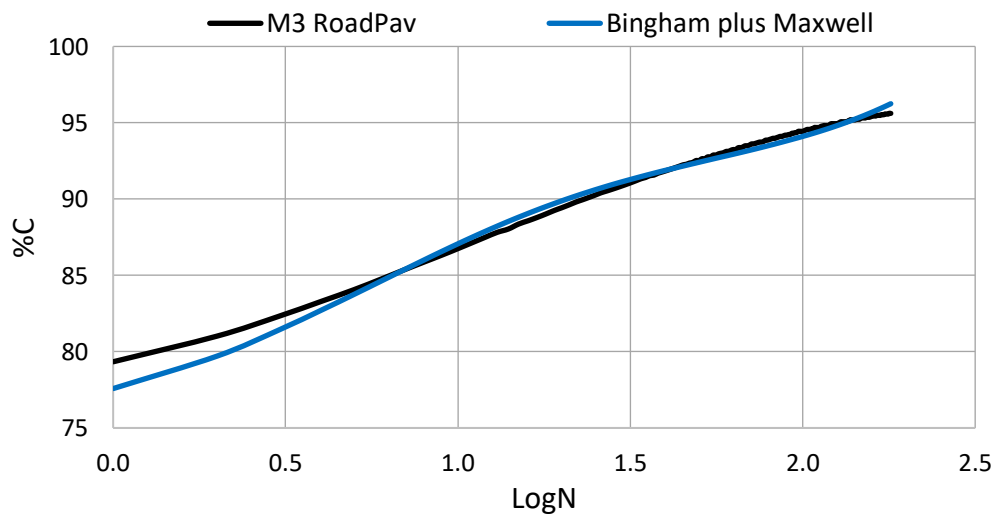
Graph 6.13: M3 - Bingham plus Maxwell model

6.   Modelling

Analyzing the graph and the errors, it is evident that the best fitting model is the Bingham plus Maxwell; another model with a low error is the Anti-Zener plus slider, but the shape of the curve is much more oscillatory, compared to the real one.

The simulation of the other materials, using these two models, are represented in the following pages.

M1 Asfaltival special

Model	M1 Asfaltival Special					
	E_1	E_2	η_1	η_2	σ_y	RMS
Anti-Zener plus slider	140	-	575	135996	574	5.14
Bingham plus Maxwell	108	9758819	1035	4616830	579	2.69

Table 6.7: M1 - Anti-Zener plus slider and Bingham plus Maxwell models
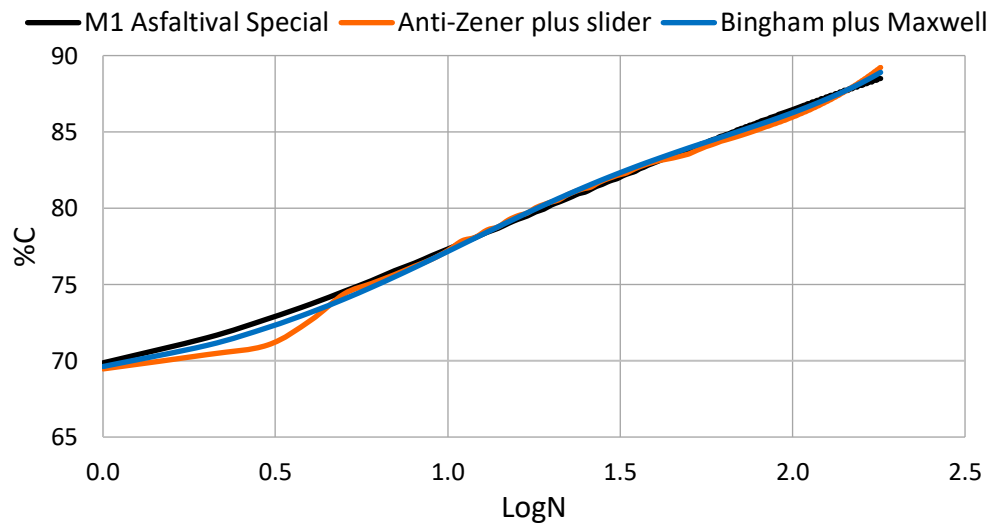
Graph 6.14: M1 - Anti-Zener plus slider and Bingham plus Maxwell models

M2 Asfaltival 2.0 Revolution

Model	M2 Asfaltival 2.0 Revolution					
	E_1	E_2	η_1	η_2	σ_y	RMS
Anti-Zener plus slider	107	-	477	122348	578	3.65
Bingham plus Maxwell	125	590	1755	4418074	572	3.81

Table 6.8: M2 - Anti-Zener plus slider and Bingham plus Maxwell models
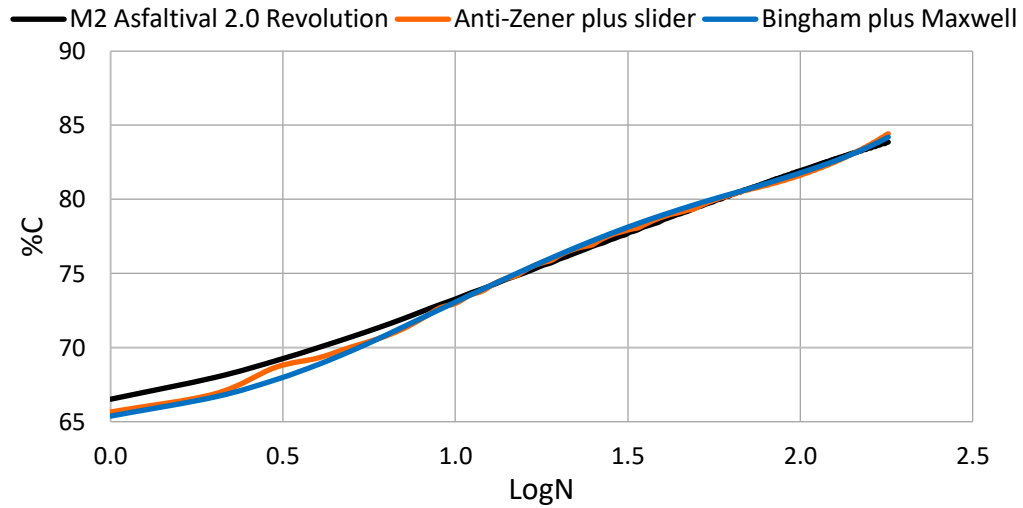
Graph 6.15: M2 - Anti-Zener plus slider and Bingham plus Maxwell models

M4 ProntoSint

Model	M4 ProntoSint					
	E_1	E_2	η_1	η_2	σ_y	RMS
Anti-Zener plus slider	141	-	737	223133	575	3.74
Bingham plus Maxwell	141	8730	1590	6018751	576	2.66

Table 6.9: M4 - Anti-Zener plus slider and Bingham plus Maxwell models
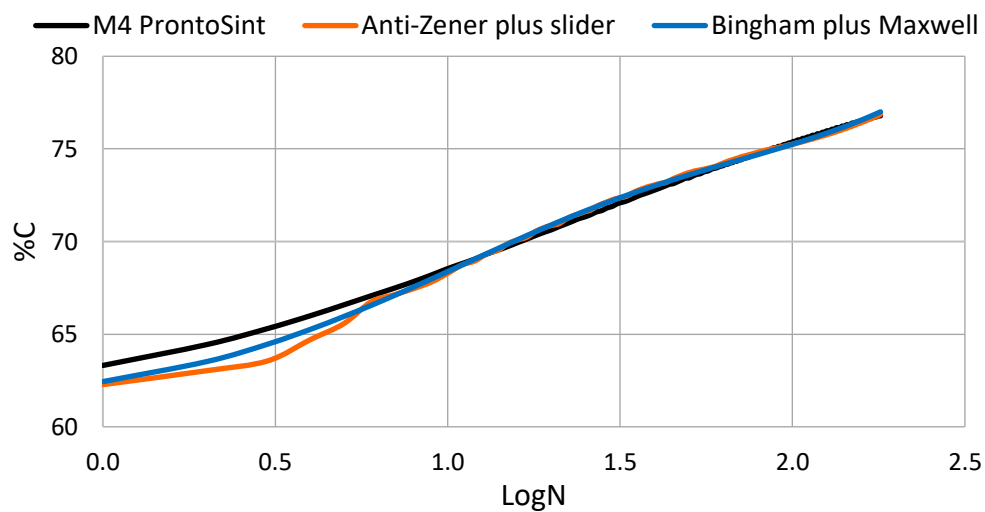
Graph 6.16: M4 - Anti-Zener plus slider and Bingham plus Maxwell models

M5 Bitem

Model	M5 Bitem					
	E_1	E_2	η_1	η_2	σ_y	RMS
Anti-Zener plus slider	134	-	639	164449	577	2.68
Bingham plus Maxwell	911	9574273	16097	4640188	456	4.43

Table 6.10: M5 - Anti-Zener plus slider and Bingham plus Maxwell models
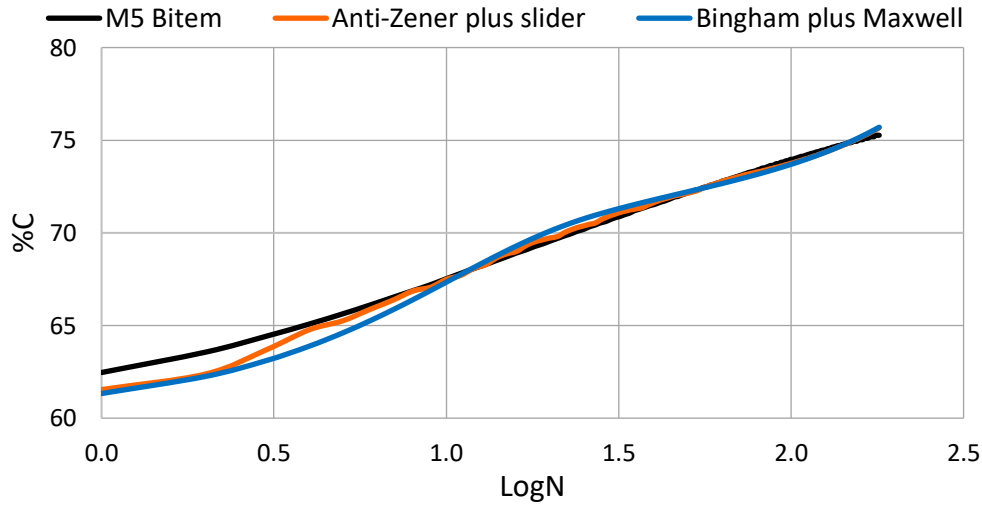
Graph 6.17: M5 - Anti-Zener plus slider and Bingham plus Maxwell models

M6 Bitux

Model	M6 Bitux					
	E_1	E_2	η_1	η_2	σ_y	RMS
Anti-Zener plus slider	109	-	699	303913	577	4.28
Bingham plus Maxwell	388	9965074	6305	4545376	530	4.63

Table 6.11: M6 - Anti-Zener plus slider and Bingham plus Maxwell models
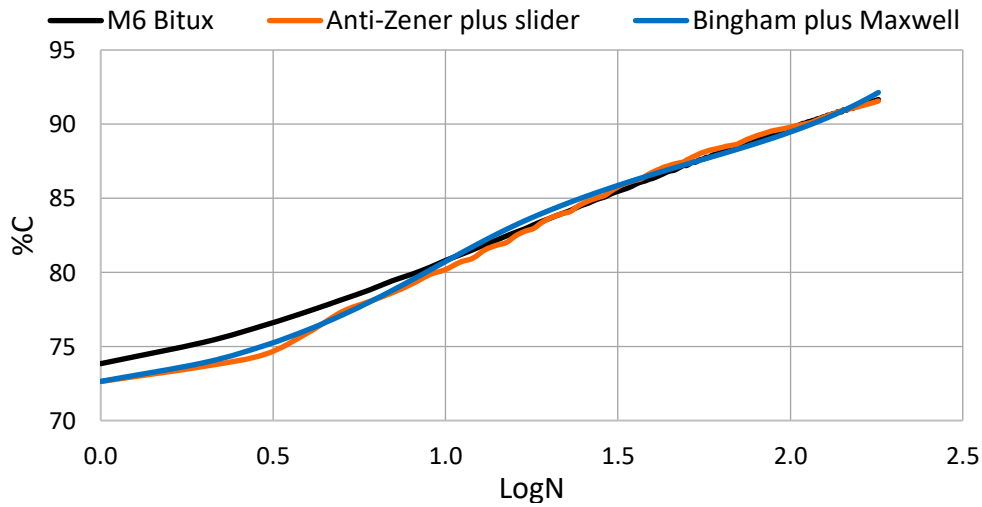
Graph 6.18: M6 - Anti-Zener plus slider and Bingham plus Maxwell models

M7 BlackTop

Model	M7 BlackTop					
	E_1	E_2	η_1	η_2	σ_y	RMS
Anti-Zener plus slider	120	-	587	365738	575	4.68
Bingham plus Maxwell	158	669263	1761	7757108	568	4.05

Table 6.12: M7 - Anti-Zener plus slider and Bingham plus Maxwell models

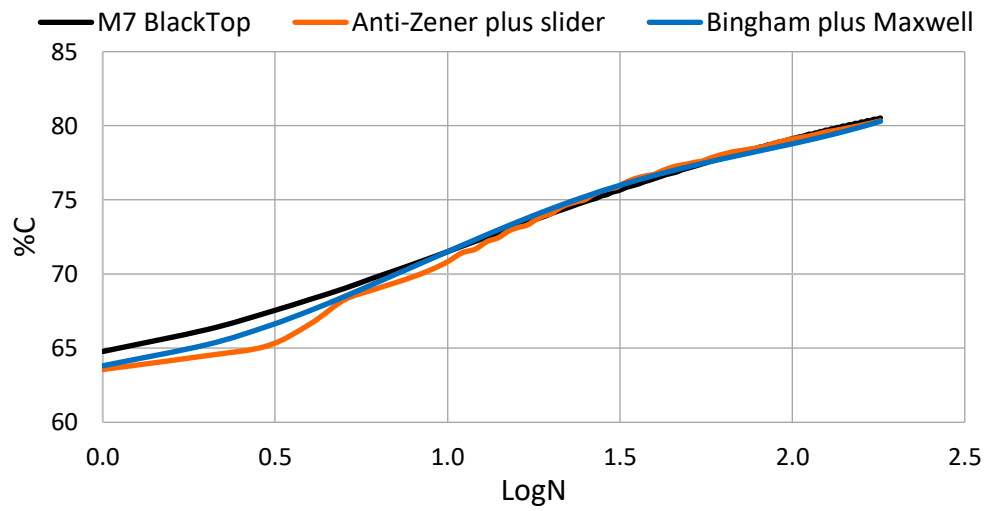*Graph 6.19: M7 - Anti-Zener plus slider and Bingham plus Maxwell models*

6.   Modelling

The results of this simulation phase, whit all the parameters for the different materials, are summarized in the following tables, one for the Anti-Zener plus slider model (_Table 6.13_), one for the Bingham plus Maxwell model (_Table 6.14_).

	Material	Anti-Zener plus slider					
		E_1	E_2	η_1	η_2	σ_y	RMS
M1	Asfaltival Special	140	-	575	135996	574	5.14
M2	Asfaltival 2.0 Revolution	107	-	477	122348	578	3.65
M3	RoadPav	110	-	496	527609	577	5.44
M4	ProntoSint	141	-	737	223133	575	3.74
M5	Bitem	134	-	639	164449	577	2.68
M6	Bitux	109	-	699	303913	577	4.28
M7	BlackTop	120	-	587	365738	575	4.68

Table 6.13: Anti-Zener plus slider model, parameters

	Material	Bingham plus Maxwell					
		E_1	E_2	η_1	η_2	σ_y	RMS
M1	Asfaltival Special	108	9758819	1035	4616830	579	2.69
M2	Asfaltival 2.0 Revolution	125	590	1755	4418074	572	3.81
M3	RoadPav	152	9758819	1065	5775154	572	4.78
M4	ProntoSint	141	8730	1590	6018751	576	2.66
M5	Bitem	911	9574273	16097	4640188	456	4.43
M6	Bitux	388	9965074	6305	4545376	530	4.63
M7	BlackTop	158	669263	1761	7757108	568	4.05

Table 6.14: Bingham plus Maxwell, parameters

From these results and from comparing the curves in the graph, it is evident that the Anti-Zener plus slider can simulate the compaction curve, but its solution is not stable, it continues to oscillate.

The Bingham plus Maxwell model has a better behavior, but it is not very accurate at the end, when it has an increase instead of remaining stable.

One of the objective of this study was to find a correlation between the parameters of the model and some properties of the real mixtures, in this case is quite difficult due to the variability of the obtained results.

For example, the stiffness parameter of the second spring (E_2) in the Bingham plus Maxwell model ranges from 590 to 9965074.

Both the model analyzed are far from the solution at the beginning of the curve, for this reason a double curve simulation was implemented. Starting from the Bingham plus Maxwell model, the simulation was divided into two main parts: one for the first ten rounds, one for the remaining 170 rounds.

The idea was that the materials have a different behavior depending on the dispersion of the aggregates inside the binder: at first there is a high air voids content and the aggregates are in loose contact, so the mixtures have a fast volume change.

After the initial compression the aggregates are in strict contact and they must rearrange to continue to compact.

For each material the simulation was performed using the Bingham plus Maxwell model, which was the most stable one. The results are shown in the following tables and graphs.

M1 Asfaltival Special

Part	Model	M1 Asfaltival Special					
		E_1	E_2	η_1	η_2	σ_y	RMS
1st	Bingham plus Maxwell	31	18143	59	832989	596	0.22
2nd	Bingham plus Maxwell	306	9851267	9897	7159219	540	0.82

Table 6.15: M1 - Bingham plus Maxwell two parts models
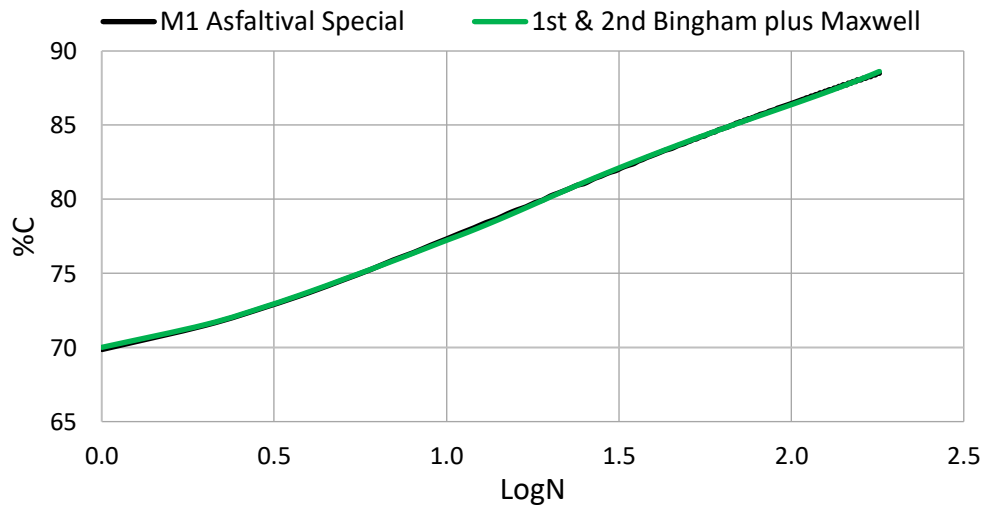
Graph 6.20: M1 - Bingham plus Maxwell two parts models

M2 Asfaltival 2.0 Revolution

Part	Model	M2 Asfaltival 2.0 Revolution					
		E_1	E_2	η_1	η_2	σ_y	RMS
1st	Bingham plus Maxwell	2222	568	7808	200961	437	0.21
2nd	Bingham plus Maxwell	1142	52566	45754	4761075	438	1.84

Table 6.16: M2 - Bingham plus Maxwell two parts models
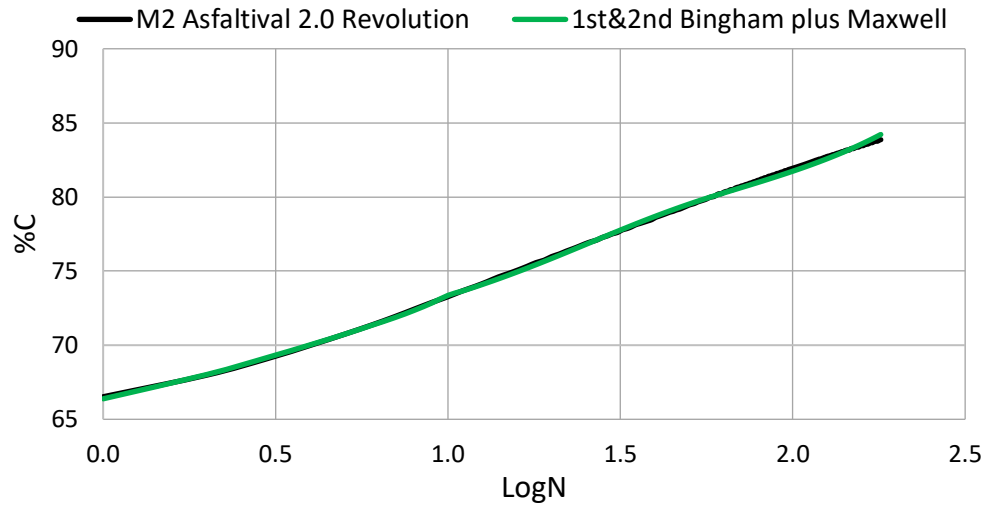
Graph 6.21: M2 - Bingham plus Maxwell two parts models

M3 RoadPav

Part	Model	M3 RoadPav					
		E_1	E_2	η_1	η_2	σ_y	RMS
1st	Bingham plus Maxwell	1679	1672	4056	217053	455	0.52
2nd	Bingham plus Maxwell	1027	110910	39728	9918215	450	1.38

Table 6.17: M3 - Bingham plus Maxwell two parts models
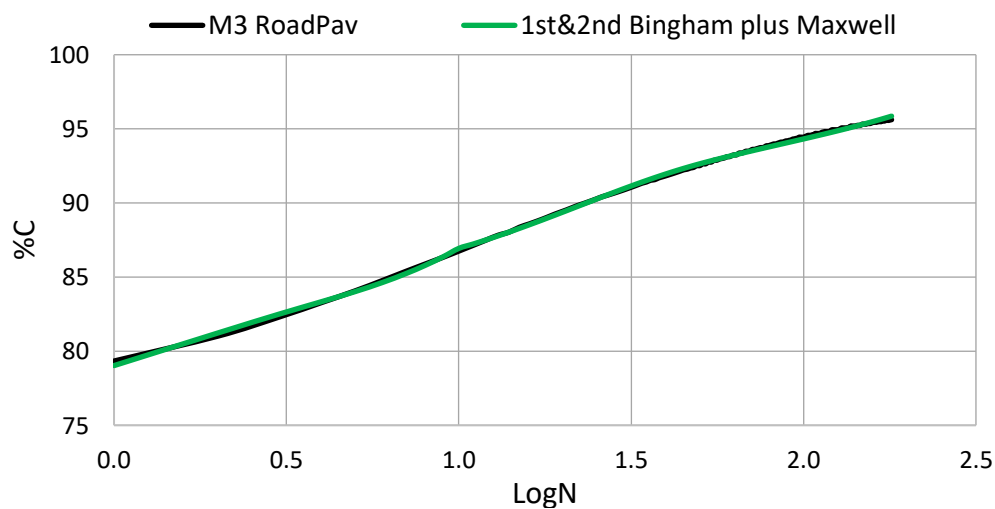
Graph 6.22: M3 - Bingham plus Maxwell two parts models

M4 ProntoSint

Part	Model	M4 ProntoSint					
		E_1	E_2	η_1	η_2	σ_y	RMS
1st	Bingham plus Maxwell	732	9.98E+09	2921	333327	543	0.22
2nd	Bingham plus Maxwell	924	9.84E+09	51109	9961959	459	1.26

Table 6.18: M4 - Bingham plus Maxwell two parts models
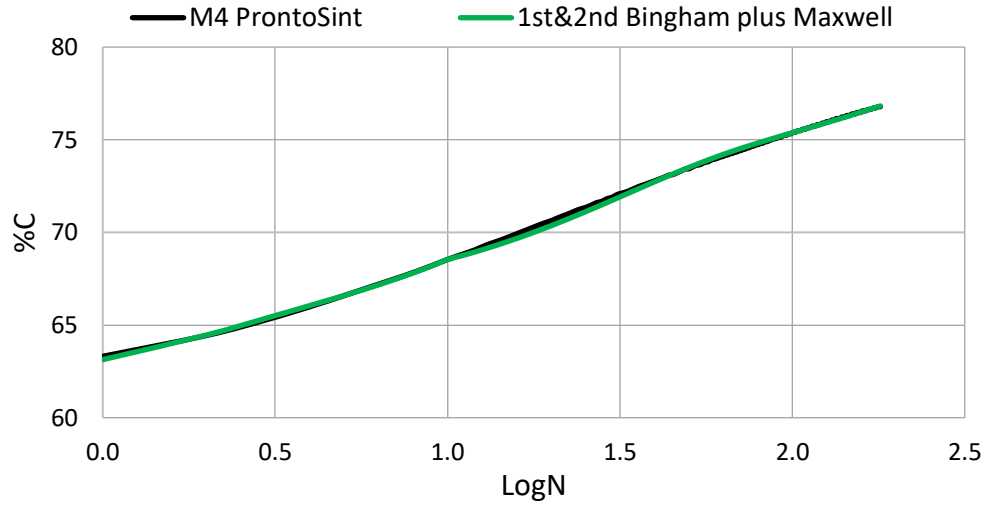
Graph 6.23: M4 - Bingham plus Maxwell two parts models

M5 Bitem

Part	Model	M5 Bitem					
		E_1	E_2	η_1	η_2	σ_y	RMS
1st	Bingham plus Maxwell	341	1285	1014	314262	573	0.19
2nd	Bingham plus Maxwell	969	9.55E+09	43952	8000491	464	0.90

Table 6.19: M5 - Bingham plus Maxwell two parts models
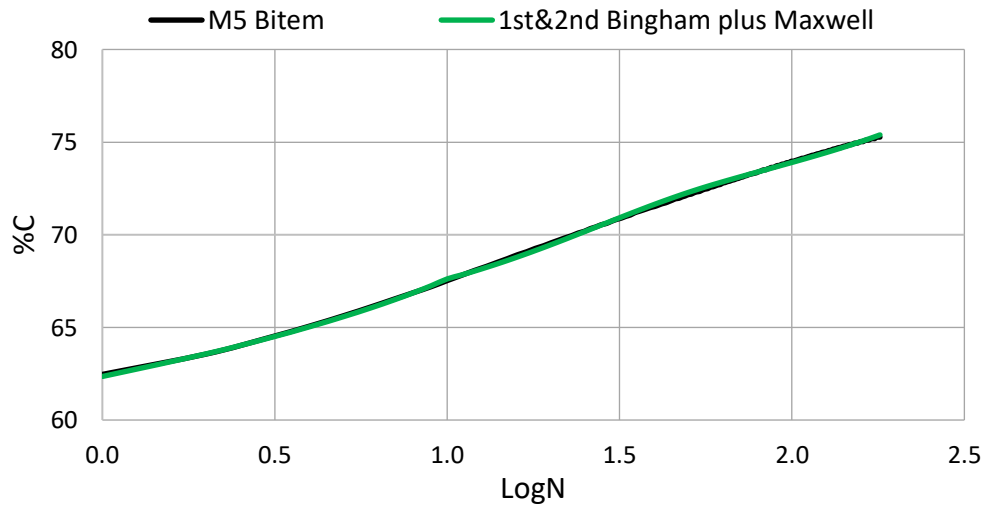
Graph 6.24: M5 - Bingham plus Maxwell two parts models

M6 Bitux

Part	Model	M6 Bitux					
		E_1	E_2	η_1	η_2	σ_y	RMS
1st	Bingham plus Maxwell	251	336	958	304803	575	0.19
2nd	Bingham plus Maxwell	1118	2913827	46745	5873269	428	1.43

Table 6.20: M6 - Bingham plus Maxwell two parts models
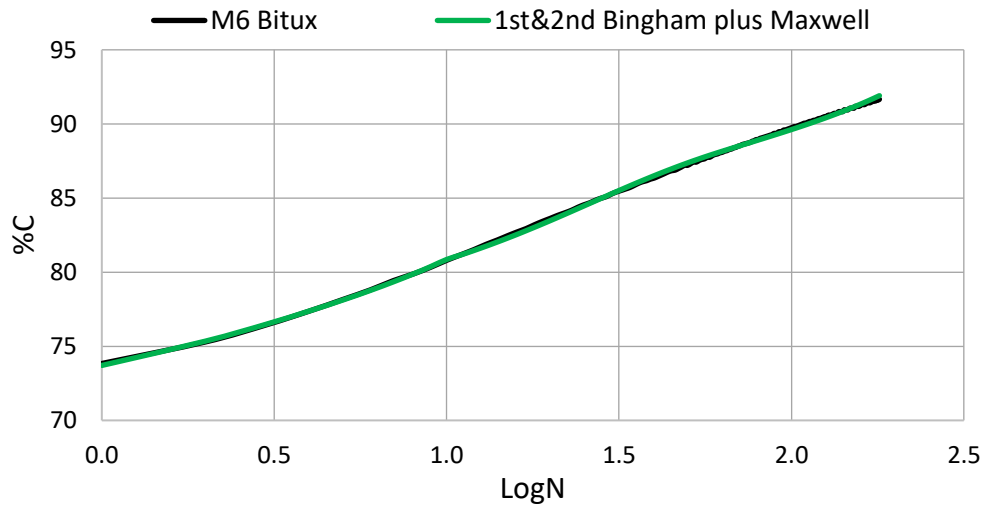
Graph 6.25: M6 - Bingham plus Maxwell two parts models

M7 BlackTop

Part	Model	M6 Bitux					
		E_1	E_2	η_1	η_2	σ_y	RMS
1st	Bingham plus Maxwell	663	9997004	3045	325377	532	0.30
2nd	Bingham plus Maxwell	621	632588	23095	8437958	493	1.02

Table 6.21: M7 - Bingham plus Maxwell two parts models
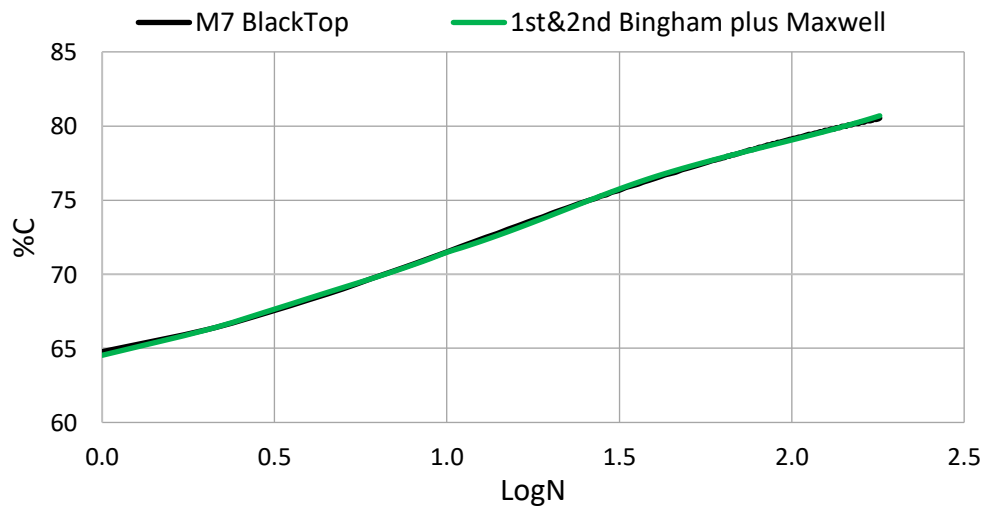
Graph 6.26: M7 - Bingham plus Maxwell two parts models

All the parameters of the model, for the different materials, are summarized in the _Table 6.22_:

Material		1st and 2nd Bingham plus Maxwell					
		E_1	E_2	η_1	η_2	σ_y	tot RMS
M1	Asfaltival Special	31	18143	59	832989	596	0.85
		306	9851267	9897	7159219	540	
M2	Asfaltival 2.0 Revolution	2222	568	7808	200961	437	1.85
		1142	52566	45754	4761075	438	
M3	RoadPav	1679	1672	4056	217053	455	1.48
		1027	110910	39728	9918215	450	
M4	ProntoSint	732	9.98E+09	2921	333327	543	1.28
		924	9.84E+09	51109	9961959	459	
M5	Bitem	341	1285	1014	314262	573	0.92
		969	9.55E+09	43952	8000491	464	
M6	Bitux	251	336	958	304803	575	1.44
		1118	2913827	46745	5873269	428	
M7	BlackTop	663	9997004	3045	325377	532	1.07
		621	632588	23095	8437958	493	

Table 6.22: Bingham plus Maxwell two parts models, parameters

The curve obtained with this model is very similar to the real one, the error is much lower compared to the simulation with only one curve; in particular, there are no more big differences at the starting point.

6.5. SUMMARY

This chapter represents a first approach to the analytical modelling of Cold Mix Asphalt, starting from the basic elastic, viscous and plastic theories until the numerical simulation of the behavior of the real materials.

From the results is possible to say that the compaction curve of these mixtures can be obtained from some analytical models, in an acceptable way with a low error. In particular the simulation performed dividing the curve in two parts gives some very good graphical results.

The main problem is the individuation of a correlation between the parameters that control the model and some properties of the real materials; until now the obtained results are not helpful from this point of view, with a variability that is too high.

This study should be carried out, with the main objective to find a model that can predict the compaction behavior of the mixtures, starting from some of their characteristics.

7. CONCLUSIONS AND FURTHER DEVELOPMENTS

In this research, seven proprietary cold mix asphalts were tested, with the aim to start an extensive analysis of this type of material, that are widely used in road repairs but suffers of a lack of information and standards.

7.1. RESULTS ANALYSIS

Generally, most of the materials are characterized by very poor characteristics and performances, making it difficult also to test some mixtures, whose sample collapses before the test.

The first difference that can be observed is the stocking quality, that can affect the durability of the material; three main stocking types are used: the material can be sold loose, or contained in plastic bags or buckets.

Regarding the composition of the mixtures, the binder content related to the aggregates ranges from 5.86% to 9.18%, but in this quantity are included also all the additives that the producers use to maintain the materials workable at low temperatures.
The seven materials have different particle size distribution, with some of them characterized by a very discontinuous curve.

CMA are usually difficult to compact, after 180 rounds in the Gyratory Shear Compactor only two out of four materials reaches a voids content lower than 10%, with two mixes that remain with more than 20% of voids.
The compaction behavior reflects the different particle size, in particular materials with a more uniform composition will compact more than the others.

After the analysis of the basic properties, the study focused on the evaluation of the materials' strength at two different compaction levels:

- Low compaction strength, related to the density after 50 rounds in the GSC, that simulates the first life of the patches, after a low compaction by the workers.

In this phase both ITS and CBR were evaluated.

- High compaction strength, related to the material after 180 rounds in the compactor, to simulate the patches after the effect of traffic load. For this analysis were estimated the resilient modulus, the quick shear resistance and was performed the wheel tracking test.

LOW COMPACTION STRENGTH

Concerning ITS, due to the weakness of the materials, four out of seven mixtures were not able to sustain the test even if a confinement element was used during the curing period.

For the other three materials, different effects of curing were observed: M6 had a constant resistance so it is not subjected to hardening, M3 had a fast increase in the first 3 days then its resistance stabilized, M7 had low resistance in the first days then it started to linearly increase.

In this phase also the CBR was performed, although it is a test for soil, it was useful because all the materials give some results, thanks to the lateral confinement.

The CBR values ranges from 26.4% of M6 to 62.2% for M3; in particular it is possible to distinguish two classes, one with the CBR around or lower than 40%, one with a ratio around or higher than 60%.

HIGH COMPACTION STRENGTH

The majority of the mixes have low resistance also after a high compaction.

In order to perform the resilient modulus evaluation, for some materials it was necessary to use a new frozen procedure that freeze the slender sample before its extrusion; also in this way, some specimens collapsed during the curing period.

After one day at 20°C, the mean resilient modulus ranges from 96 MPa to 264.8 MPa, while after 28 days it goes from 94.9 to 263.9 MPa.

Regarding the shear resistance, it is possible to recognize three different classes: mixes with a resistance lower than 400 kPa, materials with a resistance that ranges from 400 to 600 kPa, mixtures with higher resistance.

7. Conclusions and further developments

With the exception of M7, it can be observed a decrease of the modulus and the shear resistance in time.

An attempt was made in order to simulate the resilient modulus with three different models: Uzan, MEDPG and Puppala. The difference between the real and predicted modulus remain high, so these models are not representative of the behavior of cold mix asphalts.

Only M3 showed good performance during the wheel tracking test, since it has resisted to all the 30000 cycles and the average rut depth at the end was comparable to the one of a standard hot mix asphalt.

M7 gives some results only for the first 300 cycles, while all the other materials collapsed during the setting cycles.

MATERIALS CLASSIFICATION

From the results of this study, it is possible to divide the cold mix asphalts in three different categories, related to the possible final use.

The worst mixes (M4 and M5) can be used as filling of the lower lift of deep potholes, since they don't have enough strength to resist to traffic load; they are similar to unbounded materials.

The best materials (M3 and M7) can be used as ordinary maintenance, also in heavy traffic roads, due to their performances that are similar to the ones of a hot mix asphalt.

The other materials (M1, M2 and M6) can be used to perform extraordinary maintenance, to solve immediately a problem but they cannot be considered as a long term solution.

The price of the mixtures usually reflects the different classes, with the filling materials that are the cheapest and the ordinary maintenance ones that are the most expensive.

MODELLING

Different models were studied in order to simulate the compaction behavior of the materials; from the results it is possible to say that the Bingham plus Maxwell model can simulate the compaction curve with an acceptable error.

It is also possible to improve the results dividing the simulation in two parts, before and after ten rounds.

In both cases it was not feasible to find a correlation between the parameters of the models and some properties and characteristics of the real mixtures.

7.2. FURTHER DEVELOPMENTS

To improve this analysis, it would be possible to introduce different curing times for both the CBR and rutting test, to discover if there is a change in the behavior of the materials.

It would be helpful the study of the interaction between the patching mixes and the surfaces where they are applied, analyzing the cohesion between the different materials and the strength of the linkage.

It is possible to improve the modelling of the resilient modulus, by using more appropriate models or developing a new one.

However, one of the most important further development is the introduction of in situ test, to study the real behavior of cold mix asphalts during their life.

These tests should focus, along with diverse type of materials, on the different application techniques, on different weather condition during the filling of the pothole and on different traffic levels.

Regarding the modelling phase, due to the difficulties in finding a relationship between the models' parameters and the properties of the different materials, further investigation should be done on this aspect.

It would be possible to introduce a hardening behavior and a subdivision of the model to simulate the changes of the materials' behavior under compaction.

REFERENCES

AASHTO T307. (1999). Standard Method of Test for Determining the Resilient Modulus of Soils and Aggregate Materials.

Abela Munyagi, A. (2006). *Evaluation of cold asphalt patching mixes*. University of Stellenbosh.

Anderson, D. A., Thomas, H. R., Siddiqui, Z., & Krivohlavek, D. D. (1988). *More Effective Cold, Wet-Weather Patching Materials for Asphalt PavementsNo Title*.

Bahonar Brokerage (IME CO). (1999). en.bahonarbrokerage.com.

Bau- und Verkehrsdepartement des Kantons Basel-Stadt. (2010). Handbuch Strassenbau. *Switzerland*.

Bergstralh-Shaw-Newman. (1996). *Utility Cuts in Paved Roads - Field Guide*.

British Board of Agrément. (2010). Guidelines Document for the Assessment and Certification of Permanent Cold-lay Surfacing Material for the Reinstatement of Openings in Highways. *UK*.

British Standard Institute. (1995). Methods for Sampling and Testing of Mineral Aggregates, Sands and Fillers, *BS 812*.

Buertey, J. I. T., Atsrim, F., & Offei, S. W. (2016). An Examination of the Physio-mechanical Properties of Rock Lump and Aggregates in Three Leading Quarry Sites Near Accra. *American Journal of Civil Engineering*, *4*(6), 264–275.

Chatterjee, S., White, R. P., Smit, A., & River, R. (2006). *Development of mix design and testing procedures for cold patching mixtures*.

CSIR Council for Scientific and Industrial Research. (2010). Potholes - Technical guide to their causes, identification and repair. *South Africa*.

Czech Ministry of Transport. (2010). Catalogue of distress of flexible pavements. Technical regulations. *Czech Republic*.

Danish Road Directorate and Danish Road Institute. (2009). Repairing asphalt wearing course - Tuelsø trial section, Internal Memo 147. *Denmark*.

Diaz, L. G. (2016). Creep performance evaluation of Cold Mix Asphalt patching mixes. *International Journal of Pavement Research and Technology*, *9*(2), 149–158.

Dione, A., Fall, M., Berthaud, Y., Benboudjema, F., & Michou, A. (2015). Implementation of Resilient Modulus -CBR relationship in Mechanistic-Empirical (M. -E) Pavement

Design. *Alexandre Michou Revue Cames – Sci. Appl. & de l'Ing*, *1*(12), 65–71.

ERA-NET ROAD. (2012). *Study of existing standards , techniques , materials and experience with them on the European market*. Karlsruhe Institute of Technology (KIT) Institute of Highway and Railroad Engineering Department Highway Construction Technology.

Estakhri, C. K., Jimenez, L. M., & Button, J. W. (1999). *Evaluation of Texas DOT Item 334, Hot-Mix, Cold-Laid Asphalt Concrete Paving Mixtures.*

Forschungsgesellschaft für Straßen- und Verkehrswesen- Arbeitsgruppe Asphaltbauweisen. (2009). Additional technical contract terms and guidelines for maintenance of road constructions -asphalt. *Germany*.

Haddad, Y. M. (1995). Linear viscoelasticity. *Viscoelasticity of Engineering Materials*, 33–69.

Kandhal, P. S., & Mellott, D. B. (1981). *Rational Approach to Design of Bituminous Stockpile Patching Mixtures*.

Lubliner, J. (2006). *Plasticity*. University of California at Berkeley.

Maher, A., Gucunski, N., Yanko, W., & Petsi, F. (2001). *Evaluation of Pothole Patching Materials*. FHWA NJ 2001-02.

Marasteanu, M. (2018). *Pothole Prevention and Innovative Repair*. Minnesota Department of Transportation.

Mazari, M., Abdallah, I., Garibay, J., & Nazarian, S. (2016). Correlating Nonlinear Parameters of Resilient Modulus Models for Unbound Geomaterials. *Procedia Engineering*, *143*(Ictg), 862–869.

McDaniel, R. S., Olek, J., Behnood, A., Magee, B., & Pollock, R. (2014). *Pavement Patching Practices*. NCHRP Synthesis 463.

Miller, J. S., & Bellinger, W. Y. (2003). *Distress Identification Manual for the Long-Term Pavement Performance Program*. *Publication of US Department of Transport, Federal Highway Administration*. FHWA Research Report No. FHWA-RD-03-031.

Ministry of Transport - Agency Slovene Roads. (2005). Technical specification for public roads, Routine roads maintenance, Asphalt pavements. *Slovenia*.

Mitchell, M. (1996). *An introduction to genetic algorithms*.

Nazarian, S., Mazari, M., Abdallah, I., Puppala, A. J., Mohammad, L. N., & Abu-Farsakh, M. Y. (2014). Modulus-Based Construction Specification for Compaction of Earthwork

and Unbound Aggregate. *NCHRP Project 10-84.*

Nazzal, M., Kim, S.-S., & Abbas, A. R. (2014). *Evaluation of Winter Pothole Patching Methods*.

NCHRP. (1979). *Report 64*.

Ooi, P. S. K., Archilla, A. R., & Sandefur, K. G. (2004). Resilient Modulus Models for Compactive Cohesive Soils. *Journal of the Transportation Research Board, No. 1874*.

Österreichisches Normungsinstitut (Austrian Standards Institute). (2011). ÖNORM B 3587. *Austria*.

Paige-Green, P., Maharaj, A., & Komba, J. (2010). *POTHOLES: A technical guide to their causes, identification and repair*. CSIR built Environment.

Prowell, B. D., & Franklin, A. G. (1995). *Evaluation of cold mixes for winter pothole repair*.

Puppala, A. J., Mohammad, L. N., & Allen, A. (1997). *Engineering behavior of lime treated Louisiana subgrade soil*. *Transportation Research Record 1546*.

Riviera, P. P., Bellopede, R., Marini, P., & Bassani, M. (2014). Performance-based re-use of tunnel muck as granular material for subgrade and sub-base formation in road construction. *Tunnelling and Underground Space Technology*, *40*.

Robinson, H. (2014). How CE marking is working for surface treatments, 78–81.

Rosales-Herrera, V. I., & Prozzi, J. A. (2007). *Mixture Design Manual and Performance-Based Specifications for Cold Patching Mixtures* (Vol. 7). FHWA/TX-08/0-4872-2.

Santagata et al. (2016). *Strade*.

Santagata, F. A., Canestrari, F., & Pasquini, E. (2005). CIRS - Valutazione delle prestazioni di miscele Asphalt Rubber, 1–44.

SITEB - buonasfalto.it. (2018). E le buche? Perché ci sono? Retrieved from http://www.buonasfalto.it/sicurezza/e-le-buche-perche-ci-sono

Slovak Ministry of Transport, C. and R. D. (2011). Catalogue of repair techniques of distress basic type. Technical regulations. *Slovak Republic*.

The Economist Group Limited. (2016). The hole story. *The Economist*.

UNI EN 1097-6. (2013). Prove per determinare le proprietà meccaniche e fisiche degli aggregati - Parte 6: Determinazione della massa volumica dei granuli e dell'assorbimento d'acqua.

UNI EN 12697-2. (2003). Miscele bituminose - Metodi di prova per conglomerati bituminosi a caldo - Determinazione della granulometria.

UNI EN 12697-22. (2004). Miscele bituminose - Metodi di prova per conglomerati bituminosi a caldo - Metodo della traccia della ruota (Wheel tracking).

UNI EN 12697-23. (2006). Miscele bituminose - Metodi di prova per conglomerati bituminosi a caldo - Parte 23 : Determinazione della resistenza a trazione indiretta di provini bituminosi.

UNI EN 12697-31. (2004). Miscele bituminose - Metodi di prova per conglomerati bituminosi a caldo - Parte 31: Preparazione del provino con pressa giratoria.

UNI EN 12697-33. (2004). Miscele bituminose - Metodi di prova per conglomerati bituminosi a caldo - Provino preparato con compattatore a rullo.

UNI EN 12697-39. (2004). Miscele bituminose - Metodi di prova per conglomerati bituminosi a caldo - Parte 39: Contenuto di legante mediante ignizione.

UNI EN 12697-5. (2003). Miscele bituminose - Metodi di prova per conglomerati bituminosi a caldo - Determinazione della massa volumica massima.

UNI EN 13286-2. (2010). Miscele non legate e legate con leganti idraulici - Parte 2: Metodi di prova per la determinazione della massa volumica e del contenuto di acqua di riferimento di laboratorio - Costipamento Proctor.

UNI EN 13286-47. (2006). Miscele non legate e legate con leganti idraulici - Parte 47: Metodo di prova per la determinazione dell'indice di portanza CBR, dell'indice di portanza immediata e del rigonfiamento.

US Army Corps of Engineers, E. R. and D. C. (2005). Expedient Repair Materials for Roadway Pavements. *USA*.

Uzan, J. (1985). Characterization of granular material. *Journal of the Transportation Research Board*, (1022), 52–59.

Virginia Department of Transportation, M. D.-A. P. (2009). Evaluation of Vialit Asphalt's Rephalt Cold Mix Patching Material. *USA*.

Wilson P, T., & Romine R, A. (2001). *Materials and Procedures for Repair of Potholes in Asphalt-surfaced Pavements--manual of Practice*. FHWA Research Report No. FHWA-RD-99-168.